NASA Technical Paper 2870

February 1989

Simulation Evaluation of TIMER, a Time-Based, Terminal Air Traffic, Flow-Management Concept

Leonard Credeur
and William R. Capron

NASA

NASA Technical Paper 2870

1989

Simulation Evaluation of TIMER, a Time-Based, Terminal Air Traffic, Flow-Management Concept

Leonard Credeur
Langley Research Center
Hampton, Virginia

William R. Capron
PRC Kentron, Inc.
Aerospace Technologies Division
Hampton, Virginia

NASA
National Aeronautics and Space Administration
Office of Management
Scientific and Technical Information Division

1989

Contents

Symbols and Abbreviations

A/C	aircraft
AP	aim point
ATA	actual time of arrival
ATC	air traffic control
ATOPS	Advanced Transport Operating Systems
CAS	calibrated airspeed
ERM	en route metering
ETA	estimated time of arrival
FAF	final-approach fix
FMS	flight management system
IFR	instrument flight rules
ILS	instrument landing system
MF	metering fix
MLS	microwave landing system
NAS	National Airspace System
OAG	Official Airline Guide
RD_1	runway threshold delivery time error of first A/C of a pair
RD_2	runway threshold delivery time error of second A/C of a pair
RI	runway threshold interarrival time error of an A/C pair
RNAV	area navigation
ROT	runway occupancy time
SLT	scheduled landing time (at runway threshold)
T_B	time buffer added to reduce chance of separation violation
TAATM	terminal area air traffic model
TIMER	traffic intelligence for the management of efficient runway scheduling
t	time
V_a	final-approach indicated airspeed
V_{am}	final-approach airspeed at maximum landing weight
VFR	visual flight rules
VOR	VHF omnidirectional radio range
W_f	weight factor
x, y, z	Cartesian coordinate system
μ	mean value
σ	standard deviation
ϕ	bank angle, deg
4D	four dimensional (x, y, z, and time)

Summary

A description of a time-based air traffic control (ATC) concept called TIMER (traffic intelligence for the management of efficient runway scheduling) and the results of a fast-time computer evaluation are presented. The TIMER concept integrates en route metering, fuel-efficient cruise and profile descents, terminal time-based sequencing and spacing, and computer-generated controller aids to improve delivery precision for fuller use of runway capacity. The concept handles both 4D-equipped and non-4D-equipped aircraft and is designed for both evolutionary integration into the manual, voice-linked ATC system and for the accommodation of proposed system-upgrade features such as data link and further ground automation.

A fast-time parametric sensitivity evaluation of the TIMER concept with non-4D traffic was performed using a four-corner-post approach configuration to runway 26L at Denver's Stapleton International Airport. The simulated traffic consists of large and heavy transport arrival traffic operating under instrument flight rules (IFR). Results identify and show the effects and interactions of such key variables as horizon-of-control location, delivery-time error at both the metering fix and runway threshold, aircraft separation requirements, delay discounting, wind, flight technical error, and knowledge of aircraft final-approach speed. The current ATC system has a runway interarrival-error standard deviation of approximately 26 sec. Fast-time simulation results indicate that, with computer aiding, the runway interarrival-error standard deviation for non-4D-equipped traffic can be reduced to the region of 8 to 12 sec if the final-approach speed is known to the TIMER algorithm; however, the standard deviation would be in the region of 16 to 20 sec if the final-approach speed were unknown. Another major finding is that en route, metering-fix, delivery-error standard deviation should be below approximately 45 sec to achieve full runway capacity. This requirement implies a need for either airborne automation or assistance to the controller, since the current controller manual performance in today's en route metering environment is about 1.5 min.

1.0 Introduction

In the United States, air-travel delays have become a major problem, because the combination of increased passenger demand and airline deregulation is straining the current operational capacity of the nation's major airports. Since environmental considerations have restricted both the expansion of existing airports and the construction of new airports, there are many activities directed toward enhancing the capacity of existing airports. Examples of such activities include efforts to reduce aircraft longitudinal separations and the required spacing between parallel runway centerlines for independent approaches under instrument flight rule (IFR) conditions. Air traffic control (ATC) system designers should also consider options which take advantage of advances in airborne capability to improve the overall system (aircraft/ATC) performance. The development of four-dimensional (4D) flight management systems (FMS), which are capable of meeting time objectives at points along the flight path, offers the potential for exploitation in this area.

Although the current ATC system has evolved into a system based on distance separation, primarily because relative aircraft distances are displayed to controllers from radar data, time control is not new to ATC; in fact, distance was the basis of separation before radar. Indeed, the two major factors that limit longitudinal separation are time based: the time required for an aircraft's wake vortex to decay to a safe level, and the preceding aircraft's runway occupancy time. Runway arrival capacity will be used to its fullest potential only when these two time-dependent factors can be satisfactorily modeled and manipulated in the operational system. Therefore, an automated, time-based ATC system could be postulated which schedules aircraft to the runway as a function of these two factors constrained by the range of the arrival-time capability of each aircraft. Research and development in the areas of runway guidance, high-speed turnoffs, accurate weather prediction, and wake vortex modeling should eventually permit the use of variable, reduced time separation that depends on atmospheric conditions. Such a capability, together with improved delivery precision, forms the basis for significant potential increases in runway arrival rates.

In an advanced, variable-time-separation system such as just described, the ground automation would approve or schedule runway arrival times. The aircraft would employ their 4D flight-management system to precisely meet their scheduled landing times in a fuel-efficient manner. A data link could allow the airborne and ground systems to exchange information and intention. A block diagram of such an advanced time-based system to improve airport capacity is shown in figure 1.

There are some operational issues that must be resolved before such a system could be implemented, but the concept appears technically feasible. The problem is how to get to that ideal environment from the manual, separation-based ATC of today. This paper describes an extended-terminal,

flow-management concept called TIMER (traffic intelligence for the management of efficient runway scheduling) that is designed to bridge the gap between the current system and an ideal advanced time-based ATC system. The TIMER concept integrates en route metering, fuel-efficient cruise and profile descents, terminal time-based sequencing and spacing, and computer-generated controller aids to improve delivery precision for fuller use of runway capacity. Also presented in the paper are the results of a fast-time simulation evaluation of the basic TIMER concept which identified and showed the effects of such key system parameters as horizon-of-control location, delivery-time error at both the metering fix and the runway threshold, aircraft separation requirements, delay discounting, wind, aircraft heading and speed errors, and knowledge of final-approach speed.

2.0 Background

During the late 1950's, the 1960's, and the early 1970's, there was a substantial amount of effort in the areas of analysis and study of computer-aided spacing systems for terminal-area ATC. Much of that work was focused on final-approach spacing aids to the controller. Reference 1 contains an excellent summary of this activity and has an extensive bibliography. Despite all this referenced activity, there is still no terminal-area computer-aided spacing in operation. Some of the reasons these earlier efforts did not result in an operational system are as follows:

1. There was a lack of coupling or integration of en route arrival metering with computer-aided terminal sequencing and spacing.
2. The trajectory and time calculations did not use aircraft-type or model-specific performance data.
3. The limitations and state of computer, display, data-processing, and tracking technology at the time were a serious handicap.
4. Separation criteria and operational procedures that would handle the throughput achievable under current visual-flight-rule (VFR) conditions were not developed for the computer-aided or automated systems.
5. There was insufficient controller involvement early in the design phase and a lack of emphasis on the controller-machine interface.
6. There was inadequate flexibility and consideration of real-world requirements, such as missed approaches, pop-ups, active-runway changes, and weather disturbances.

The TIMER concept, together with advances in computers, displays, and tracking technology, addresses the first three shortcomings. Also, TIMER introduces a needed perspective and consideration of aircraft and avionic capability and development. The resolution of the fourth shortcoming depends more on criteria definition and procedural factors than on technical limitations. Further development is required before the important concerns of the fifth and sixth shortcomings are satisfied.

The process of keeping the runways fully occupied and aircraft safely separated normally requires aircraft to take spacing delays (vectoring and extensive trombone maneuvers) which are not fuel efficient. The inherent aircraft delays required to space random-arrival traffic during heavy periods can be taken in a more fuel-efficient manner relative to current procedures. However, improving fuel efficiency requires a more sophisticated ground-airborne interactive process, which must be strategic in nature to control the en route/transition/terminal region. Previous activities oriented toward that approach are documented in references 2 and 3. While the current United States en route metering (ERM-1) is a time-based process, it is characterized by relatively coarse planning, with no aircraft performance modeling and no controller aids to help deliver aircraft at the scheduled times (ref. 4). Also, it is not a coupled process, since the terminal facility controls the resultant aircraft stream from the ERM-1 process without knowledge of its intended sequence or target times.

3.0 Concept Development

An approach is needed that is broad enough to simultaneously address the following several issues. How can aircraft operations during peak demand periods be improved? How can ATC take advantage of aircraft with advanced avionics while still handling conventionally equipped traffic? What can be done to improve delivery precision and reduce interarrival separation so as to increase capacity? Can fuel efficiency be improved and still achieve maximum runway throughput? The answers lie not in the specific fields of communication, navigation, or surveillance but in a system approach that covers the areas of ATC/aircraft interaction, flexible fuel-efficient 4D flight-management systems, and automated controller aids.

An ATC/aircraft system oriented approach is being taken by the Langley Advanced Transport Operating Systems (ATOPS) Program Office. One of the principal thrusts of the program is to define and evaluate evolutionary ATC concepts which improve the capability, reliability, and economy of extended terminal flow operations (final en route cruise segment, transition, and terminal flight to the runway) when used with the proposed ground and avionic

hardware. The TIMER concept is an output of that activity. It was designed to perform the task of assisting the air traffic controller with traffic management in the extended terminal area. The TIMER concept is a step in the direction of using computers for control assistance, not just for data formatting and transfer. It is evolutionary in nature and accommodates today's aircraft as well as 4D-equipped advanced-technology aircraft. The algorithm, which uses simplified aircraft-specific performance models, is designed for integration into the manual, voice-linked ATC system and, later, to accommodate proposed National Airspace System (NAS) features such as data link and further ground automation (ref. 5). The TIMER concept was also designed to bridge the gap between today's en route terminal process for handling arrival traffic at major terminals and the future automated ATC system situation (fig. 1), for which most of the aircraft will presumably have advanced 4D flight-management systems capable of data exchange with ground automation.

4.0 Operational Description of TIMER Concept

The TIMER concept is an integrated extended terminal-area flow-control concept which begins its control at the horizon of control back in the en route airspace. The major operational features of the TIMER concept are summarized as follows:

1. The arrival stream into the extended terminal is derandomized at the horizon of control by establishing a proposed aircraft landing sequence and building a list of aircraft target landing times based on safe separation. The desired metering-fix time as a result of the assigned landing time is also determined.
2. Nominal estimated times of arrival used in step 1 are based on fairly simple yet representative aircraft-specific performance models. Using these models and predicted winds, a ground-computed trajectory is determined to meet the aircraft's assigned target landing time.
3. Computer-generated assistance is given to the controller to help meet aircraft target times based on the trajectory calculations.
4. Adjustments to the target landing times, and even changes in the landing sequence, are made to accommodate errors and anomalies.
5. The aircraft trajectory is fine-tuned in the final-approach region to meet the final target landing time with limited uncertainty.

Some of the TIMER features and its areas of operation are shown in figure 2. The features are shown in greater detail in figure 3. An operational description of the TIMER concept is accomplished by reviewing the sequence of events an aircraft would undergo as it flies from the horizon of control to the runway on the upper northwest route depicted in figure 3.

4.1 Sequencing and Scheduling

The horizon of control is encountered when an aircraft is an estimated fixed flight time from the metering fix. When aircraft reach their horizon of control, the TIMER system begins the process of determining the landing sequence and schedule (events 1 and 2 in fig. 3). Nominal arrival speeds, route segment distances to the runway, and predicted winds are used to determine the aircraft's undelayed estimated times of arrival (ETA). The sequencing criterion currently used is a projected first-to-reach-runway ordering based on the undelayed ETA's.

With the aircraft at the horizon of control, there is a range of earliest and latest landing times that the aircraft can achieve by varying its speed between nominal approach values and the slowest possible speeds imposed by performance and operational considerations. Assigned landing times are not permitted to be earlier than that achieved by flying at nominal speeds. The initial scheduled landing time (SLT) for the aircraft (event 2 in fig. 3) is determined by taking the larger of the following: (1) The undelayed, estimated landing time or (2) The landing time of the previously scheduled aircraft plus the separation criteria plus T_B. A time buffer T_B is added to account for system delivery uncertainty. If the assigned landing time exceeds the latest attainable speed-control time, the additional delay must be absorbed by either path stretching or holding.

4.2 En Route and Terminal Trajectory Computations

The time and distance associated with all descent and deceleration segments are calculated from aircraft-type-specific, point-mass equations of motion for a clean configuration at flight-idle thrust with predicted winds accounted for. The TIMER trajectory computations and aircraft model parameters used are described in more detail in reference 6. As shown in figure 4, the flight path (which corresponds to events 3 and 4 in fig. 3) is divided into a cruise segment and several descent and constant-altitude deceleration segments. An iterative process employing the *regula falsi* method (ref. 7) computes the required metering-fix altitude to continue to fly a clean-configuration, flight-idle-thrust descent inside the terminal to the aim point (shown in fig. 4 where clean, flight-idle-thrust descent normally ends). The

algorithm inputs are the aim-point altitude, the nominal segment speeds, the segment distances from the metering fix to the aim point, and the wind. With the metering-fix altitude established, the nominal flight time from the metering fix to the runway is computed and the desired metering-fix time is determined, given the scheduled runway time. Another iterative process using the *regula falsi* method is used to calculate the cruise Mach, the Mach/CAS descent speeds to the metering fix, and the time to begin the descent, so that the aircraft arrives at the metering fix at the prescribed time, altitude, and speed.

It should be noted that the TIMER simulation results presented subsequently do not have the entire en route 4D trajectory deterministically modeled. The simulation had only the time dimension with appropriate delays and time errors modeled from the horizon of control to the metering fix (event 3 of fig. 3). The simulation employed a full 4D deterministic model of aircraft flight from the metering fix to the runway.

Once the SLT and metering-fix time are established, the trajectory calculations described previously provide the non-4D aircraft with the desired metering-fix time, the cruise Mach number, the time to begin to perform the descent, and the Mach/CAS schedule during the descent. This information would be displayed to the controller and would enable him to assist the non-4D aircraft to meet its schedule in a fuel-efficient manner. The 4D-equipped aircraft could be given either its metering-fix or aim-point time. Figure 5 presents examples of the en route types of controller messages envisioned for both 4D and non-4D traffic.

There are many 4D path solutions possible. Thus, proper coordination and interfacing between ground-system designers and airborne flight-management-system designers are essential if there is to be compatibility between the paths flown by 4D and non-4D aircraft. Ideally, the only difference would be the greater time precision expected from the 4D aircraft.

4.3 Metering-Fix Rescheduling and Terminal Speed Control

The SLT may be changed when the aircraft arrives at the metering fix, either because of the action of preceding traffic or because of the aircraft's own metering-fix time error. The TIMER system is flexible enough to accommodate aircraft time errors. This flexibility is particularly important in the initial implementation when, presumably, a large percentage of unequipped aircraft are present. Depending on the circumstances, the SLT may be slipped forward or backward, or the landing sequence may be altered if the schedule slippage warrants such action.

Beginning at the metering fix, control action is performed at prespecified geometric points along the approach route (labeled speed adjustment points in fig. 3). The ETA at the runway threshold is compared with the updated SLT. The segment speed needed for the aircraft (indicated airspeed) to maintain its SLT is computed at the beginning of each segment. Those speeds are displayed to the controller and issued to the aircraft. Sample controller messages that show how TIMER would handle traffic inside the metering fix (event 4 of fig. 3) are also shown in figure 5. Initially, all the traffic would probably be handled similarly inside the terminal. It is envisioned that when the bulk of the traffic becomes 4D equipped, the desired aim-point time will be given and the aircraft will calculate its own speed profile along the specified path to meet the assigned time.

4.4 Fine-Tuning Region

In the final-approach region there are two computer-aided, fine-tuning maneuvers (events 5 and 7 in fig. 3) which are designed to further reduce runway delivery error. The fine tuning consists of timing both the turn-to-base (event 5) and the turn-to-final (event 7) maneuvers. In keeping with the evolutionary mode, the design was configured to be similar in geometry and procedures to the conventional approach performed today. That is, the pilot would not be able to distinguish between a TIMER assisted final approach and a conventional-radar, manual-controlled approach.

The fine-tuning process is based on a regularly updated ETA calculation which displays how early the aircraft would be if its turn instructions were issued immediately. This process gives more information than a straight clock countdown display, which would only indicate the time remaining in which to issue the turn command. With expected communication and response times of both the controller and pilot factored in, the data tag of each aircraft on the controller display is enhanced to indicate when, and to what heading, the controller would vector the aircraft for the base and localizer intercept segments. The fine-tuning region must accommodate minor schedule changes due to preceding-aircraft errors, wind-estimate errors, or own-aircraft flight errors which have accumulated since the last speed-control point.

4.5 Operational Benefits

The TIMER concept described has several operational benefits. The initial metering, sequencing, and scheduling of aircraft to the terminal take place

early enough in the en route airspace so that most of any required delay can be taken by more fuel-efficient speed reduction rather than flying holding patterns. The en route and terminal control processes are integrated and coupled so that fuel-efficient, clean-configuration, flight-idle-thrust descents are continued into the terminal area, all the way to the aim point, which is near the final-approach region. The 4D-equipped aircraft are allowed to use and benefit from their capability. The Mach/CAS, clean-configuration, flight-idle type of descent profiles calculated can be flown with today's conventionally instrumented cockpits. The final-approach controller spacing aid is based on the turn instructions normally issued to landing aircraft. Its use would be transparent to the pilot and would not impose any operational approach-procedure changes.

5.0 Description of Parametric Sensitivity Analysis

5.1 Method and Parameters Studied

The TIMER concept was incorporated into the terminal area air traffic model (TAATM) simulation (ref. 8) so that the effect of significant parameters could be studied. Various modules and their relationships within the simulation model are discussed in appendix A. The TAATM is a flexible dynamic simulation of the airborne, navaid, ground-control, and communication aspects of the terminal-area environment which can run in either fast-time (batch mode) or real-time (with controller-pilot interaction). Pertinent en route times, delays, and errors are stochastically modeled only in the time dimension within the TAATM. From the metering fix to the runway, the entire en route 4D trajectory is deterministically modeled with errors included. A fast-time parametric sensitivity evaluation of the basic TIMER concept was performed. The parameters studied and their values assigned are shown in table 1.

5.2 Performance Evaluation

Data collected from fast-time data runs of the TAATM simulation were used as a basis for evaluation. The objective was to determine the sensitivity or change in a particular system measure of performance as the parameter under study was varied. The various measures of performance used were: aircraft mean en route delay between the horizon of control and the metering fix; aircraft mean terminal-area delay; runway arrival rate; and aircraft-pair interarrival-error standard deviation at the runway threshold. The particular performance measure selected for each parameter depended on the relevancy and sensitivity of the measure to the parameter under study.

Table 1. Simulation Parameters Studied

Parameters varied	Values
Horizon of control, min	10, 20*, 30, 45, 60
Wake-vortex separation criteria (described in section 5.3), n.mi.	3/4/5*, 2.5/3.5/4.5, 2/3/4
Metering-fix delivery-error σ, sec	0, 15, 30*, 60, 90, 120
Input traffic rate, A/C per hr	30, 35*, 40, 55
Terminal speed control discounted, percent	0*, 30, 50, 70, 100
Runway-threshold interarrival-error σ, sec	0, 6.1*, 12.1, 20.0
Combined controller-pilot reaction-error σ, sec	0, 2, 3.5*, 5, 6.5
Aircraft heading-error σ, deg	2*, 6, 10
Wind strength (direction aligned with runway), knots	0*, 10, 20
Wind error for 20 knots wind-strength case, knots	−12, −8, −4, 0*, 4, 8, 12
Expected-final-approach-speed-error σ, knots	0*, 4, 8
Weight-factor σ ($\mu = 0.5$)	0*, 0.05, 0.10, 0.15, 0.20
Knowledge of expected-final-approach speed	Known*, unknown
Final-approach fix to runway distance, n.mi.	3.5, 5.5*

*Baseline values; kept constant while the parameter under study was varied.

Each of the measured and plotted points of performance is a statistical combination of the aircraft performance achieved during at least two independent data runs for the conditions simulated. The individual data runs each contain 2 hr of simulated aircraft landing data. The data period for the landing data began following a settling time after the first traffic was introduced at the horizon of control. The settling time was equal to the horizon-of-control-to-metering-fix flight time plus 40 min. In dealing with stochastic models, one can expect occasional low-probability events to occur. If the output performance measure of each run in a set did not agree (both measures within the range of each other's 95-percent confidence interval), an additional two-run set was performed. The total was then combined in a pooled estimate of the performance measure of interest.

5.3 Simulation Configuration

The Stapleton approach routes, a runway-26L landing configuration (fig. 6), instrument flight rules, and airline transport arrival traffic were simulated in the TAATM. One of the 1982 Official Airline Guides (OAG) was used to generate a generic traffic sample with route-loading and aircraft-type distributions. Data collected from the OAG were for transport arrivals on weekdays at Stapleton. All the traffic entered the terminal area at the metering fixes. The metering fixes are KEANN, KIOWA, BYSON, and DRAKO. The simulated arrival traffic was distributed to the four metering fixes, or corner posts, in the following manner:

Metering fix	Percentage of total traffic
KEANN	26
KIOWA	32
BYSON	26
DRAKO	16

The traffic consisted of a mix of large and heavy weight class, transport-type aircraft, with 8.6 percent of the traffic in the heavy category. Large aircraft are those with 12 500 lb to 300 000 lb maximum certified takeoff weight. Heavy aircraft are those capable of takeoff weights of 300 000 lb or more regardless of their actual weight (ref. 9). None of the simulated traffic had onboard 4D trajectory computing capability.

The minimum requirement used in the simulation for wake-turbulence separation distance was a function of the weight class of both the lead and trail aircraft of a pair. By using aircraft velocities and simulated winds, the separation distances are converted to separation times for scheduling purposes in the TIMER algorithm. The distance separation criteria used in terms of the lead and trail aircraft of a pair are as follows:

Lead	Trail	
	Large	Heavy
3/4/5 n.mi. criterion		
Large	3	3
Heavy	5	4
2.5/3.5/4.5 n.mi. criterion		
Large	2.5	2.5
Heavy	4.5	3.5
2/3/4 n.mi. criterion		
Large	2	2
Heavy	4	3

6.0 Simulation Results and Discussion

6.1 Horizon of Control

A major goal of the TIMER concept is to meter, sequence, and initially schedule arrival aircraft early enough in the approach so that any delays needed to derandomize the traffic can be taken in a fuel-efficient manner. The trade-off is to determine how early or at what expected flight time to the metering fix the horizon of control should be located without extending too far back in time from the airport to cause coordination problems between centers. Figure 7 shows the measured mean en route delay (delay between horizon of control and metering fix) and its standard deviation for both the long and short terminal approach routes for various horizons of control. For the runway-26L configuration of figure 6, the western routes (DRAKO and BYSON) are the long approach routes, and the eastern routes (KEANN and KIOWA) are the short approach routes.

The delay data plotted in figure 7 were obtained from simulation runs with a traffic arrival rate equal to the measured runway arrival rate (35 aircraft per hour) for a traffic sample of large and heavy aircraft using IFR 3/4/5 n.mi. separations and a metering-fix time-error standard deviation of 30 sec. Since the horizon of control is defined as a fixed time from the metering fix for all routes, the sequencing scheme (projected first-to-reach-runway ordering) in some aircraft-delay cases imposes longer en route delays to aircraft on the shorter terminal routes. The result is longer overall average delays for the shorter routes when operating at or near the system acceptance rate. Therefore, for the conditions simulated, the

short-route delay requirement is the limiting case which will be used to define the desirable horizon-of-control boundary. The plotted values indicate that average en route delays are not significantly influenced by the value of horizon of control.

Also shown in figure 7 are the contours of delay possible by speed reduction to Mach 0.63 from a range of initial cruise speeds. The en route delay capabilities were determined using the trajectory computation procedure of reference 6. The plotted values are the difference in the travel times of a Boeing 737 (B-737) aircraft flying two different trajectories (similar to that of fig. 4) from the same initial x, y location at 35 000 ft altitude and at the same initial designated Mach cruise speed. In the first trajectory, the aircraft cruises at 35 000 ft and the designated Mach number until the computed time when it performs a designated-Mach/265-knot CAS clean-configuration, flight-idle-thrust descent. Upon reaching 19 500 ft, the aircraft maintains constant altitude in order to reduce its airspeed to 250 knots as the metering fix is crossed. In the second trajectory, the aircraft immediately slows to the cruise Mach number of 0.63 and maintains 35 000 ft until the time to begin its descent. At the computed time, the aircraft performs a Mach 0.63/250-knot CAS flight-idle-thrust descent in order to cross the metering fix as the aircraft reaches 19 500 ft. The time difference between the two trajectories is the amount of delay between the selected horizon of control and the metering fix achievable by speed reduction from the initial cruise speed to Mach 0.63.

Both the horizon of control and initial cruise speed clearly have a strong effect on the amount of delay possible by speed control. The nominal cruise speeds of commercial aircraft vary with aircraft type as well as policies of the individual airlines. Using the Mach 0.78 data as a sample cruise speed case, a horizon-of-control boundary of 27.5 min (fig. 7) from the metering fix is enough so that speed control will handle all the simulated en route delays that are less than the expected delay plus 1σ (approximately 84 percent of the delay cases if the distribution is Gaussian). If the criterion is the ability to handle all delay less than the expected delay plus 1.28σ (90 percent of delay cases), the horizon of control would be 30.2 min. The 1.65σ (95 percent of delay cases) criterion would place the horizon of control at 32.7 min.

Just as changing the horizon of control had a slight effect on the aircraft average en route delay, there is a corresponding effect on the terminal delay which may have to be considered. From the moment an aircraft is scheduled at the horizon of control and begins its flight toward the metering fix, there are schedule changes that occur as a result of both the metering-fix time errors of the preceding traffic and flight technical (path and response time) errors inside the terminal. The SLT is updated as a result of metering-fix time errors of the preceding traffic. However, the continual SLT slippages, caused by the terminal flight technical errors of the preceding traffic, are not always accounted for by the TIMER algorithm while the aircraft is still in the en route region between the horizon of control and the metering fix. The rationale is that the time controllability inside the terminal area will be used to deliver the aircraft to their updated SLT's rather than constantly making minor adjustments to the metering-fix scheduled time while flying in en route airspace. Consequently, when an aircraft arrives at the metering fix, its SLT could have been shifted from the earlier assigned landing time, which originally established the metering-fix target time. The longer the flight time from the horizon of control to the metering fix, the more the SLT is likely to have shifted and to result in longer terminal delay. Figure 8 shows this effect.

The delay results differ slightly from those shown in figure 7 of reference 10. In the simulation runs of TIMER in reference 10, the effect of terminal-area dynamic SLT slippage of the preceding aircraft was never added to the metering-fix target time. In the data of this report, the accumulated dynamic slippage since the originally scheduled SLT is sometimes added to the metering-fix target time of an aircraft. Specifically, this updating only occurred on those occasions when the metering-fix target time was pushed back (delayed) as a result of a metering-fix error by a preceding aircraft.

A TIMER goal is to use fuel-efficient speed control as much as possible inside the terminal as well as en route. What is needed is a horizon of control that is large enough to handle most of the expected en route delays and yet does not impose terminal-area delays that exceed the terminal speed-control and path-stretching capability. In figure 8, the measured mean expected terminal-area delays, plus their pooled σ about the fitted curve, are shown as a function of horizon of control for the same traffic and error conditions that existed in figure 7. Also shown are the boundaries of speed-control delay capability within the terminal area of the nominal routes and the combined speed and path delay capability using the maximum delay routes of the final-approach region shown by the longest-path dashed lines of figure 6. For the range of simulation conditions studied, and using the current schedule adjustment algorithm, the data indicate that no upper boundary was imposed on the horizon of control by terminal delays resulting from the terminal area SLT dynamic shifts.

Figure 9 shows the same information as figure 7 but for a traffic arrival rate equal to the runway acceptance for a 2/3/4 n.mi. separation criterion. The two cases shown in figures 7 and 9 span the range of separations likely to be used in the foreseeable future. For the same initial speed conditions, the horizon-of-control boundaries are less than for the larger separation conditions of figure 7. Using the same initial Mach 0.78 example, the horizons of control needed with the 2/3/4 separation are 24.5 min for mean delay plus 1σ (84 percent of delay cases), 26.2 min for 1.28σ (90 percent of delay cases), and 28.5 min for mean delay plus 1.65σ (95 percent of delay cases). Figure 10 may be used to verify the situation observed in figure 8. There is no upper horizon-of-control boundary imposed by the terminal area within the range of conditions simulated.

Figures 7 and 9 reveal several factors that an ATC system designer must consider in selecting the design value for horizon of control. Clearly, aircraft cruise speed is an important factor. A representative weighted, expected nominal cruise Mach number must be determined from expected airline company operational policies and projected aircraft types. The terminal-area separation standard to be used must also be considered. Slower cruise speeds, which were more widely used during the energy shortage to conserve fuel, require a larger horizon of control, but reduced separations tend to reduce the required horizon-of-control time. Without the benefit of detailed aircraft type or operational policy projections, a working number of 30 min for the horizon of control appears reasonable. This translates to about 220 n.mi. for an aircraft cruising at Mach 0.78 at 35 000 ft, no wind, then descending and crossing the metering fix at 250 knots.

6.2 Metering-Fix Delivery Accuracy

It is described in section 4.0 how, in concept, the aircraft would be delivered by en route control to the four metering fixes or corner posts with a target time which is computed to meet the scheduled landing time. This process is simulated in the TAATM by assigning the aircraft to appear at the metering fix at the scheduler-calculated target time plus a statistical time error to represent delivery error. The metering-fix time error was picked from a normal distribution with a mean of zero and a specified variance. Depending on the magnitude of sign (early or late) of the metering-fix error, and operating within the boundaries of terminal controllability, the scheduler attempts to minimize the schedule slippage of the following aircraft stream. The result is that under certain circumstances an aircraft at the metering fix may have its place in the sequence changed to reduce capacity loss caused by its metering-fix time error.

When aircraft arrive at the metering fix earlier than their scheduled time, the application of time delay is used to preserve the schedule first by speed reduction and then by path stretching, if necessary. In figure 6, the nominal approach routes are shown by the solid lines, and the region of path-distance variability is shown by the dashed lines. The range of time controllability varies with aircraft type and winds aloft. Table 2 gives the range of terminal controllability for each approach route, without wind, for a B-737 aircraft. In a similar manner, the ability to recoup late arrival errors depends on the time catch-up or forward-schedule-slippage capability of the various routes. The eastern (short) routes (KEANN and KIOWA) have only about 18 sec of catch-up capability, relative to their nominal paths, while the western (long) routes (DRAKO and BYSON), because of their "trombone" configuration, have approximately 88 sec.

Table 2. Speed and Path Time Control of Terminal Approach Routes for B-737 Aircraft

Routes	Delay control, sec		Catch-up control, sec
	Speed	Speed and path	Path
KEANN	44	114	18
KIOWA	38	106	17
BYSON	73	237	87
DRAKO	71	237	89

Figures 11 and 12 show the terminal traffic flow patterns for metering-fix arrival-error standard deviations of 30 sec and 120 sec, respectively. Figure 12 illustrates greater use of both path reduction and stretching, relative to the nominal route, than does figure 11; this greater use is an attempt to accommodate the larger metering-fix arrival errors.

The following factors determine what runway arrival-rate loss, if any, results from a metering-fix time error: the route the aircraft is on, the route and SLT's of adjacent aircraft in the sequence for swapping, and the magnitude of the metering-fix error itself. Figure 13 indicates the cumulative effect of these factor interactions. The figure presents the runway arrival rate for three separation standards plotted as a function of various metering-fix arrival-time-error standard deviations. For an en route/terminal coupled, time-based, flow-control system with the conventional geometry simulated, the

plot suggests that en route metering-fix delivery-error standard deviations should be kept to less than a number somewhere between 35 and 45 sec to realize full runway capacity. This is consistent for all the separations simulated. The TIMER system uses the time controllability inside the terminal region to prevent the smaller metering-fix errors from adversely affecting runway capacity. Figure 14 confirms that metering-fix delivery-error standard deviations of less than 45 sec show no significant capacity loss at different runway delivery errors or at different separation criteria.

Keeping the metering-fix delivery-error standard deviation below 45 sec implies the need for ground or airborne assistance to the controller, since the manual performance in today's en route metering environment (ERM-1) is from 1 to 2 min (ref. 11). The controller aids described in section 4.0 would provide the ground assistance to improve the delivery performance of aircraft without 4D capability. The TIMER concept uses representative point-mass models of aircraft to calculate, and then indicate to the controller, the Mach cruise speed, the time or distance to start the descent, and the Mach/CAS flight-idle-thrust descent speed to be issued to the flight crew in order to meet the scheduled metering-fix time. Experiments conducted from the cockpit of commercial airlines (ref. 12), with a simple model and similar open-loop commands, have shown that a delivery error at a metering fix of less than 45-sec σ is readily achievable in real-world operational conditions.

Aircraft with 4D, closed-loop guidance could arrive at the metering fix with time-error standard deviations of considerably less than 45 sec (refs. 11 and 13 to 16). However, for the type of terminal-area control and geometry simulated, figure 13 shows that increased precision at the metering fix would do little to improve the arrival rate. On the other hand, the differences in the runway arrival rate for the various runway delivery-error curves of figure 14 indicate that reducing the time error as much as possible is desirable at the runway threshold. These results taken together indicate that 4D flight-management-system designers should use a time-accuracy criterion which reduces as the remaining time or distance to the runway decreases.

6.3 En Route Delay Discounting

As shown in the previous section, runway capacity is influenced by large arrival-time errors ($\sigma \geq 45$ sec) at the metering fixes. The primary factor in this relationship is late arrivals at the eastern or short-route metering fixes (KEANN and KIOWA). Whereas late arrival times at the long approach route metering fixes (BYSON and DRAKO) can generally be made up by shortening the downwind leg of the approach, the geometry of the short approach routes allows very little catch-up capability (table 1). Therefore, there is a slippage of schedules and subsequent gaps of excessive separation on final approach.

Some of the schedule disruptions caused by large metering-fix arrival-time errors can be smoothed out by using a technique called delay discounting. This technique, applied between the horizon of control and the metering fix for the aircraft to be delayed, reduces any calculated en route delay needed to meet its target metering-fix time by some specified amount. As implemented, the specified amount of delay discounted en route to all four metering fixes is a constant percentage of each particular route's terminal speed-control delay capability between the metering fix and the runway. The aircraft's terminal path-stretching capability to achieve time delay is not considered for discounting purposes but is kept in reserve to accommodate errors and uncertainties. For example, aircraft that had delay discounting applied and arrived on time at their metering fix without an assigned landing-time change can expect a delay in the terminal area that is equal to the discounted or postponed amount. Early arrivals at the metering fix are kept on schedule by first using any remaining speed-control delay capability not used to accommodate the delay discounting and then by path stretching.

The discounting benefit results from having been applied to late-arriving aircraft at the metering fix, particularly the short approach routes. The effect of these late-arriving aircraft is reduced, since the limited time-catch-up capability is only needed when the aircraft's metering-fix overdue time error is larger than the amount of en route delay that was discounted or postponed. Thus, the schedule impact caused by larger, late, metering-fix time errors on the short approach routes is reduced.

Parametric data runs were made using 0, 30, 50, 70, and 100 percent of terminal speed-control capability for en route delay discounting and 30, 90, and 120 sec for the metering-fix arrival-error standard deviations σ. The results of these data runs are presented in figure 15 and show the runway arrival rate as a function of the upper boundary (percentage of terminal speed control) available for discounting when en route delay was needed. For a 30-sec metering-fix-error σ, delay discounting had no capacity effect. The 30-sec-σ case represents full runway capacity (fig. 13). Therefore, the difference between the 30-sec-σ plot and the values plotted at zero-percent discounting in figure 15 for the 90- and 120-sec cases depicts the capacity lost because of metering-fix errors. The plots indicate that a full

100-percent discounting recovers about half of the capacity loss due to metering-fix arrival errors with large standard deviations. If the system were to operate without any en route controller aids to improve the metering-fix delivery precision of non-4D aircraft, then delay discounting should be considered. However, if an enhanced en route system and 4D aircraft are able to restrict metering-fix-error standard deviations to approximately 45 sec or less, there is no capacity benefit to be gained by delay discounting.

When the metering-fix delivery-error standard deviation is 30 sec, the decrease in average en route delay is matched by an equal increase in average terminal delay as the percentage of delay discounted is increased from 0 to 100 percent. That situation is illustrated in figure 16. Since there is no capacity gain for metering-fix delivery-error standard deviations below about 45 sec, delay discounting should not be used; higher altitude en route speed-reduction delays are more fuel-efficient than speed-reduction delays of the same length taken at terminal altitudes. As would be expected, since delay discounting improved the capacity for the 90- and 120-sec metering-fix delivery-error cases, the reduction in average en route delay is greater than the corresponding increase in average terminal delay when delay discounting is applied to a traffic sample of 35 aircraft per hour. Figures 17 and 18 illustrate this significant reduction in average en route delay at the expense of a slight average increase in terminal-area delay.

6.4 Final-Approach Delivery Performance

6.4.1 Relation of Separation and Delivery Precision

The TIMER scheduler adds a delivery-error-dependent interarrival-time buffer to the minimum permitted separation time (distance separation standard converted to time) on final approach to keep separation violations to a low probability level. The scheduled time separation between two aircraft is illustrated in figure 19. The time relation between single-aircraft delivery precision and the buffer added to keep violations between aircraft pairs below 5 percent is defined as follows:

$$\sigma_{RI}^2 = \sigma_{RD_1}^2 + \sigma_{RD_2}^2 \quad (1)$$

$$T_B = 1.65\sigma_{RI} \quad (2)$$

where

σ_{RD_1} runway delivery-error standard deviation of the first of two successive aircraft

σ_{RD_2} runway delivery-error standard deviation of the second of two successive aircraft

σ_{RI} aircraft-pair runway interarrival-error standard deviation

T_B buffer time added to minimum separation because of delivery uncertainty

6.4.2 Runway Arrival-Rate Sensitivity to Delivery Precision

Runway arrival rate is shown in figure 20 as a function of aircraft-pair interarrival-error standard deviation at the runway threshold for the three separation standards defined in section 5.3. Since 4D FMS performance is normally given in terms of single-aircraft delivery-error standard deviation, that axis was included in figure 20 for comparison. The pair interarrival-error σ is $\sqrt{2}$ times the σ of single-aircraft delivery error if Gaussian distributions are assumed. The plotted data of figure 20 were obtained under the assumption that runway occupancy time (ROT) was not a limiting factor. If current procedures of prohibiting simultaneous occupancy of a runway by more than one aircraft are adhered to, then the maximum ROT is 37.6, 50.4, and 63.3 sec for the 2/3/4, 2.5/3.5/4.5, and 3/4/5 n.mi. separation criteria, respectively (ref. 17).

As shown in figure 20, the final delivery precision has considerable affect on the runway arrival rate for the three separation criteria evaluated. However, the impact becomes even more pronounced as separations are reduced. The slope or rate of arrival-rate change increases as the separation criterion is made smaller. Because of its significant effect on arrival acceptance rate, runway interarrival-error standard deviation is used as the measure to evaluate the system effect of several parameters.

It is anticipated that when a terminal-area time-based ATC system is first introduced, many if not most of the aircraft will not be equipped with 4D guidance. Until most of the aircraft are 4D equipped, the performance of a time-based system will be constrained by the runway delivery precision achievable with non-4D aircraft. A major goal of this study is to determine where on the runway delivery precision axis of figure 20 the resultant performance of non-4D aircraft falls when operating with computer aiding for the controller. This will define the initial time-based system performance before additional airborne and ground automation are introduced.

As a point of reference, the delivery precision (interarrival-error standard deviation) of current manual control at the final-approach gate (normally 6 to 8 mi. from the runway) is about 18 sec (ref. 18). Furthermore, the delivery precision at the runway threshold is further degraded by variation in aircraft final-approach speeds as a result of varied landing weight and piloting procedure. Figures 21 and 22 show aircraft separation distributions at the outer marker (final-approach fix) and at the runway threshold. Although these data were collected under conditions of visual aircraft separations, they illustrate that final-approach-speed variations increase the spread of the separation distribution at the runway threshold relative to the speed at the final-approach fix (outer marker). One documented value of runway-measured interarrival-error standard deviation for manually vectored aircraft is 25.6 sec (ref. 19).

6.4.3 Non-4D-Equipped Aircraft With Known Expected-Final-Approach Speed

There are several parameters which directly affect the runway delivery performance of non-4D-equipped aircraft in the TIMER environment. One of the principal factors is the variability in final-approach speed, because it is highly dependent upon gross weight of the aircraft, atmospheric conditions, and piloting procedures. If the final-approach speed is known to the flow-control system, then other factors will determine the lower bounds of delivery precision. The impact of these factors such as pilot and controller response times, aircraft heading error, heading command resolution, wind velocity, wind velocity error, and piloting procedures is examined individually.

6.4.3.1 Pilot and controller response time. There is embedded in the TIMER ETA calculations an assumed time for the controller response to the computer-generated aids and the pilot response to the resultant ATC message. Clearly, a time error will be introduced if either the controller or the pilot reacts differently from the assumed time. A consistent reaction-time error will introduce a bias in the individual aircraft arrival times, but the interarrival aircraft time error will not be affected. Two aircraft that are either early or late by the same amount of time will be properly separated relative to each other; however, variability in the response time will affect the runway interarrival error.

Figure 23 shows the resultant runway-interarrival-error standard deviation as a function of the combined controller and aircraft system reaction-time-error standard deviation. The nominal combined controller and pilot reaction value used in the baseline runs was a standard deviation of 3.5 sec. This value yielded an interarrival-error standard deviation of 6.6 sec with no winds. The reaction-time variability impact on the interarrival-error standard deviation gets considerably larger for high-reaction-time standard deviations in the region above 3.5 sec.

6.4.3.2 Aircraft heading error. When an aircraft is given vector instructions in the fine-tuning region (downwind, base, and turn-to-final), the accuracy to which those vectors are followed has some effect on the runway arrival-time accuracy. The TIMER calculations are based on a trajectory made up of segments with specific headings. If the aircraft's path or flight distance differs from those used in the calculation, a time error will occur. Figure 24 shows the runway-interarrival-error standard-deviation sensitivity to aircraft-heading-error standard deviation for two wind-strength conditions (270° wind aligned with runway). Aircraft heading-error σ is not expected to exceed 6°; therefore, the heading-error effect is not a major factor. The nominal value used in the baseline runs was a heading-error standard deviation of 2°. Increasing the heading-error σ to 6° added only about 0.75 sec to the interarrival-error σ for both wind conditions shown.

6.4.3.3 Heading command resolution. The TIMER algorithm calculates a precise heading required for the aircraft to follow a desired ground track with the assumed winds. When that heading instruction is displayed and issued to the aircraft, it is rounded to a specific resolution. This rounding causes the heading-angle error to vary somewhere between $\pm 1/2$ the resolution angle. Current ATC practice is to issue vectors to the nearest 10°; however, there are situations for which a 5° resolution is used. For stable, known wind conditions and no heading error, the resolution rounding or aliasing error is a steady-state or constant value, because the final intercept ground track is fixed and, as a result, so is the exact calculated heading. For nonvarying conditions, the resolution-induced heading error causes a fixed bias in the runway delivery time of successive aircraft but does not affect the aircraft-pair interarrival error.

On the other hand, variations in the resolution rounding error, caused by factors such as changing winds, altitude, aircraft speeds, and approach path headings of different routes, affect the runway interarrival error of successive aircraft. The values plotted in figure 25 show the measured interarrival-error standard deviation as a function of heading-command resolution with a uniform distribution model of resolution rounding error for both a 2° and a 6° heading-error standard deviation from that commanded. The fitted regression curves represent

an upper boundary of the effect due to resolution rounding errors, since operational rounding errors are not as varied or random as those generated by the uniform model. Even so, the measured interarrival-error standard deviation is not very sensitive to heading-resolution-induced errors if the heading-command resolution is kept to 10° or less. For example, the error contribution that results from the 10° resolution will be between 0 and 0.9 sec interarrival-error standard deviation, depending on the extent of wind and aircraft trajectory variations.

6.4.3.4 Wind. As the curves of figure 24 indicate, the TIMER system final-approach performance is degraded by winds as well as heading and response-time errors. Figure 26 shows the measured runway interarrival-error standard deviation as a function of wind strength for aircraft heading-error standard deviations of 2° and 10°. Since the TIMER ETA calculations account for wind, the interarrival error would not be expected to change with wind strength. However, figure 26 indicates that wind strength magnifies the effect of one or more errors or uncertainities to such an extent that a slight wind-strength effect exists. For example, an increase in the surface wind from 0 to 20 knots results in an increase of 2.3 sec interarrival-error standard deviation.

In addition to the interarrival-error effect, there is a further arrival-rate reduction due to reduced ground speeds caused by the head-wind component on final approach. This reduction is characteristic of a system constrained by a distance-separation criterion as opposed to a time-based criterion. Figure 27 shows this compounding effect on the runway arrival rate. The upper curve represents the simulation arrival rate for the given wind condition but for the no-wind interarrival-error buffer value. The interarrival-error standard deviations measured were then used to adjust the separation and project the arrival rates shown by the lower curve.

Another consideration is the contribution of wind-strength error to interarrival error. This error is defined as the difference between the actual and predicted values of wind. A specific wind error will generate a different time error for two aircraft flying different approach airspeeds. The result is a wind-error-generated interarrival error. Figure 28 shows the measured interarrival-error standard deviation for various wind-strength errors for a predicted 20-knot surface head wind aligned with the runway. Unfortunately, wind-strength errors also affect the final heading vector calculation. Since a particular ground track is desired, there is an interplay between the calculated heading value, the given wind-error condition, and the heading resolution to the nearest 10°. This interplay tends to scatter the data slightly. Nevertheless, the wind-error effect is apparent in figure 28. For airport wind errors of up to 8 knots, the effect is not more than 3.4 sec on the interarrival-error standard deviation. However, for larger wind errors there is a significant increase in interarrival-error σ.

6.4.3.5 Pilot-induced variation in expected-final-approach speed. For each aircraft type, there exists a final-approach and landing speed (typically 1.3 times the stall speed) which, for the recommended flap setting, is approximately a linear function of aircraft landing weight for the range of weights normally found in transport operations. The speed-weight curves are contained in company and pilot manuals and in tabular form in the pilot's take-off-and-landing-speeds flip chart. Generally, pilots add a wind correction equal to one-half the surface head wind plus the gust value, up to a maximum of nominally 20 knots, to the indicated flip-chart speed. This resultant value is referred to as the expected-final-approach speed. However, there is some variability in the wind adjustment from pilot to pilot as well as in the precision of flying the selected final-approach speed. Other considerations are the type of terminal and traffic load as well as the increasing wind-shear concern. These latter characteristics of higher-than-expected-final-approach speed may be modeled, but some variability is inevitable.

The effect of final-approach piloting procedure was modeled by adding an additional increment of speed to the expected-final-approach speed with the assumption that the landing weight of the aircraft was known. This pilot-induced uncertain speed increment was represented by a Gaussian distribution of zero mean and specified standard deviation. Figure 29 presents measured runway interarrival-error standard-deviation sensitivity to the standard deviation of error in the expected-final-approach speed. Variability in actual final-approach speed that is different from the expected speed significantly degrades the runway delivery precision. A pilot-induced, final-approach-speed standard deviation of 4 knots would add about 3.5 sec of runway interarrival-error standard deviation to the situation when the expected-final-approach speeds, for the aircraft landing weights, were precisely flown.

6.4.3.6 Interarrival error with known expected-final-approach speed. In the terminal simulation, the variability in final-approach speed that is due to the gross landing weight of the aircraft is accounted for by varying a quantity called weight factor W_f. The approach-speed/weight/weight-factor relationship is illustrated in figure 30. Weight factor is a value normalized to the particular

aircraft type which characterizes the actual aircraft landing weight. A weight factor of 1 is equivalent to the maximum landing weight, and 0 is equivalent to the operating empty weight. Since the recommended final-approach speed is almost linear over the defined range of weight factor, a straight-line approximation to the final-approach-speed/weight-factor relation was used in the TIMER calculations. Therefore, the final-approach indicated airspeed V_a is defined by

$$V_a = V_{am} - (1 - W_f)(\Delta V_a) \tag{3}$$

where

V_{am} = Final-approach airspeed at maximum landing weight for A/C type

$\Delta V_a = V_{am}$ – Approach airspeed at A/C OEW (4)

$$W_f = \frac{\text{A/C landing weight} - \text{A/C type OEW}}{\text{A/C type max landing weight} - \text{A/C type OEW}} \tag{5}$$

and OEW is operating empty weight.

If the landing weight were available to the TIMER system, the specific aircraft final-approach speed could be estimated from parameters stored for that aircraft type and from equations (3), (4), and (5). One approach to estimating the weight would be to have expected landing weight included as part of the flight-plan information entered into the ATC system. A related technique would be to have departure weights entered and to approximate the landing weight by using the aircraft fuel-burn rate. The use of data link to convey weight, or even better, the pilot's planned final-approach speed, will be feasible when that system becomes operationally available for ATC control purposes. Before data link, a manual entry of the pilot's intended final-approach speed into the flow-control system could be used instead of estimating the expected speed. However, this could present some operational problems and additional work load, particularly to the controller.

Another ground-system method of estimating the final-approach speed would be to request each aircraft of a type to fly a specific indicated airspeed. Either a common speed plus wind correction would be agreed to by pilots and airlines and included in company manuals or it would be requested by ATC. The aircraft-type-specific airspeed would be selected to allow the heavily loaded aircraft of the class to land safely in existing wind conditions. This procedure would simplify the ground-system requirements, but would require the lighter loaded aircraft to fly faster than normal final-approach speeds. Either a mutually agreed upon common final-approach speed or an ATC requested final-approach speed is a change from current operating procedures and pilot-company acceptance would be a major issue. Other considerations such as tire-wear cost, blowout hazard, runway lengths, and exit locations would influence operational acceptance of this procedure.

If the final-approach speed is known to the TIMER system, the lower bounds of non-4D-equipped aircraft delivery precision are determined by several other factors. These factors include pilot and controller response times, aircraft heading error, heading-command resolution, wind velocity, wind-velocity error, and final-approach piloting procedure. The parametric evaluation of how these factors degrade runway delivery accuracy indicated that the runway interarrival-error standard deviation for non-4D-equipped traffic was judged to be in the region of 8 to 12 sec (figs. 23 to 26, 28, and 29) with computer aiding to the controller. By comparison the interarrival-error standard deviation of manual control is about 26 sec at the runway threshold (ref. 19). Using the same 5-percent-violation criterion defined in section 6.4.1, the improvement of computer aiding over the manual system would theoretically yield an arrival-rate increase in the range of 16 to 25 percent when operating in an arrival-only mode under either the 3/4/5 or 2.5/3.5/4.5 n.mi. separation criteria.

6.4.4 Non-4D-Equipped Aircraft With Unknown Expected-Final-Approach Speed

In today's operational environment, the weight, and thus the expected-final-approach speed of a specific aircraft, is not known to the ATC system. Flying the last 5 or so miles at a different speed from that assumed introduces a time error to the runway-threshold crossing time. In section 6.4.3.6 with known landing speed, the overall expected interarrival-error standard deviation was judged to be between 8 and 12 sec. Clearly, if the expected-final-approach speed is an unknown variable value, an additional degrading of the delivery precision results. The questions are how much reduction in delivery precision results if the expected landing-weight speed is unknown, how significant is this effect, and should an effort be made to obtain the aircraft's landing weight?

Ten different types of transport aircraft (Boeing and McDonnell Douglas) were simulated in the arrival traffic. The values of their possible approach-speed variations are shown in table 3. These approach-speed variations were compiled after consulting a number of sources such as *Jane's All the World's Aircraft, Aviation Week's* commercial transport table, and airline operation manuals. In making the time calculation, when the aircraft's actual

landing weight or expected-final-approach speed was not known, the procedure used was to choose the speed value corresponding to the mean of the weight-factor distribution. Traffic samples with a mean weight factor of 0.5 and various standard deviations were created to obtain their impact on interarrival delivery precision.

Table 3. Final-Approach-Speed Differential Due to Weight Variability of Simulated Aircraft

Aircraft designation	Final-approach-speed differential, knots
B-720F	14
B-727	30
B-727-200	32
B-737	32
B-747	30
DC-8	26
DC-8 (60, 70 series)	30
DC-9 (10, 20 series)	35
DC-9 (30 80 series)	31
DC-10	25

Figure 31 shows the measured interarrival-error standard deviation as a function of weight-factor standard deviation. Under the conditions simulated, operating with unknown expected-final-approach speeds had a considerable effect on measured system interarrival error for landing-weight-factor standard deviations greater than 0.075. That being the case, a key issue is whether the operational weight factor spreads for transport aircraft are likely to have a standard deviation greater than 0.075.

Figure 32 presents the probability distribution of weight factors for all arriving B-737-200A aircraft of a major U.S. carrier landing at Chicago's O'Hare International Airport (ORD) between January 1, 1986, and April 30, 1987. The mean weight factor for the B-737-200A was 0.435, and the standard deviation was 0.176. Figure 33 presents the same information for that carrier's B-737-200 aircraft. The mean weight factor for the B-737-200 was 0.541 with a standard deviation of 0.196. While these distributions may not represent all situations, the fact that it is a major carrier means its distribution characteristics have a significant impact on total-population statistics.

Based on the available weight data, operational weight-factor standard deviations greater than 0.075 are indeed likely to be encountered. In fact, the weight-factor standard deviations are probably in the range of 0.15 or higher. That means that operating without aircraft-specific landing-speed knowledge substantially increases delivery error at the runway. Figure 31 indicates that the increase in interarrival-error standard deviation is between 6 and 10 sec, depending on the actual weight factor or final-approach-speed spread.

Figure 34 shows a comparison of the measured runway interarrival-error standard deviation for situations with the expected-final-approach speeds known and unknown to the TIMER algorithm. The weight-factor distribution of the input traffic had a mean of 0.5 and standard deviation of 0.15 for both cases. Arriving at a single number to characterize the effect of unknown final-approach speed is not straightforward; the interarrival error depends on several contributing factors, some of which are interactive (i.e., not independent) with the knowledge of final-approach speed. Therefore, root-sum squaring of the effects is not proper.

The overall interarrival-error standard deviation was judged to be from 16 to 20 sec if the final-approach speed were unknown to the flow-control system. This range was arrived at by selecting the medium value, 8, from the 6 to 10-sec increase in interarrival-error standard deviation due to the weight-factor effect on final-approach-speed variation. Further support for an 8-sec degrading effect emerges from the delivery-precision values achieved during manual control. There is about an 8-sec difference between the 18-sec standard deviation at the final-approach fix (ref. 18) and the 25.6-sec standard deviation at the runway threshold. If an interarrival-error σ of 8 to 12 sec from section 6.4.3.6 is used to represent the TIMER performance with known final-approach speed, degrading these values by 8 sec results in an interarrival-error σ of 16 to 20 sec.

Using the interval of 8 to 12 sec as the runway interarrival-error σ with expected-final-approach speeds known, a degrading of the σ to an interval between 16 and 20 sec represents about a 10-percent loss in arrival capacity. This magnitude of difference in arrival rate suggests that if an operationally feasible approach to obtaining final-approach speeds exists, it should be pursued. Some possible techniques were discussed in section 6.4.3.6.

6.4.5 4D Flight-Management System

Studies and flight-test programs have shown that aircraft equipped with an advanced 4D flight management system (FMS) can achieve delivery precisions of 5 sec or less standard deviation (refs. 10, 12, 14, and 15). Figure 35 shows the runway arrival rate as a function of unequipped aircraft runway delivery error for various levels of 4D-equipped

aircraft. The curves were obtained by a process of mathematical extrapolation, using data from the 2.5/3.5/4.5 n.mi. separation curve of figure 20, with an assumed delivery-error standard deviation for the 4D aircraft of 4.3 sec. The 4.3 sec was a plotted point on the single aircraft delivery standard-deviation axis of figure 20 and is compatible with the referenced 4D FMS performance.

The analysis was made assuming that average interarrival time is the result of the following factors: (1) Separation standard, (2) Arrival gaps due to system inefficiency, and (3) Added interarrival buffer to handle delivery uncertainty. Since arrival rate is the reciprocal of the average interarrival time, the combined value of the first two factors was determined from the figure 20 data to be 39.7 aircraft per hour. Holding the value of the first two factors constant, the arrival-rate effect of a new weighted buffer was extrapolated. The weighted-buffer time T'_B used in the revised average interarrival time was calculated by using equations (1) and (2) and the following expression:

$$T'_B = \sum_{j=1}^{2} \sum_{i=1}^{2} T_{B,ij} P_i P_j \qquad (6)$$

where

T'_B	weighted-buffer time
$T_{B,ij}$	buffer time defined in equation (2) for aircraft pair ij
P	probability that aircraft is either 4D equipped or non-4D equipped depending on values of i and j
i	first aircraft of a pair
j	second aircraft of a pair
1	designates a 4D-equipped aircraft
2	designates a non-4D-equipped aircraft

Figure 35 indicates that even if the final-approach interarrival delivery error for non-4D-equipped aircraft is reduced with computer aiding to about 10 sec (7.1 sec single A/C delivery error), there is some incremental capacity gains (theoretical 8-percent gain for 100-percent equipage) to be obtained by using 4D flight-management systems with the accuracies assumed.

6.5 Final-Approach-Region Geometry

It was postulated in sections 6.2 and 6.3 that metering-fix errors and delay discounting affected capacity primarily because of the limited time catch-up or forward-schedule-slippage capability on the two short approach routes. To test this hypothesis, the final-approach geometry was modified in the simulation as shown in figure 36. The dashed lines show the shorter minimum paths obtained by relocating the final-approach fix for runway 26L to a distance of 3.5 n.mi. rather than the normal 5.5 n.mi. from the runway threshold. The revised configuration increased the forward-schedule-slippage capability of the short routes from about 18 sec to about 31 sec. The forward-schedule-slippage capability of the long routes was increased from about 88 sec to about 160 sec. The delay capability remained virtually the same as shown in table 1.

Figure 37 is a comparison of the arrival rate between the nominal and new geometry under three metering-fix delivery-error conditions. The result of the revised geometry was a slight increase of about 1 aircraft per hour for the 3/4/5 n.mi. separation standard. This suggests that the increase in the forward-schedule-slippage capability, particularly on the short approaches, slightly improves the ability of the scheduler to accommodate metering-fix late arrivals.

The improvement for the large metering-fix delivery-error conditions might be expected to be more dramatic than for the 30-sec delivery-error case. However, the forward-schedule-slippage improvement of the revised geometry for the shorter routes was only about 13 sec. If some technique were possible to give considerably greater forward-schedule-slippage capability, it seems likely that the capacity improvement at larger metering-fix delivery-error values would have been greater. Such a result would reduce the sensitivity to metering-fix delivery error and would make the curves of figure 13 even flatter. Although current operational considerations restrict the shortening of the common final-approach path, the implementation of the microwave landing system (MLS) may allow a reconsideration of the constraints (ref. 20). Designing as much time catch-up capability as possible in the short routes and delay discounting if aircraft are likely to have considerably larger than 30-sec metering-fix errors are techniques that the ATC system designer can use to reduce the short-route limitation of the conventional four-corner-post terminal geometry.

7.0 Major Results and Concluding Remarks

A study was conducted with the broad objective of defining and evaluating a time-based air traffic control (ATC) concept TIMER (traffic intelligence for the management of efficient runway scheduling). The TIMER system provides the basis for an

evolutionary transition from today's manual separation-based ATC to a future, automated, time-based ATC system with most aircraft capable of using onboard 4D flight guidance to meet their respective scheduled times. The TIMER concept integrates en route metering, fuel-efficient cruise and profile descents, terminal sequencing and spacing, and computer-generated controller aids to fully use runway capacity and to improve the efficiency of delay absorption in extended-terminal operations (en route approach, transition, and terminal flight to the runway).

A fast-time parametric sensitivity evaluation of the basic extended terminal-area flow-control concept with non-4D-equipped aircraft was performed using a four-corner-post, runway-26L configuration at Denver's Stapleton International Airport with commercial instrument flight rule (IFR) arrival traffic. The results of this study identify and show the effects and interrelationships of key system variables. The following is a summary of the major findings:

1. A parameter of interest is the horizon of control (i.e., the sequencing and scheduling boundary) which, if chosen properly, would enable most of the delays that are needed to derandomize arrivals to be taken en route using cruise speed reduction and fuel-efficient profile descents. The desired value of horizon of control depends on the separation standard in use and the airline nominal cruise speeds. The data indicate that a value of 30 min to the metering fix is a reasonable number to use in the design of an extended-terminal flow-control design.

2. Data runs indicate that the en route delivery error at the metering fix should be kept to a standard deviation less than 45 sec to realize full runway capacity. Time precisions at the final-approach fix and at the runway are critical to capacity, but the impact is considerably less at the metering fix. The system is more robust (tolerant) to metering-fix errors because of the speed and fine-tuning control capability within the terminal area. This tolerance implies that the delivery precision design criteria for a 4D flight management system (FMS) at the metering fix could be relaxed from the potentially achievable value of 5-sec standard deviation. Limiting the metering-fix delivery-error standard deviation to 45 sec or less indicates the need for automated controller aids in the process of controlling aircraft without 4D capability. The current manual performance in today's en route metering environment (ERM-1) is on the order of 1 to 2 min.

3. Delay discounting, or postponing the execution of some of the en route delays because of runway scheduling until the aircraft arrive in the terminal area, was shown to be beneficial in reducing the capacity loss of metering-fix delivery-error standard deviations greater than 30 sec. If no en route controller aiding is used, delay discounting should be applied. However, if automated advisories and 4D-equipped aircraft reduce the metering-fix-error standard deviation to about 30 sec or less, as expected, no delay discounting should be used. The rationale is that taking delays en route is more fuel efficient than taking them within the terminal area.

4. As expected, the TIMER concept capacity is sensitive to runway delivery precision, because a delivery-error-dependent time buffer is added to the time separation to keep separation violations to a low probability. The IFR capacity of a first generation time-based system, such as TIMER, will be constrained by the delivery precision achieved with aircraft not equipped with 4D guidance. Assuming that the expected-final-approach speeds of all aircraft are known, there are several other factors which will determine the lower bounds of delivery precision, such as pilot and controller response time, aircraft heading error, heading command resolution, wind effects, and final-approach piloting procedure. A fast-time parametric evaluation of these factors indicates that, with computer aiding to the controller, the runway-interarrival-error standard deviation for unequipped traffic could be reduced to the region of 8 to 12 sec from the approximately 26 sec that is typical of the current manual control system. In an "arrival-only" runway configuration, that precision improvement would ideally translate to an increase in the range 16 to 25 percent in capacity under either the 3/4/5 or 2.5/3.5/4.5 n.mi. separation criterion.

One of the principal factors which affect the runway delivery performance of non-4D-equipped aircraft is the variability in final-approach speed as a result of varying landing gross weights. Fast-time simulations of operations, without aircraft-specific expected-final-approach-speed knowledge, indicate that the overall runway interarrival-error standard deviation would be between 16 and 20 sec. This represents about a 10-percent less arrival capacity than when final-approach speed is known. These results indicate that developing an operational process to determine aircraft landing weights or expected-final-approach speeds plays an important part in the establishment of a precision delivery time-based ATC system.

The introduction of 4D flight management systems into a time-based ATC system such as TIMER offers further incremental increases in capacity with increases in fleet equipage. With 100-percent equipage, the arrival capacity is theoretically about 8 percent greater than with the non-4D-equipped case, even when the expected-final-approach speed

is known. It should be noted that all the calculated gains mentioned previously are under conditions with separation distances rigidly defined and adhered to.

5. It was postulated that large, late-arrival time errors at the metering fixes have more impact on capacity than early-arrival errors of equal magnitude. The reason is that the simulated four-corner-post terminal geometry has much greater delay capability to accommodate early errors than it has catch-up or forward-schedule-slippage capability to accommodate late errors. This is especially true of the two shorter routes. Shortening the minimum path length by moving the extended-runway centerline intercept 2 mi. closer to the threshold improved the capacity by one aircraft per hour. This improvement indicates that increasing the forward-schedule-slippage capability improves the flexibility of the scheduler to handle metering-fix late-arrival errors. The microwave landing system (MLS) may provide an opportunity for the time-based, terminal automation planners to design some additional forward-schedule-slippage capability into the terminal approach geometry to reduce the effect of the current shorter route limitation.

NASA Langley Research Center
Hampton, VA 23665-5225
December 21, 1988

Appendix A

TIMER Simulation Functional Description

This appendix describes the various modules of the terminal area air traffic model (TAATM) program within which the TIMER (traffic intelligence for the management of efficient runway scheduling) concept algorithms are embedded. The functional relationships and brief descriptions are presented herein.

A block diagram of the independent programs that form the basis of TIMER experiments is shown in figure A1. The components relating to real-time operation are not subjects of this report but are included in the block diagram for completeness.

Sample Generation of Aircraft Traffic

The Official Airline Guide (OAG) was used to determine a set of statistics for generating a generic aircraft traffic sample for the TAATM. The data collected from the OAG were for transport arrivals on a typical weekday at Denver's Stapleton International Airport. The data for each arriving flight include origin, airline company, and aircraft type. For these data, statistics were generated on arrival distribution to the four arrival corridors, distribution of airlines for each of the four arrival routes, and distribution of aircraft types for each airline on each route. These statistics were then used to generate a dense, 5-hr master traffic sample from which subsamples were selected for the parametric study. Statistically, the master traffic sample represents an operation rate of 2400 aircraft/hr with a Poisson distribution of the intervals between aircraft simulation entry times. Numerous subsamples were selected by specifying integer starting points and noninteger selection intervals within the master sample. At least four subsamples were chosen for each operation rate selected within the range of 18 to 60 aircraft/hr.

Description of TAATM Input Database

General

The TAATM input database consists of data necessary to describe the terminal area geometry and wind conditions, traffic control points, aircraft performance characteristics, and numerous program constants and configuration parameters. The data include flight-path segment descriptions for all defined paths; descriptions of all relevant estimated time of arrival (ETA) points, intersections, and area navigation (RNAV) waypoints; navigation and surveillance aids with characteristic error models; ATC control types, separation criteria, conflict resolution options, and communication parameters; aircraft performance tables and aircraft/pilot-error model parameters; and selectable traffic samples. Most of the array-type data are stored internally as packed integers to conserve computer memory. The input data are scaled to a desired resolution and then packed in fixed or variable field widths, depending on the type of data. Fixed-field data require three descriptors (field width, scale factor, and location within the packed array), and variable fields require four descriptors per data item. These are field width, sign indicator, scale factor, and location of field within the packed word.

Terminal Area Data

The flight paths are described by individual segments which are linked together by a path descriptor array. Each segment is described by a flight navigation mode (e.g., VOR, RNAV, vector), a terminating condition (e.g., navigation fix passage, VOR radial intercept, controller message), an altitude objective, available speed options, message type, if any, associated with the segment, and ground-track distance and heading. Nominal and optional flight paths are generated from the flight segments during control computations.

Terminal area intersections and RNAV waypoints are defined by their location and ground-track information. Several ETA points are defined to allow model performance assessment. Ground navigation and surveillance aids are defined by their locations and associated error model parameters. The database contains several sets of wind model parameters that are user selectable.

Aircraft Characteristics

Aircraft performance tables include nominal values for 20 aircraft types for several flight conditions. The tables contain climb-descent and acceleration-deceleration rates, speeds, and arrival-departure runway occupancy times. The rate and speed tables allow for variations in aircraft weight. Extensive data tables are included for flight-idle-thrust descent calculations for the major transport aircraft types. These tables include minimum and maximum weights, wing area, drag polars as a function of Mach number, and thrust data as a function of altitude and lift coefficient.

ATC Control Descriptors

Several different types of ATC control functions provide flexibility in the TAATM program. The control logic for a particular action may be time-based, such as at the horizon of control; may be

fixed geographic points, such as terminal area entry, speed control, and firm sequencing points; or may be a combination of both, such as direct course error (DICE) computations, which are initiated at specified points and then updated at regular time intervals.

The TIMER algorithms employ the following types of ATC control points as an aircraft progresses from the horizon of control to the runway:

1. Initial scheduling from the horizon of control
2. Metering-fix en route holding and departure inbound
3. Schedule maintenance (speed control)
4. Firm scheduling with optional path assignment
5. Direct course error (DICE)
6. Optional transition-speed control on final approach

Each of the control types involves ETA computations to the runway for the remaining nominal and optional flight paths, predicted-conflict detection at the runway and possibly at intermediate path intersections, and conflict resolution using specified options.

Description of TAATM Program Flow

Overall Flow

The major components of the TAATM program are database initialization, controller communications, aircraft dynamics (tracking), and ATC functions (control). The TIMER algorithms are embedded in the control section of the TAATM. Figure A2 is a flowchart of these components. After all external data are stored in common areas, the program executes at a specified integration rate, normally 4 sec, which corresponds to the aircraft surveillance radar (ASR) sweep rate. Each of the three main program modules (communications, tracking, and control) is invoked in order during each iteration step or "scan." The major enhancements that differentiate the current TAATM simulation capability from its predecessor (ref. 8) are the addition of flight-idle-thrust profile descent dynamics (ref. 6) and associated ETA algorithms for the major transport aircraft types, extensive reconfiguration of the terminal area geometry to reflect the current four-corner-post arrival corridors, and refinements to the scheduling and conflict resolution processes. The primary functions of each of the three modules are described in the following sections.

Controller Communications

The communication subprogram monitors the controller message queues and pending aircraft entry times. As the delivery times for controller-generated messages are approached, the pending-message information is changed from future to current status and inserted into the transmission flow based on a priority system. When a message transmission is completed, the appropriate aircraft data are updated, the message is documented in the primary output file, and the message is deleted from the active queue. After the message queues for all the simulated controllers are updated, the entry times of pending aircraft are compared with the current program time. As each entry time is approached, information on the aircraft is placed in the appropriate control queue for system entry.

Aircraft Dynamics (Tracking)

The positions of all aircraft within the terminal area bounded by the metering fixes are updated every scan. The tracking process includes updating the flight schedule as each flight segment is completed, computing a four-degree-of-freedom (x, y, z, and ϕ) trajectory with 1-sec integration steps over the scan interval, documentation of actual time of arrival (ATA) at specified fixes, and entry of aircraft information into control queues as criteria for generating ATC functions are satisfied. Output from the tracking subprogram includes recording the aircraft position, status, and current flight segment for each aircraft on each scan and, when an aircraft is deleted from the system, recording pertinent estimated times of arrival (ETA) and ATA data accumulated during its flight.

ATC Functions (Control)

The general concepts employed in the various TIMER control types are discussed in section 4.0 of the main text. The particular characteristics of each concept, namely the criteria for initiating the function, conflict detection points, and conflict resolution options, are concentrated on in this appendix.

In general, the sequence of events that occurs during the control process for each aircraft in the control queue is as follows:

1. Get relevant aircraft performance parameters, ATC procedure parameters, and path data from the database.
2. Compute ETA's to runway threshold (minimum, nominal, miminum speed, minimum speed/maximum path, and delayed action).
3. Compute desired scheduled landing time (SLT) based on separation criteria with respect to other aircraft.
4. Determine urgency of imposing a delay maneuver, if any, to maintain proper spacing.

5. If immediate delay action is required, step through available options (speed reduction, alternate path assignment, resequencing, hold) to resolve conflict.

6. Assign flight segments and generate messages to accomplish desired objectives.

7. Record on secondary output file the computed data used in the decision process. Some of the control types also employ procedures to maintain proper spacing at other points such as the metering fixes and flight-path intersections.

The following list summarizes the characteristics of the six types of control listed in the TAATM input database description:

1. Initial scheduling from horizon of control:

   Initiation criterion: entry time of new aircraft
   Conflict checks:
   a. Metering fix
   b. Runway threshold
   Conflict resolution option: en route delay with possible delay discounting. May generate en route delays for other aircraft because of projected "first-to-reach-runway" scheduling process.

2. Metering-fix departure inbound with optional holding:

   Initiation criterion: metering-fix arrival time
   Conflict check: runway threshold
   Conflict resolution options:
   a. Speed reduction
   b. Resequencing
   c. Delayed alternate path
   d. Hold at metering fix

3. Schedule maintenance:

   Initiation criterion: passing imaginary line through specified point
   Conflict check: runway threshold
   Conflict resolution option: speed control

4. Firm sequencing:

   Initiation criterion: passing imaginary line through specified point
   Conflict checks:
   a. Intersecting flight paths
   b. Runway threshold
   Conflict resolution options:
   a. Resequencing
   b. Alternate paths

5. Direct course error (DICE):

   Initiation criteria:
   a. Downwind leg of western routes and base leg of eastern routes: passing line through specified point
   b. Base leg of western routes: elapsed time since base leg clearance
   Conflict check: runway threshold
   Conflict resolution option: Timed reinsertion into control queue. Clearance to final approach is mandated if projected flight path crosses extended-runway centerline.

6. Optional transition speed control on final approach:

   Initiation criterion: ILS flight navigation mode
   Conflict check: desired SLT
   Conflict resolution option: reinsertion into control queue until approach gate intercept

Relationships of Subprograms

The TAATM simulation program is executed within an overlay shell structure to reduce computer central memory requirements. As shown in figure A3, the base program, TAATMFT, executes the primary overlay, TATINT, which installs the TAATM database in conjunction with the subprograms INIT and PDDATA. It then executes the primary overlay, TATMAIN, which in turn executes the secondary overlays, TATREST (internal variable and array initialization) and TATOPER (simulation control overlay).

The diagrams presented in figures A4 and A5 show the relationships of all major subprograms in the TAATM. For simplicity, the data manipulation utility subroutines such as those used to pack and unpack variables are not included. The diagrams are not intended to represent a chronological sequence of events; they are intended to show the interconnections of all routines in hierarchial order from left to right.

Subprogram Descriptions

The subprograms depicted in figures A3 through A5 are briefly described in alphabetical order as follows:

ACEPTAC: moves aircraft from traffic entry queue into active traffic of model

AHGS: computes aircraft heading and ground speed based on altitude, wind, indicated airspeed, and desired ground track; entry point in HEADSPD

AHLDSPD: assigns a holding speed for an aircraft that is scheduled to enter a holding pattern

AHTSGS: computes aircraft heading, true airspeed, and ground speed; entry point in HEADSPD

AIMALT: computes projected aim-point altitude of an aircraft flying profile descent mode

ALTMSG: develops specified controller message that assigns a new altitude to lower an aircraft in holding stack

AUTOHLD: determines if an aircraft has to hold because an aircraft ahead is in holding stack

AVGWND: computes wind impact on a segment or set of segments assigned to flight path of an aircraft

CALROC: calculates rate of climb (or descent) for aircraft in a profile descent

CCD: calculates drag coefficient

CDCD: calculates Reynolds number correction to drag coefficient for a Lockheed L-1011

CEVENT: establishes event array information and computes total elapsed time for an aircraft to fly a subsegment. An event is determined by a change of indicated airspeed, a change in altitude, or no change.

CHDGDIF: determines whether an aircraft has passed a specified point by examining relative location of aircraft's present position with respect to a perpendicular line through the specified point

CHOLDT: computes amount of time an aircraft will fly a holding pattern, given the amount of time needed to delay and information on whether aircraft is flying under IFR (instrument flight rules) or radar conditions. The initial type of turn required, the hold exit method, and the type of pattern are also taken into consideration.

CLBSBSG: calculates subsegments necessary for an aircraft to climb to a specified altitude

CNTRLAC: governs ATC functions section of TAATM model. The list of aircraft needing control actions accumulated during a scan interval is examined, and appropriate procedures are executed for each, based on the specified type of control action. Predicted separation violations between pairs of aircraft are flagged, and diagnostic information about the control action is recorded.

COMMUN: places controller messages for active traffic aircraft in transmission queues and monitors input traffic sample for entering aircraft into system

CTHRST: calculates thrust coefficient

DICESPD: generates optimal time to reduce to outer marker speed on final approach. This procedure is an optional fine-tuning mechanism to reduce runway delivery error.

DICEVEC: computes direct course error (DICE) to runway threshold for vectoring aircraft onto base and final-approach flight legs

ETACOMP: calculates flight time for a given set of segments

ETADEL: deletes an aircraft from ETA array associated with a particular checkpoint when criteria for passing checkpoint have been satisfied

ETAPASS: utilizes predetermined criteria to ascertain whether an aircraft has passed a checkpoint. A flag is set within the subroutine indicating the status of the aircraft with respect to the checkpoint.

ETAR: calculates ETA at runway

ETASAVE: makes initial entry of an aircraft into ETA arrays of information. The information is arranged chronologically with respect to runway ETA's.

ETASEPC: computes time for an aircraft to fly designated separation distances back-calculating from the ETA point and using the segment distances established in EVENT array. In this manner, desired separation distances are converted to time parameters.

FLTPSCH: detects and resolves predicted conflicts in scheduled landing times

FPINIT: performs initial scheduling at horizon of control

GRNDDST: calculates distance traveled over ground in a vector turn, including wind effects

HEADSPD: determines various parameters associated with aircraft dynamics. See AHGS, AHTSGS, and ISTS.

INIT: performs initialization of program pointers, arrays, and indicators

INITSTA: determines initial SLT based on projected first-to-reach-runway ordering at runway threshold and on other aircraft headed for same metering fix

ISTS: computes indicated airspeed and true airspeed based on observed ground speed, altitude, wind, and ground track

ISWAPF: determines desired sequence of two aircraft on different routes based on geometry of intersecting flight paths

LOCACS: locates an aircraft in an SLT/ETA array

MDELET: examines current and future message queues of a specified controller and deletes designated messages for delivery to a specified aircraft

MFALT: calculates metering-fix altitude that is required to attain desired aimpoint altitude at end of a profile descent

MFEXIT: develops terminal area schedule for an aircraft arriving at a metering fix. This subprogram may resequence and/or hold the aircraft.

MFHLDEX: determines when an aircraft can exit a hold at metering fix; entry point in MFEXIT

MLSERR: determines aircraft position offsets based on calculated microwave landing system (MLS) bias and random errors for both azimuth and slant range

MSGDEV: enables complete specification of verbal communications between controllers and an aircraft. Both general flight messages and messages which alter the flight on a segment are developed from an examination of the conditions and requirements of each segment of the aircraft's assigned flight path.

MSGORD: places messages in pending-message arrays based on transmit time and priority

MSGREC: modifies assigned flight segments of an aircraft receiving a transmitted message according to information in message

PDACEL: calculates average deceleration when changing from one speed to another at idle thrust and at a given altitude

PDCHAR: places characteristics of a specified class of aircraft in proper variables for calculating profile descent information

PDDALT: calculates time and distance required to descend in a constant calibrated-airspeed profile from a given altitude to another, taking winds into consideration, with a limit on distance. If the distance is exceeded, the final altitude attainable is returned.

PDDATA: installs part of database necessary to make profile descent calculations

PDDESC: calculates time and distance required to descend in a constant calibrated-airspeed profile from a given altitude to another

PDDSPD: calculates distance and time traveled while changing speed during a profile descent, including wind effects, with a limit on distance. The attainable speed is returned if the distance limit is inadequate for the desired speed change.

PERFTAB: unpacks the performance rates for a given aircraft class into appropriate internal arrays

PFRATE: calculates descent and deceleration rates at a given altitude, including wind effects

PWIND: computes estimated wind velocity for a given altitude

RECORD: writes output data to document a given run for later analysis

RNAVDST: examines relative location of upcoming waypoints along an aircraft's current path and computes a "turn anticipation distance" before aircraft should initiate RNAV turn to respective waypoint

RNVTURN: defines turn-profile information for an aircraft about to make an RNAV turn to an upcoming waypoint. The turn radius, turn distance, and the point on the turning arc are determined.

SBOUNDS: computes ETA's to be used as limits to set SLT's. Minimum, nominal, nominal max, and maximum ETA's are calculated.

SCHED: establishes flight segments to be added to the active schedule of an aircraft from the master flight-segment data as a result of an ATC function. For each new segment, the appropriate heading, speed, and altitude objectives are determined.

SEGCHAR: unpacks segment characteristics from master flight-segment data into appropriate internal arrays

SEGUPD: updates active schedule of an aircraft when criteria for terminating current flight segment are satisfied

SEPAHED: determines a time-separation requirement with the aircraft directly ahead of a specific aircraft flying toward the same ETA point. The separation time is based on the order of the aircraft pair and is a function of the performance classes of the pair.

SEPBHND: determines a time-separation requirement with the aircraft directly behind a specific aircraft on a given path. The separation time is based on the order of the aircraft pair and is a function of the performance classes of the pair.

SHSKED: establishes holding segments which can be flown by an aircraft to realize required holding time computed by CHOLDT

SLIPSTA: initiates schedule slippage for those aircraft which have been firmly sequenced. Runway ETA's are fine-tuned to account for minor errors as the aircraft are turned onto final approach, and unnecessary gaps between aircraft are closed. No resequencing of aircraft takes place.

SPDOPT: calculates a new airspeed to be assigned to a designated aircraft to achieve its scheduled runway threshold arrival time

STACOMP: determines desired order of aircraft in ETA queues and dynamically adjusts landing sequence and scheduled runway arrival times to account for errors and maintain adequate separation between aircraft pairs. The position of an aircraft in the landing sequence may not be changed once it has passed its firm-sequencing point.

STOREDT: stores time of day and delay time associated with an ATC function for postprocessing

TAATMFT: controls loading and execution of primary overlays of program

TATINT: installs database and traffic sample and initializes constants; primary overlay

TATMAIN: initializes arrays and output files and controls execution of simulation; primary overlay

TATOPER: directs the three main operating sections of program—communications, tracking, and control; secondary overlay

TATREST: initializes internal variables, arrays, and files. This is a secondary overlay primarily for real-time operation to initialize run-dependent variables.

TIMTOPT: calculates time to fly from current position to a point at which ETA calculations are to begin

TRACKAC: updates active traffic information on all aircraft in terminal area

TRNCAL: computes flight events associated with a turn subsegment

TRNDST: establishes parameters necessary to compute distance traveled in a vector turn

TRNSBSG: generates subsegments and events arrays to contain turn information

TRUWND: computes actual wind affecting aircraft movement; includes wind error added to predicted value; entry point in PWIND

TURNANG: calculates turn angle and direction to change from one heading to another

TURNC: computes turn information for an aircraft: turn direction, heading of aircraft, ending coordinates of turn, and turn distance

TURNDST: computes distance traveled by an aircraft in a turn

TURNTO: computes end point and distance in a turn for an aircraft making a heading change to a specified point

UPKCA: unpacks ATC function parameters into appropriate internal arrays

XY: computes intersection point of two straight lines

Output and Analysis of TAATM

Output of the TAATM consists of binary and coded files for post-run analysis. The primary file from which system performance is evaluated is the aircraft dynamics data file. This file contains the aircraft data records for each active aircraft for every scan of the simulation run, a record of each transmitted and each received controller message, a record of en route delays for each active aircraft, and a record of terminal area ETA's and ATA's at specified points of interest (metering fix, outer marker, runway threshold) for each aircraft that lands during the run. These data are then postprocessed to produce various statistics, histograms, and position plots for a specified time period within the run. Recorded output of all ATC functions performed during the run is digested separately to produce time-history plots of ETA's and SLT's for visual evaluation of system efficiency. Detailed descriptions of output and analysis files are contained in reference 21.

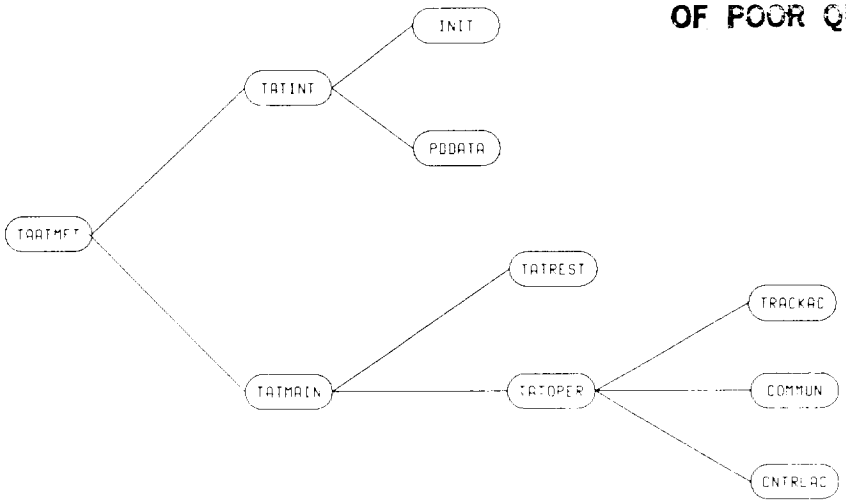

Figure A3. Functional relationships of TAATM shell.

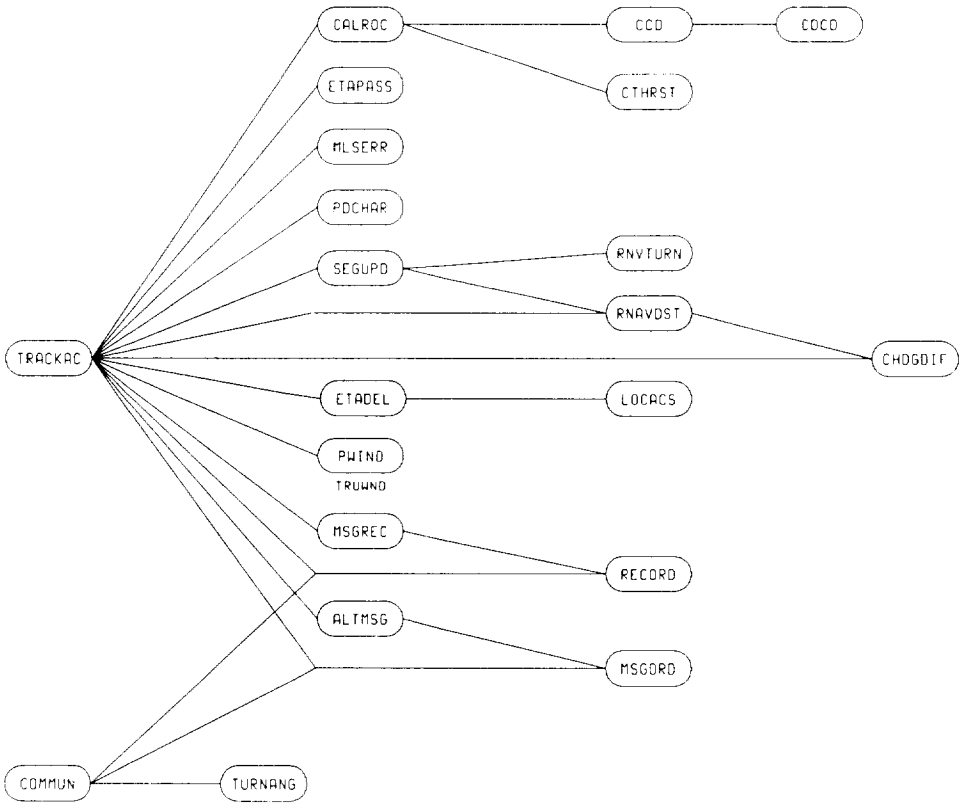

Figure A4. Diagram of aircraft dynamics and communications.

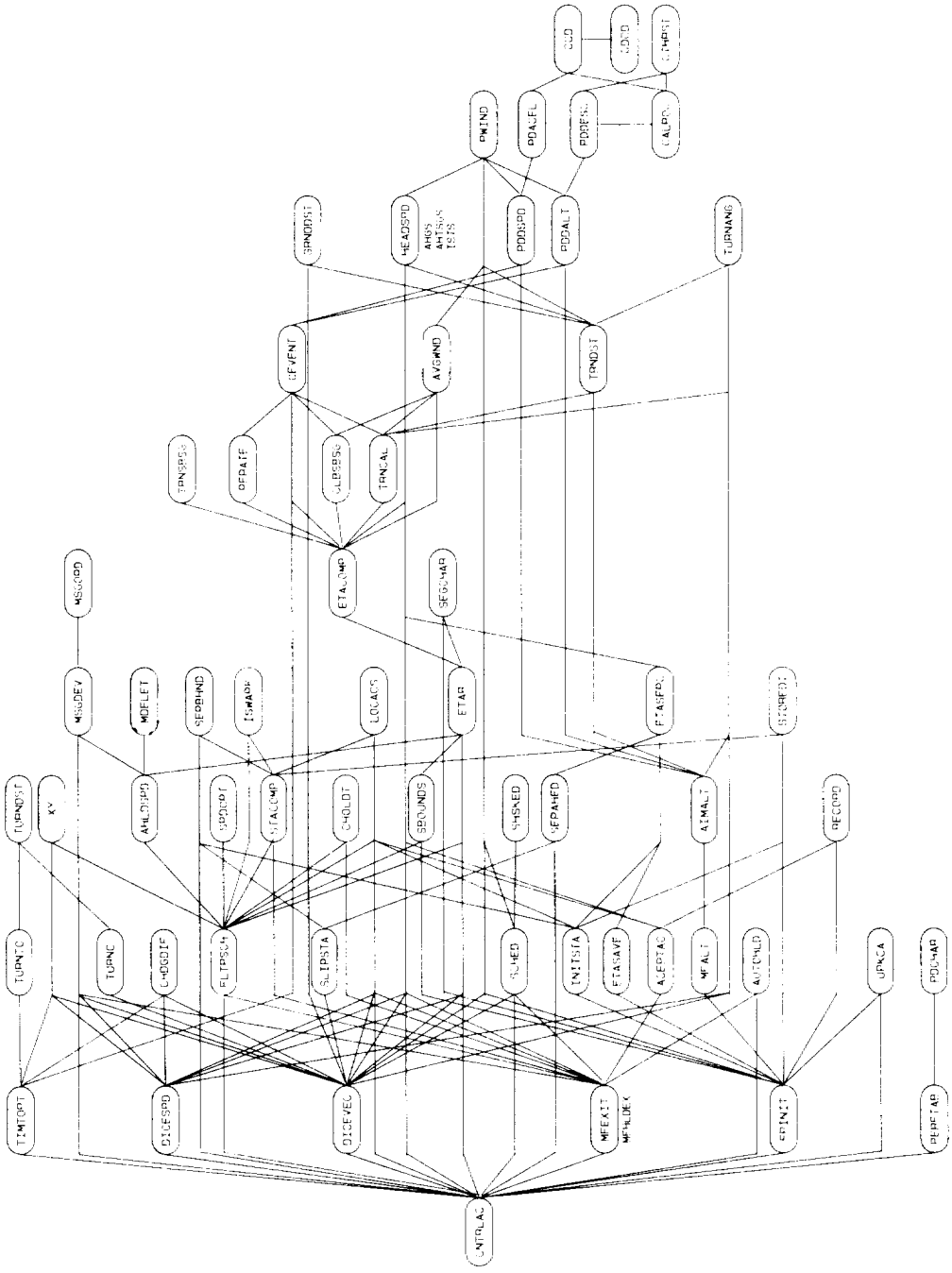

Figure A5. Relational diagram of ATC functions.

References

1. Holland, F. C.; and Garceau, T. V.: *Genealogy of Terminal ATC Automation.* M70-9, Revis. 2, MITRE Corp., Mar. 1974.
2. Benoit, Andre; and Swierstra, Sip: Dynamic Control of Inbound Flights for Minimum Cost Operation. *Air Traffic Control in Face of Users' Demand and Economy Constraints,* AGARD-CP-340, Feb. 1983, pp. 11-1–11-32.
3. Erwin, Ralph L., Jr.: Strategic Control of Terminal Area Traffic. *Plans and Developments for Air Traffic Systems,* AGARD-CP-188, Feb. 1976, pp. 3-1–3-9.
4. Groce, J. L.; Izumi, K. H.; Markham, C. H.; Schwab, R. W.; and Taylor, J. A.: *An Investigation of TNAV-Equipped Aircraft in a Simulated En Route Metering Environment.* NASA CR-178031, 1986.
5. *National Airspace System Plan—Facilities, Equipment, Associated Development and Other Capital Needs.* Federal Aviation Adm., June 1988.
6. DeJarnette, Fred R.: *Effects of Aircraft and Flight Parameters on Energy-Efficient Profile Descents in Time-Based Metered Traffic.* NASA CR-172338 and Addendum to NASA CR-172338, 1984.
7. Conte, S. D.; and de Boor, Carl: *Elementary Numerical Analysis—An Algorithmic Approach,* Third ed. McGraw-Hill Book Co., c.1980.
8. Credeur, Leonard; Davis, Christina M.; and Capron, William R.: *Evaluation of Microwave Landing System (MLS) Effect on the Delivery Performance of a Fixed-Path Metering and Spacing System.* NASA TP-1844, 1981.
9. *Air Traffic Control.* 7110.65E, Federal Aviation Adm., Apr. 9, 1987.
10. Credeur, Leonard; Williams, David H.; Howell, William E.; and Spitzer, Cary R.: Advanced ATC: An Aircraft Perspective. *Efficient Conduct of Individual Flights and Air Traffic or Optimum Utilization of Modern Technology for the Overall Benefit of Civil and Military Airspace Users,* AGARD-CP-410, Dec. 1986, pp. 43-1–43-14.
11. Heimbold, R. L.; Lee, H. P.; and Leffler, M. F.: *Development of Advanced Avionics Systems Applicable to Terminal-Configured Vehicles.* NASA CR-3280, 1980.
12. Knox, Charles E.; Vicroy, Dan D.; and Simmon, David A.: *Planning Fuel-Conservative Descents in an Airline Environment Using a Small Programmable Calculator—Algorithm Development and Flight Text Results.* NASA TP-2393, 1985.
13. Bruckner, Juergen M. H.; Benson, Fred B.; McCormick, Larry J.; and Sharpe, Tom G.: *3D/4D Area Navigation System Design, Development, and Implementation. Volume I. Main Text.* Rep. No. FAA-RD-77-79, I, July 1977. (Available from DTIC as AD A056 605.)
14. Knox, Charles E.; and Cannon, Dennis G.: *Development and Test Results of a Flight Management Algorithm for Fuel-Conservative Descents in a Time-Based Metered Traffic Environment.* NASA TP-1717, 1980.
15. Adam, V.; and Lechner, W.: Investigations on Four-Dimensional Guidance in the TMA. *Air Traffic Control in Face of Users' Demand and Economy Constraints,* AGARD-CP-340, Feb. 1983, pp. 12-1–12-11.
16. Moor, Donald A.: Time Flies—An In-Service Evaluation of a 4-D Flight Management System. *6th Digital Avionics Systems Conference,* American Inst. of Aeronautics and Astronautics, Dec. 1984, pp. 54–59. (Available as AIAA-84-2607.)
17. Swedish, William J.: *Evaluation of the Potential for Reduced Longitudinal Spacing on Final Approach.* Rep. No. FAA-EM-79-7, Aug. 1979. (Available from DTIC as AD A076 434.)
18. Haines, Andrew L.: *Parameters of Future ATC Systems Relating to Airport Capacity/Delay.* Rep. No. FAA-EM-78-8, Apr. 1978. (Available from DTIC as AD A055 482.)
19. Martin, Donald A.; and Willett, Francis M., Jr.: *Development and Application of a Terminal Spacing System.* Rep. No. NA-68-25 (RD-68-16), Federal Aviation Adm., Aug. 1968.
20. White, William F., compiler: *Flight Demonstrations of Curved, Descending Approaches and Automatic Landings Using Time Reference Scanning Beam Guidance.* NASA TM-78745, 1978.
21. Capron, W. R.; and Rodgers, W. G.: *An Operator/User Guide for the Terminal Area Air Traffic Model (TAATM) Fast-Time and Real-Time Simulation Programs.* NASA CR-165662, 1981.

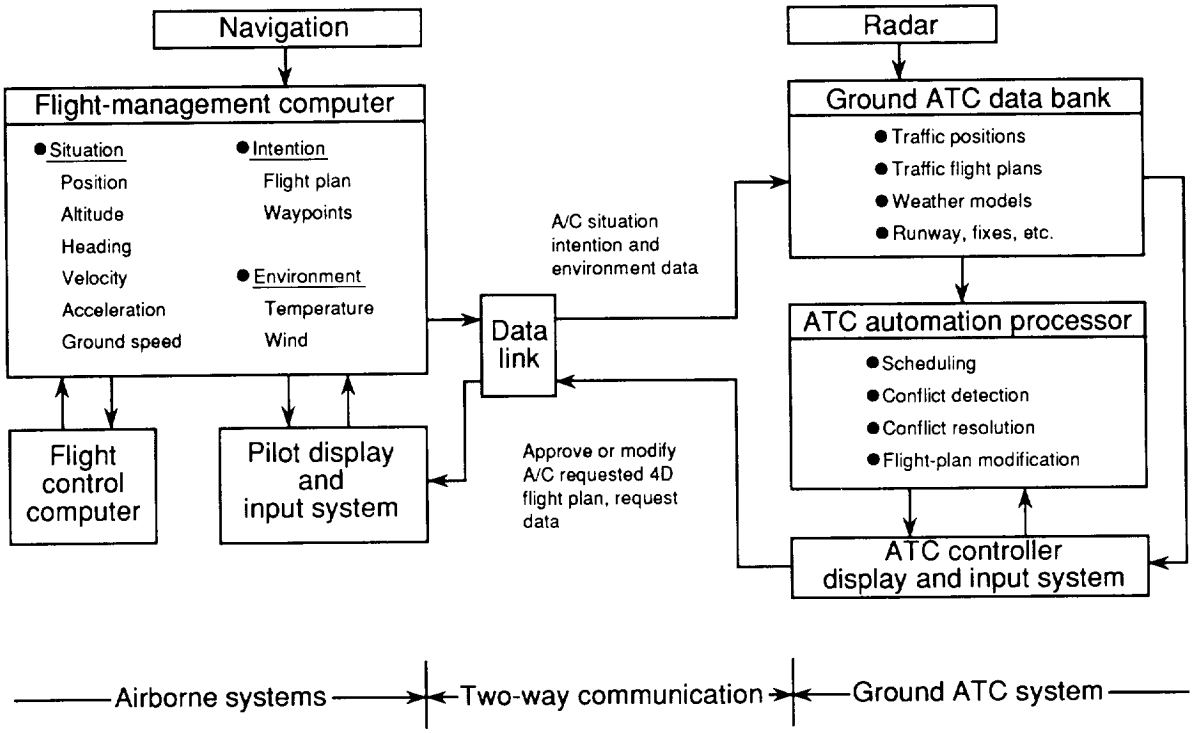

Figure 1. Possible integration of airborne capability in an advanced ground-based automated ATC system.

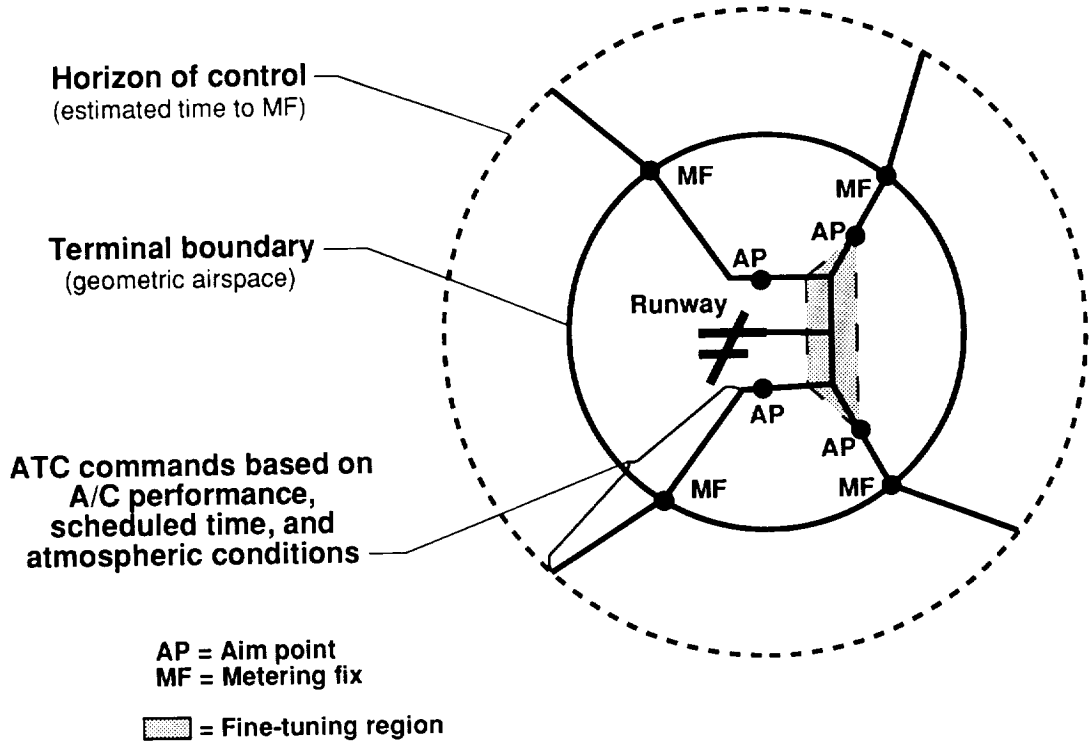

Figure 2. Principal features and areas of operation of TIMER concept.

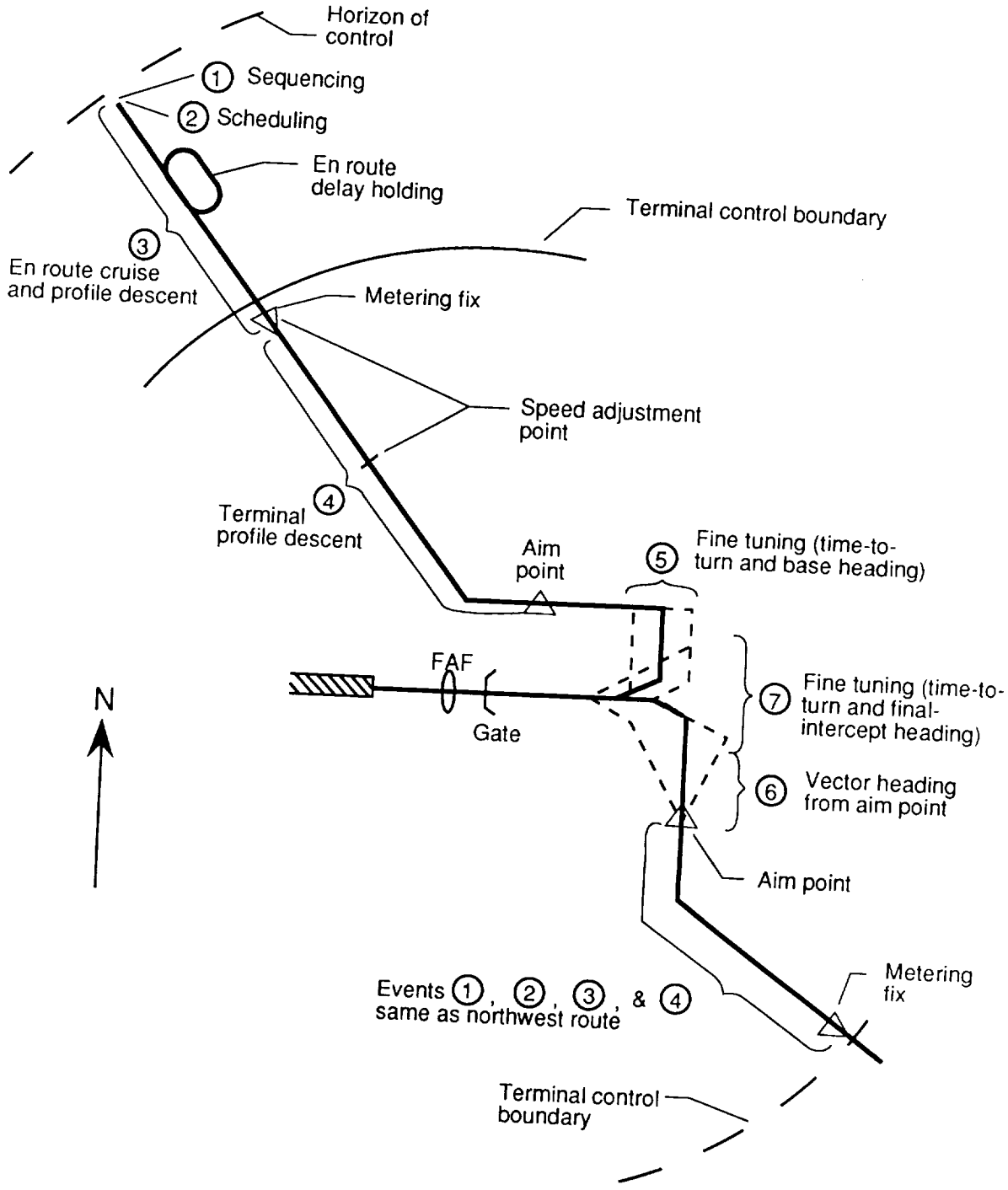

Figure 3. Sequence of events an arrival aircraft would experience in TIMER concept.

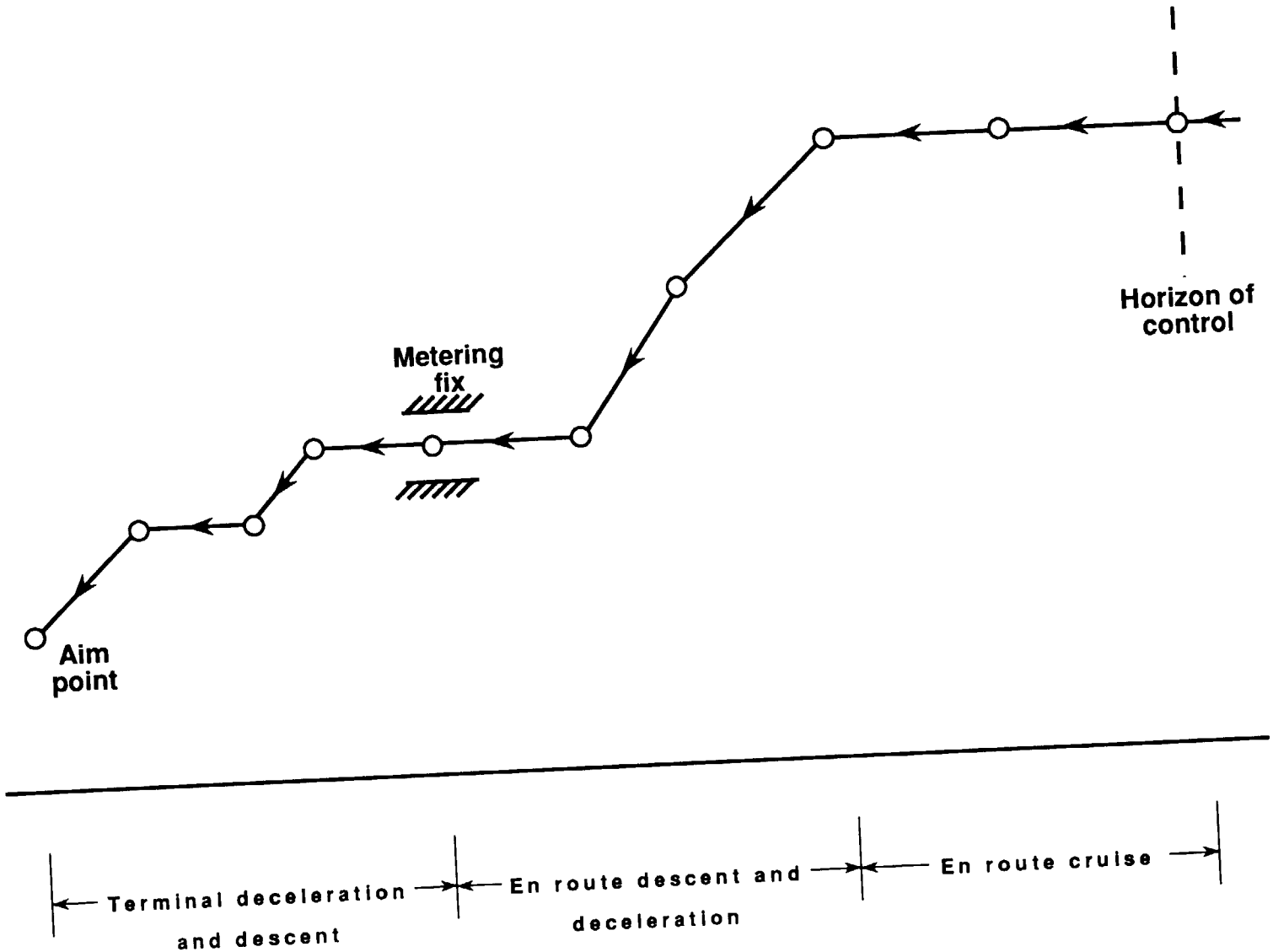

Figure 4. Division of each arrival path (from its horizon of control to aim point) into a cruise deceleration segment, a constant Mach cruise segment, and several constant-speed descent and level deceleration segments into the terminal using a Mach/CAS flight thrust, profile descent.

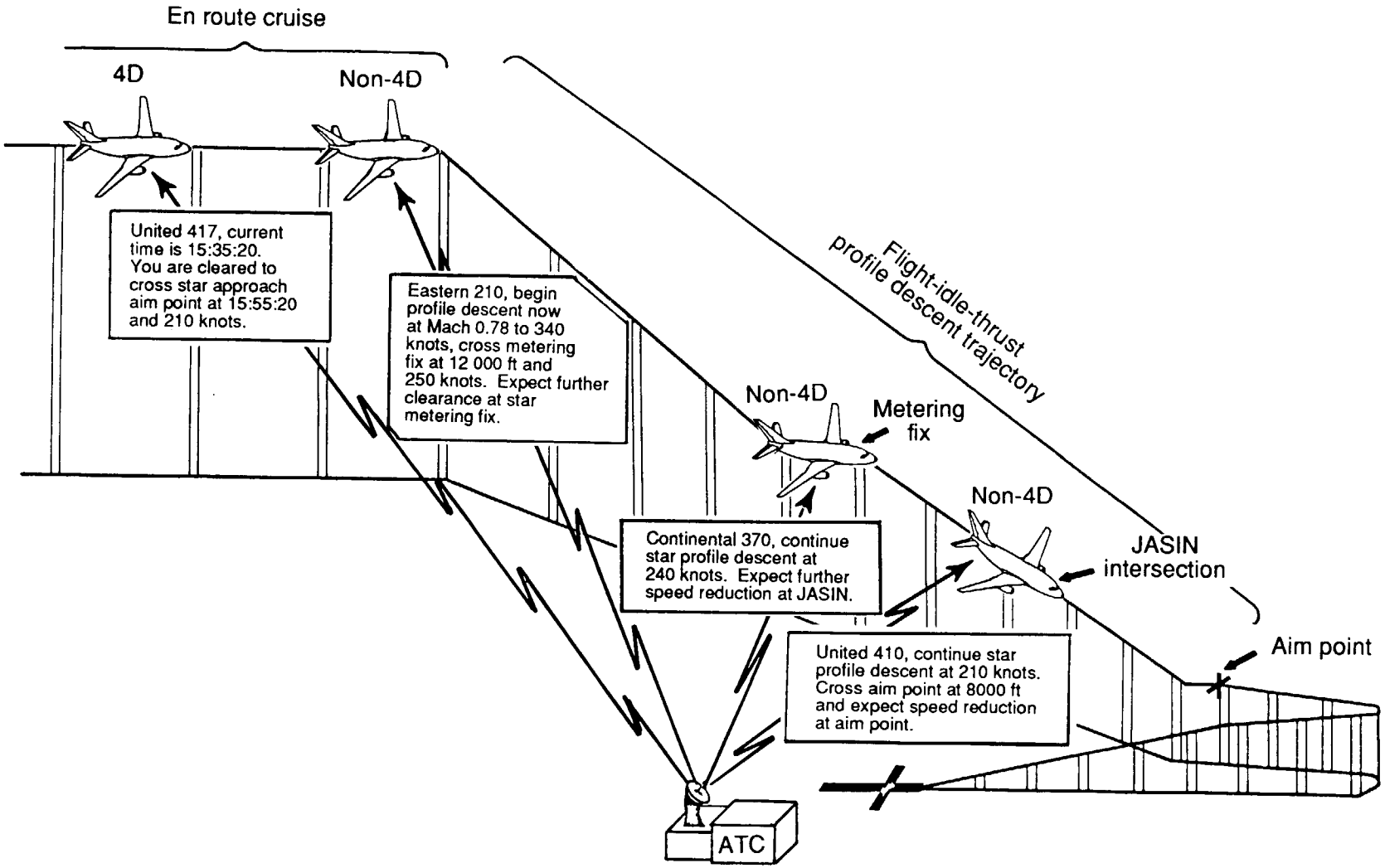

Figure 5. Sample TIMER control instructions for 4D- and non-4D-equipped aircraft performing flight-idle-thrust, profile descent approaches.

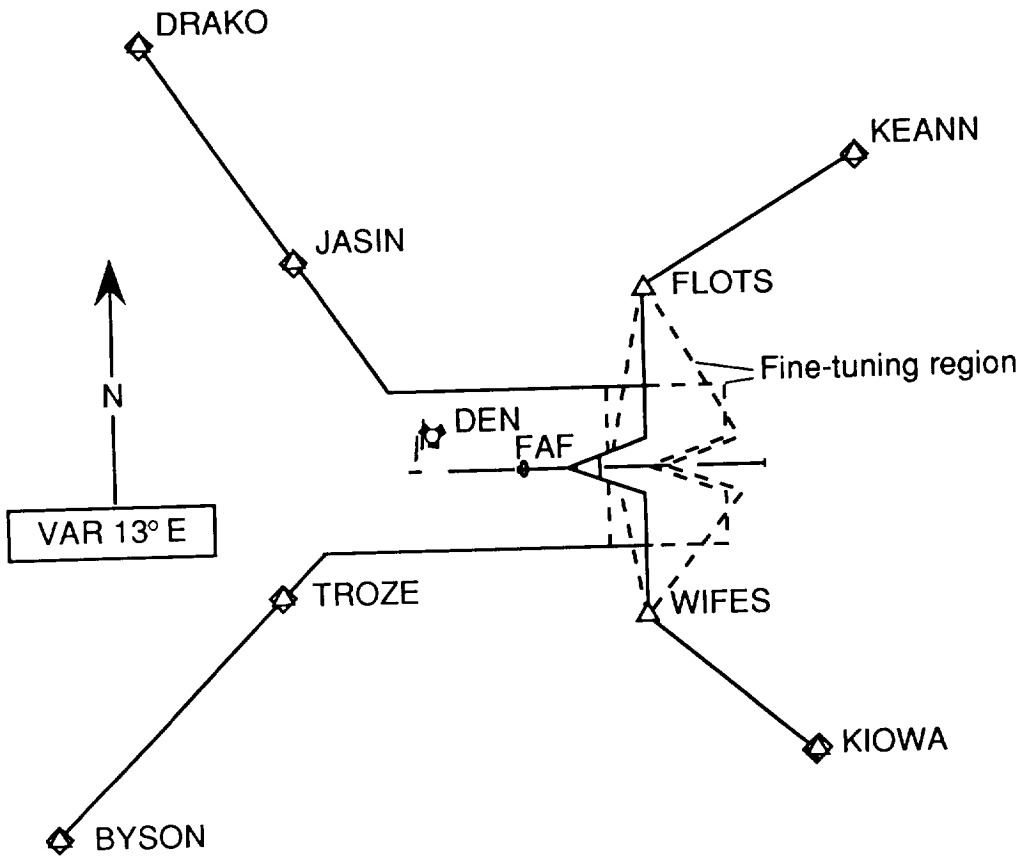

Figure 6. Terminal geometry simulated for approaches to runway 26L at Denver's Stapleton International Airport.

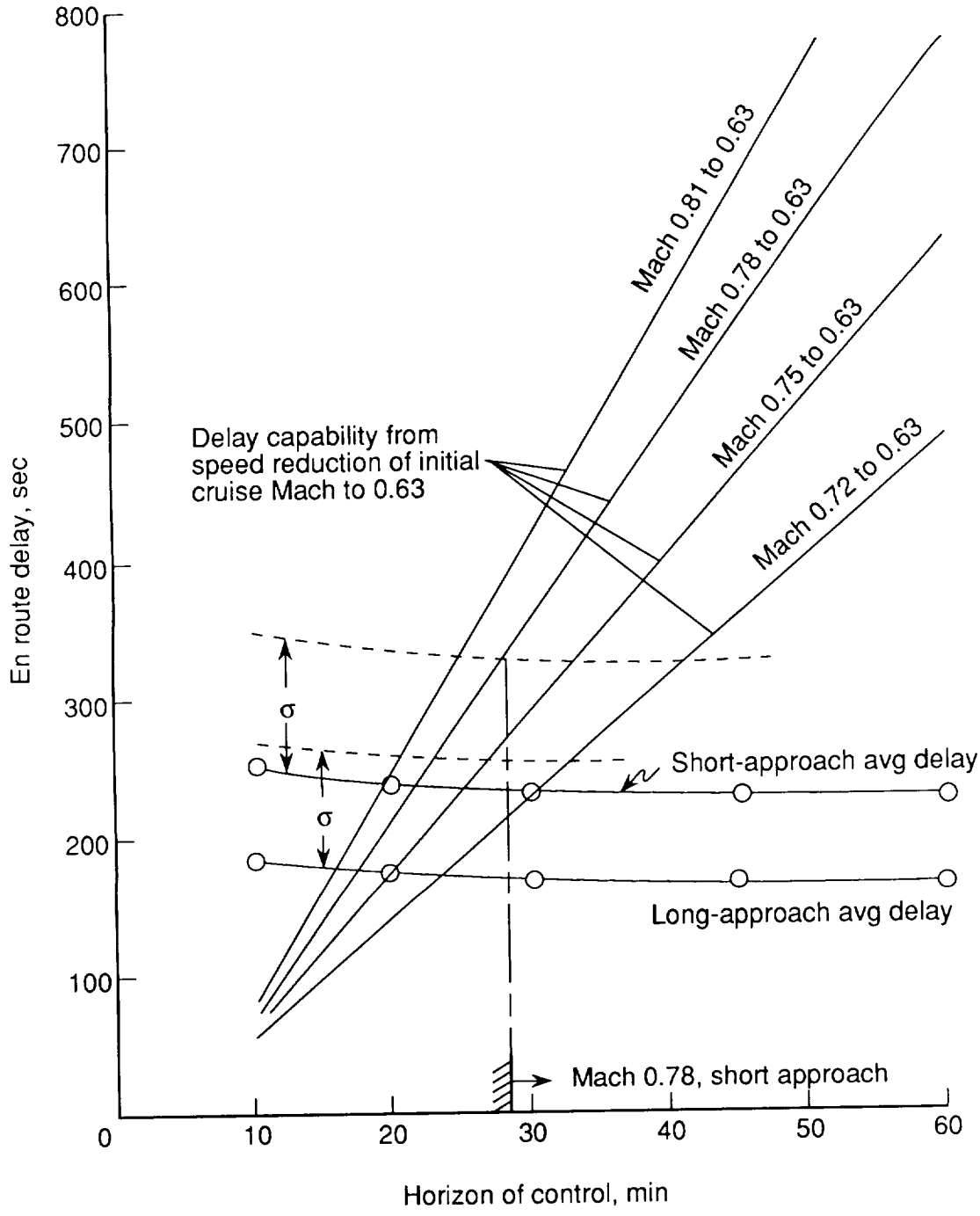

Figure 7. Horizon of control needed to efficiently absorb delay for range of initial cruise speeds (3/4/5 n.mi. separation criteria).

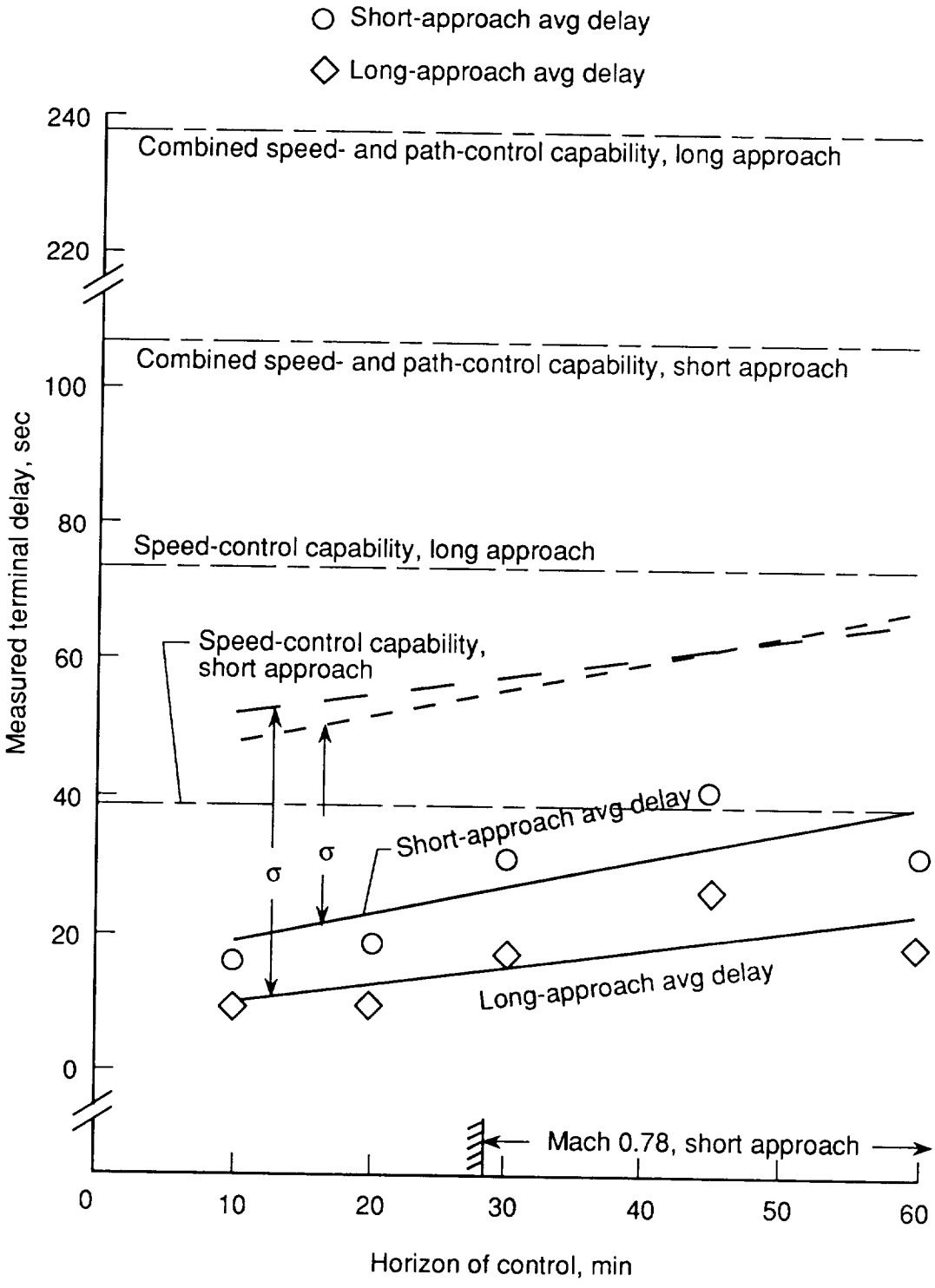

Figure 8. Horizon-of-control region needed to stay within terminal area nominal delay capability (3/4/5 n.mi. separation criteria).

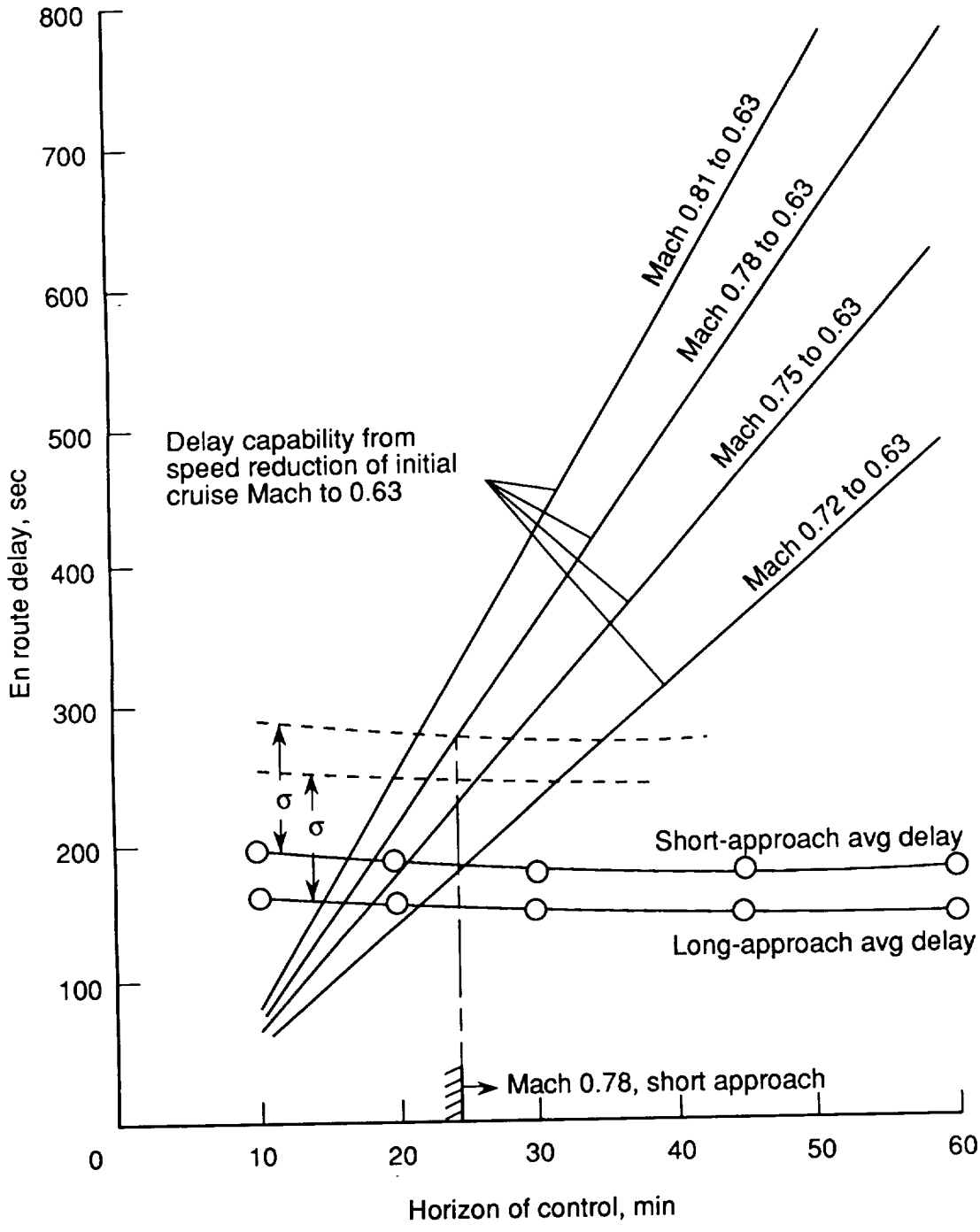

Figure 9. Horizon of control needed to efficiently absorb delay for range of initial cruise speeds (2/3/4 n.mi. separation criteria).

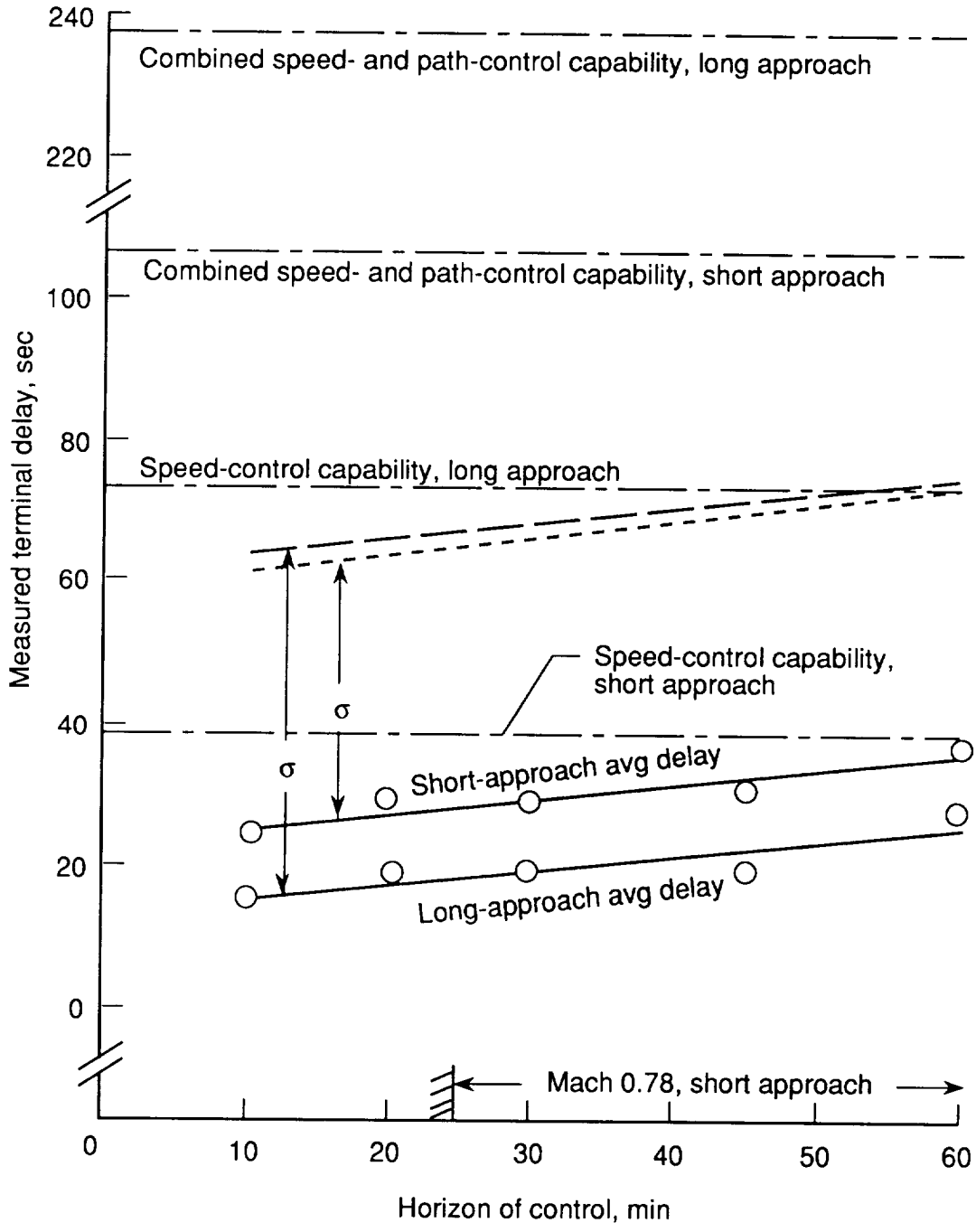

Figure 10. Horizon of control needed to stay within terminal area nominal delay capability (2/3/4 n.mi. separation criteria).

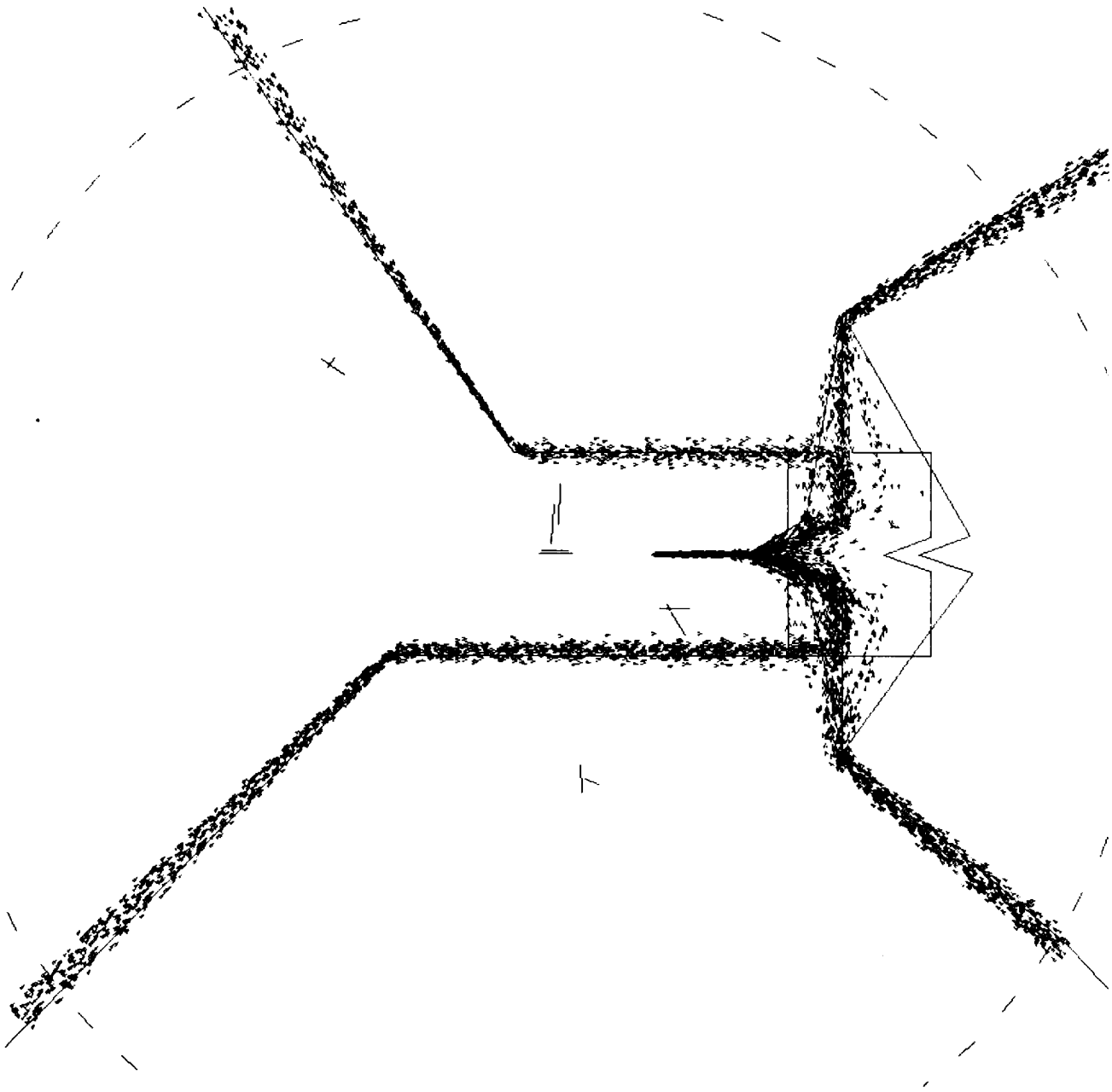

Figure 11. Terminal flow pattern for a metering-fix, arrival-error, standard deviation of 30 sec.

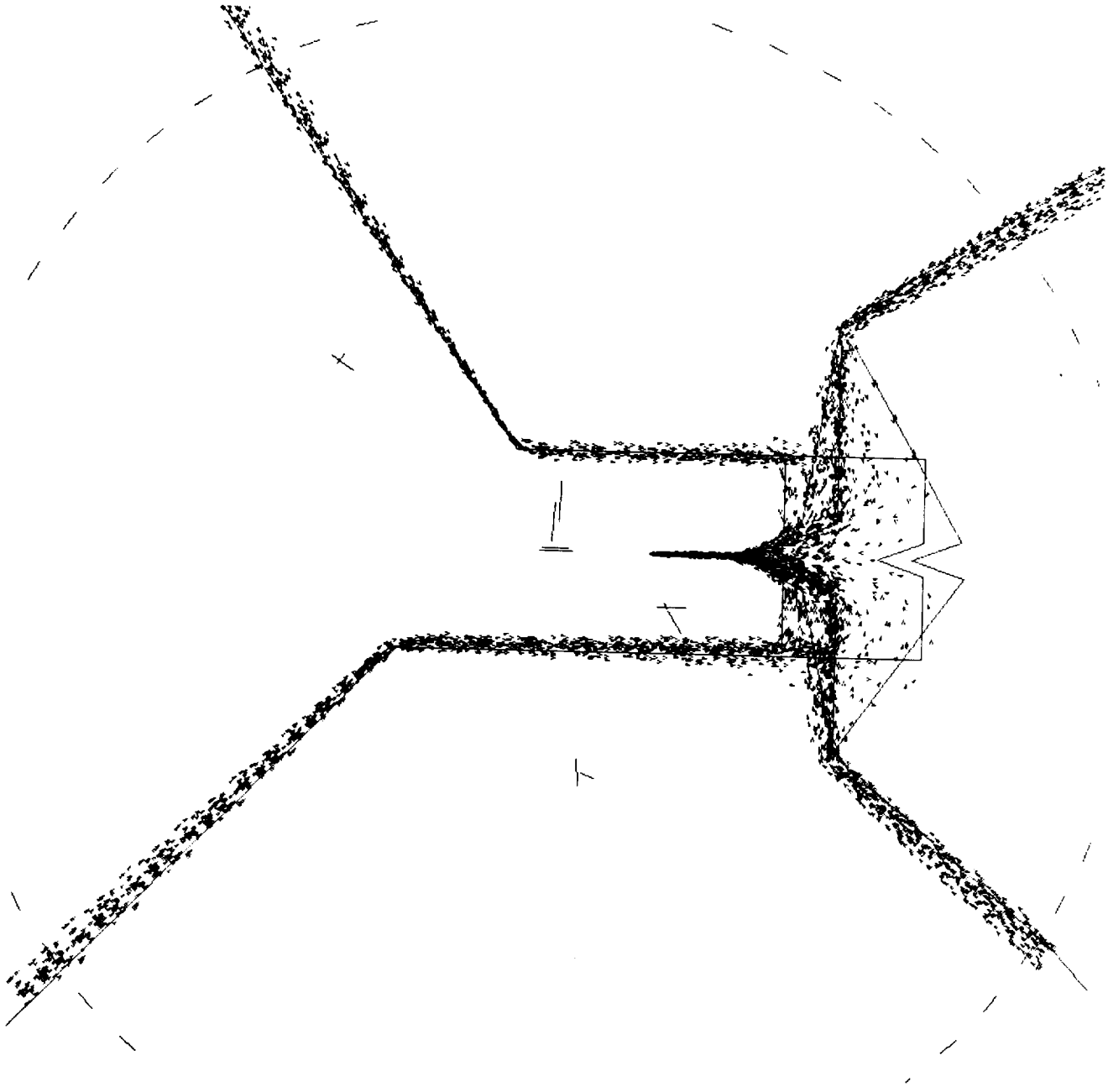

Figure 12. Terminal flow pattern for a metering-fix, arrival-error, standard deviation of 120 sec.

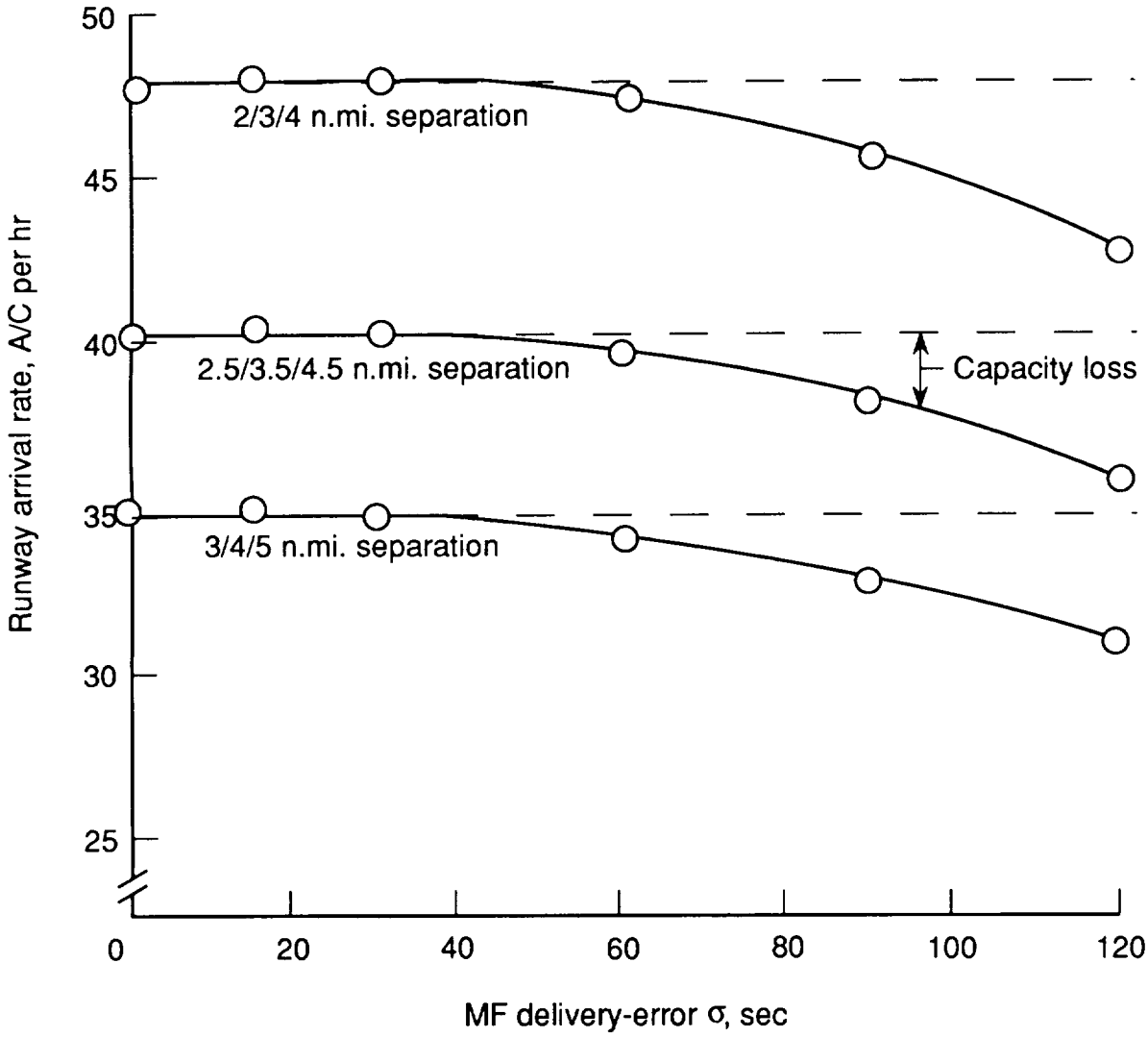

Figure 13. Impact of metering-fix delivery error on runway arrival rate.

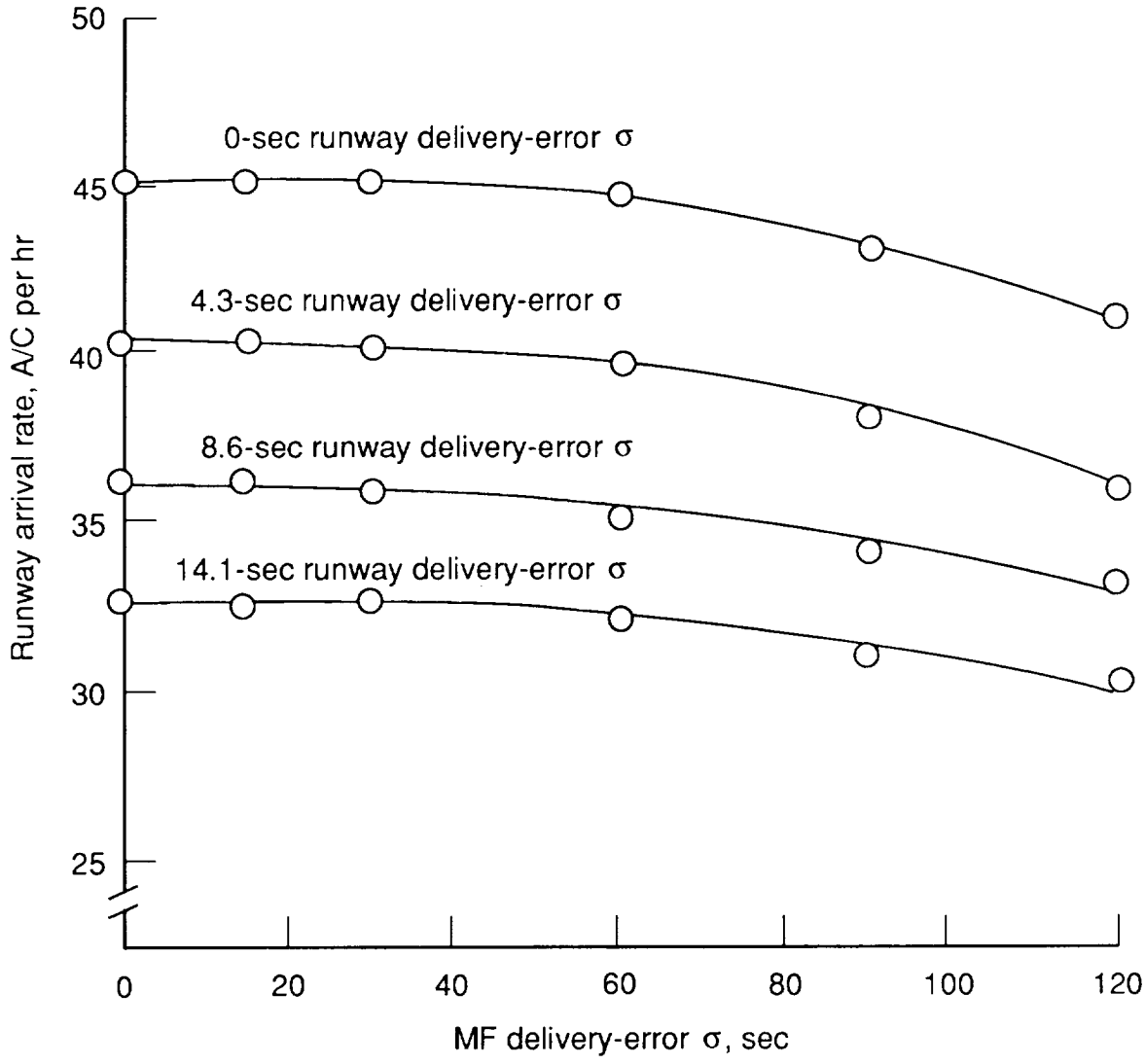

Figure 14. Impact of metering fix and runway delivery error on runway arrival rate (2.5/3.5/4.5 n.mi. separation criterion).

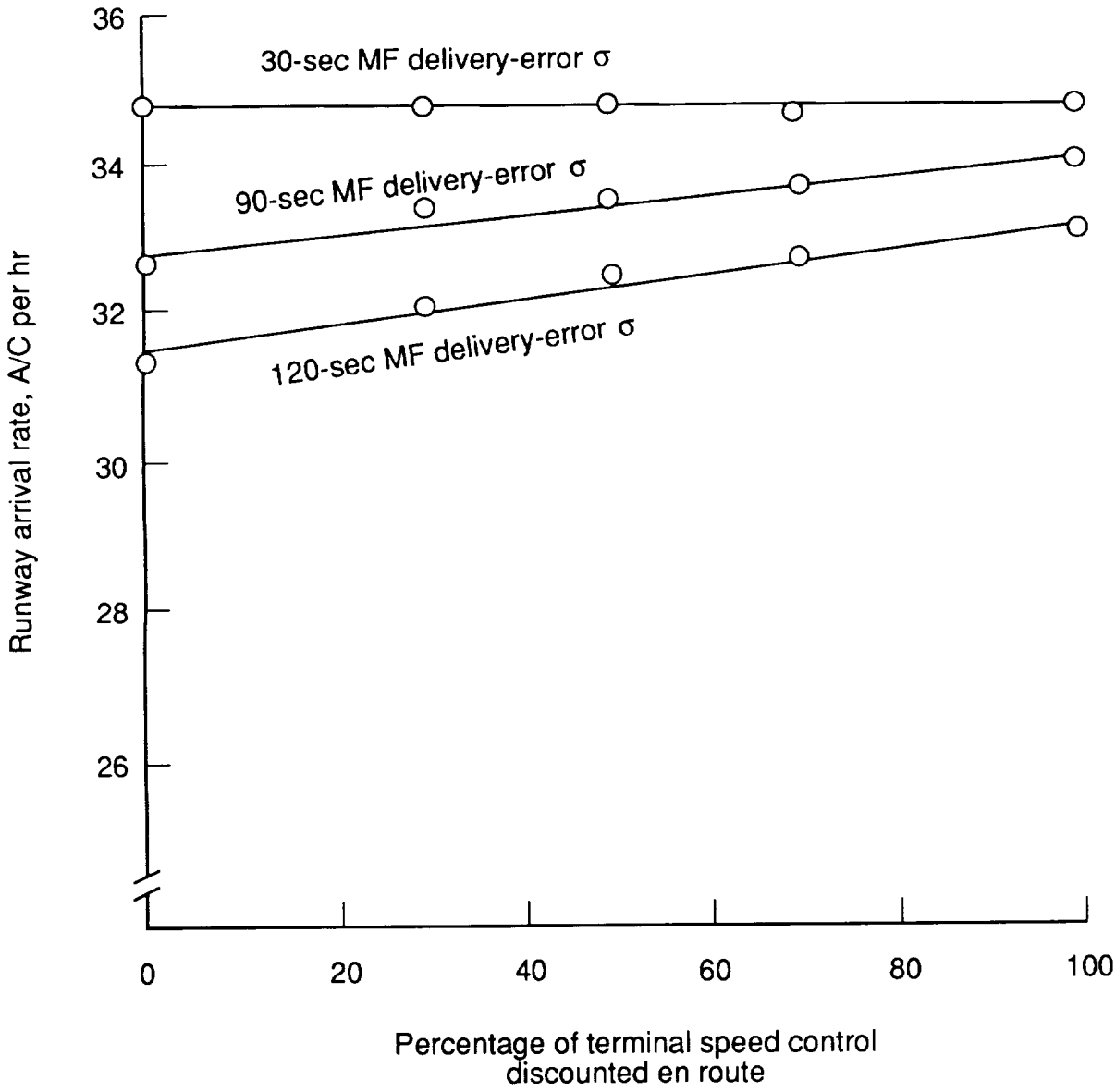

Figure 15. Effect of en route delay postponement on runway arrival rate.

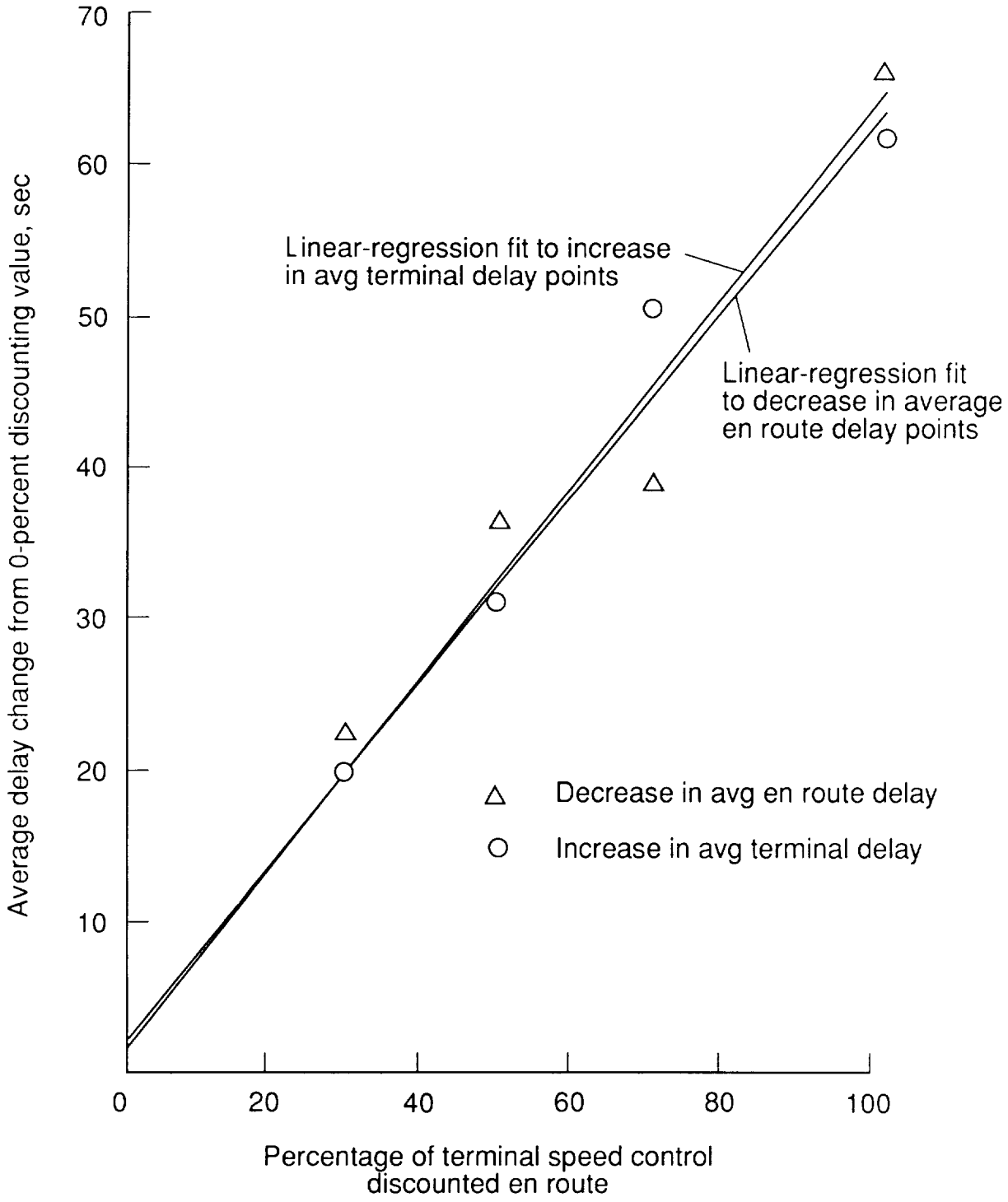

Figure 16. Decrease in average en route delay and increase in average terminal delay as a function of en route delay postponement for a 30-sec metering-fix, delivery-error, standard deviation.

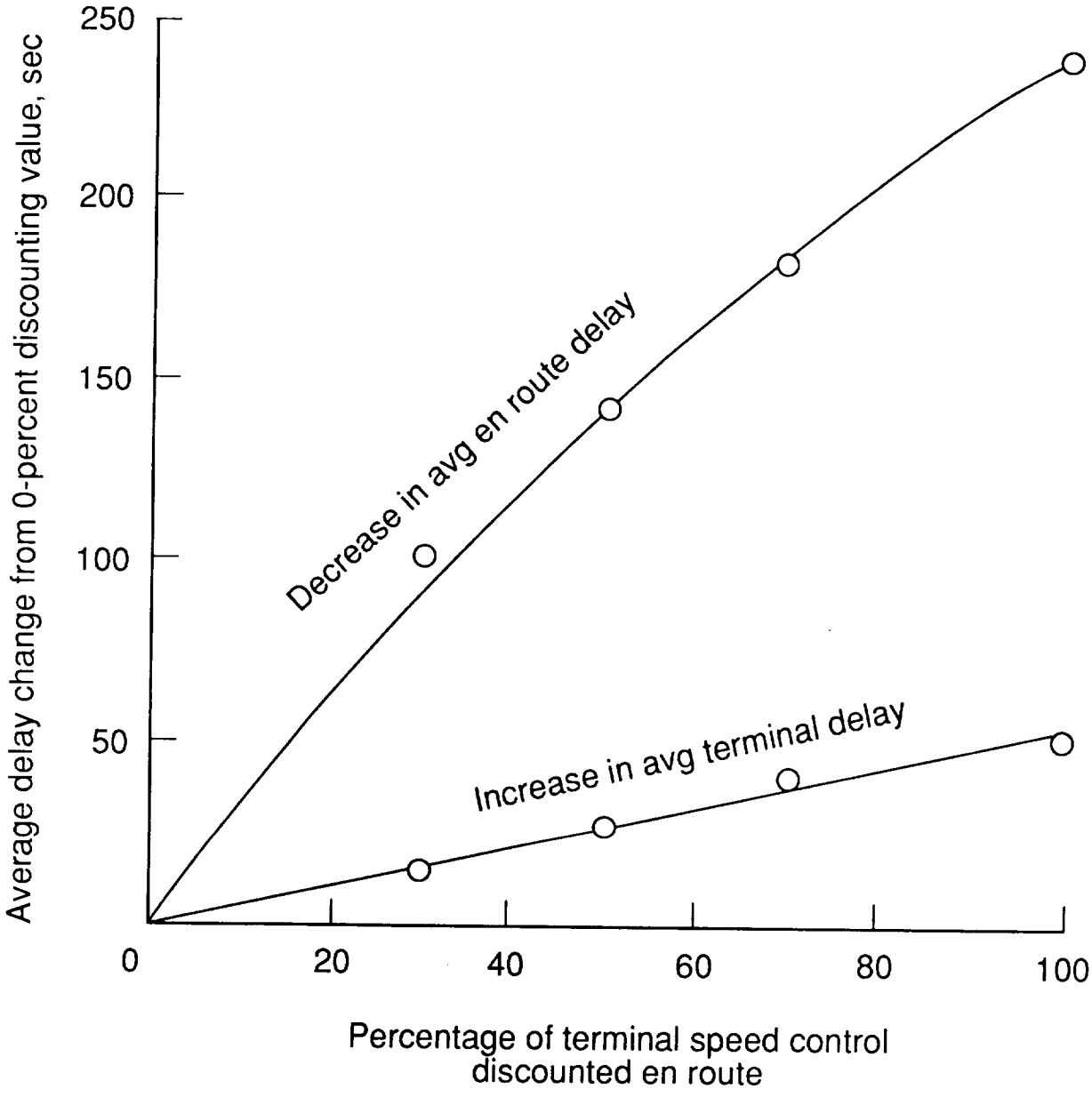

Figure 17. Decrease in average en route delay and increase in average terminal delay as a function of en route delay postponement for a 90-sec metering-fix, delivery-error, standard deviation.

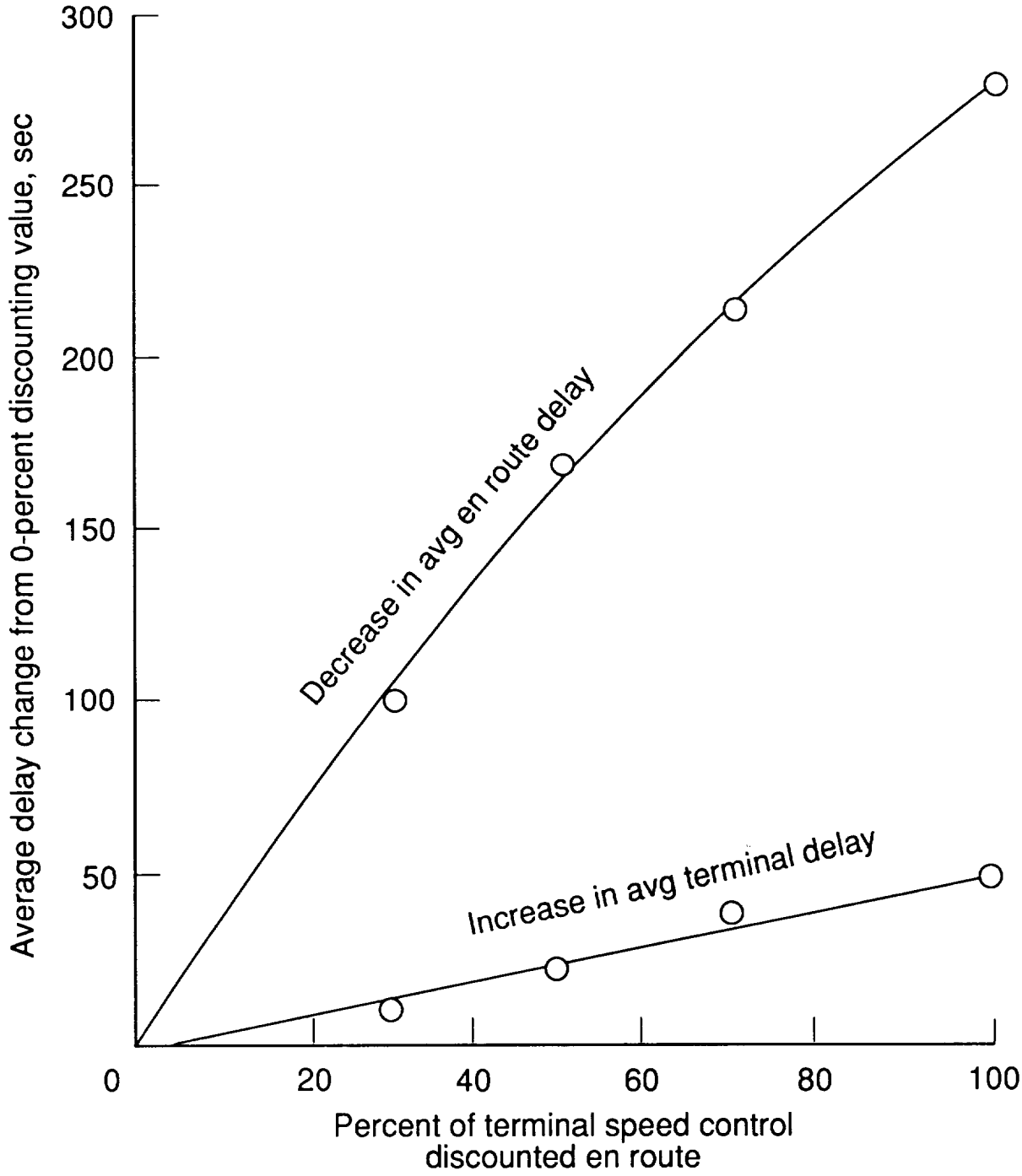

Figure 18. Decrease in average en route delay and increase in average terminal delay as a function of en route delay postponement for a 120-sec metering-fix, delivery-error, standard deviation.

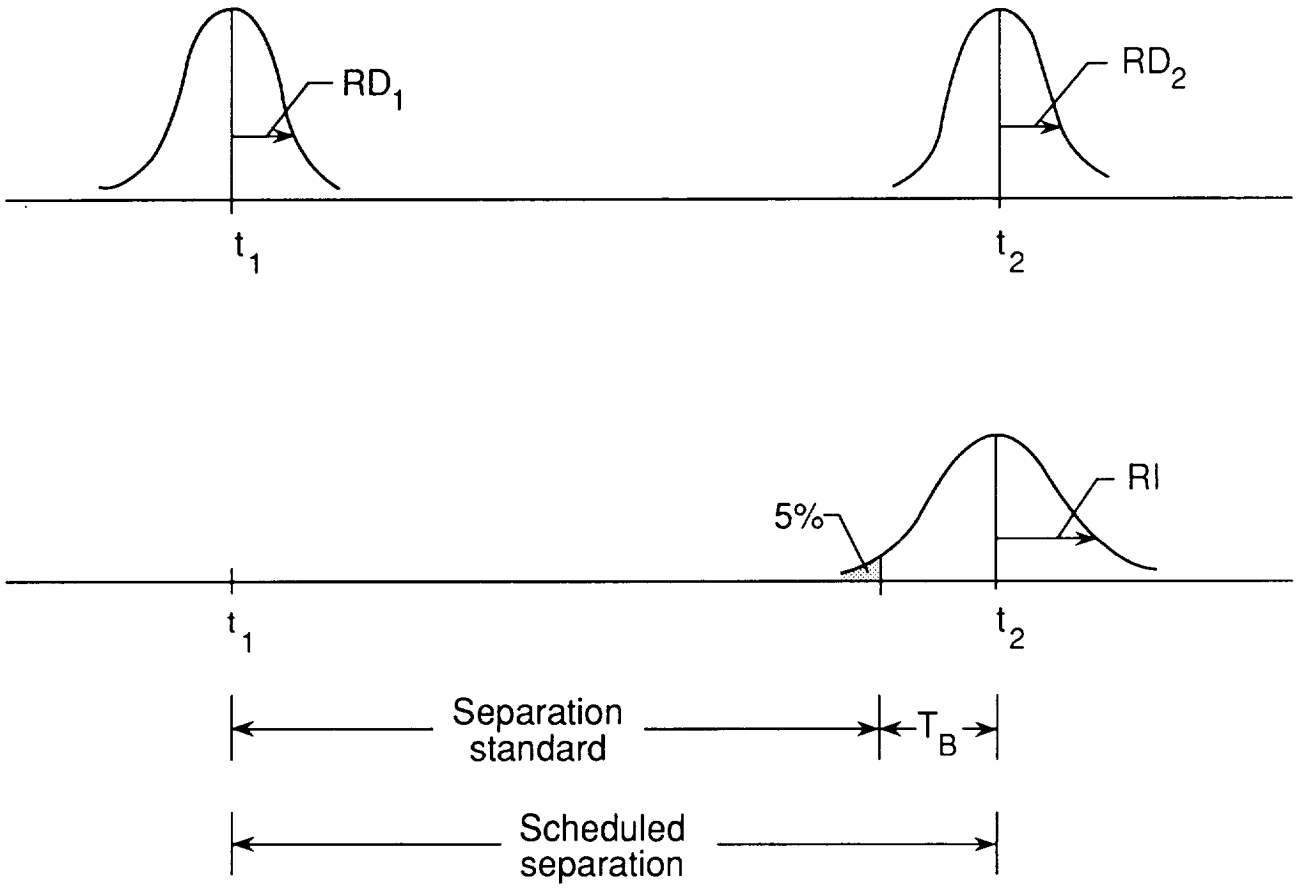

Figure 19. Time relation between individual delivery error, separation standard, and scheduled separation of two successive landing aircraft.

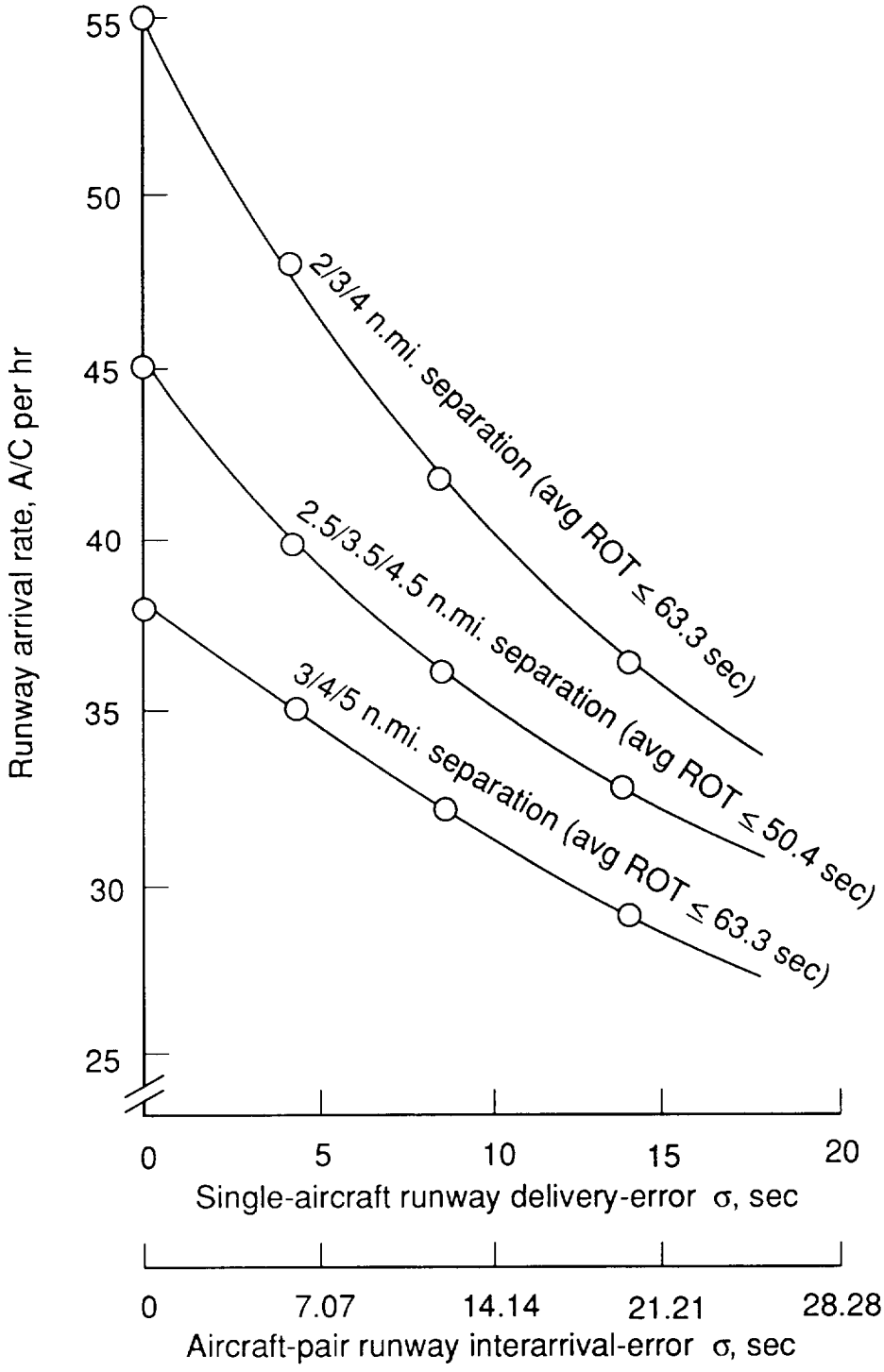

Figure 20. Impact of runway delivery error on capacity. 8.6 percent heavy aircraft.

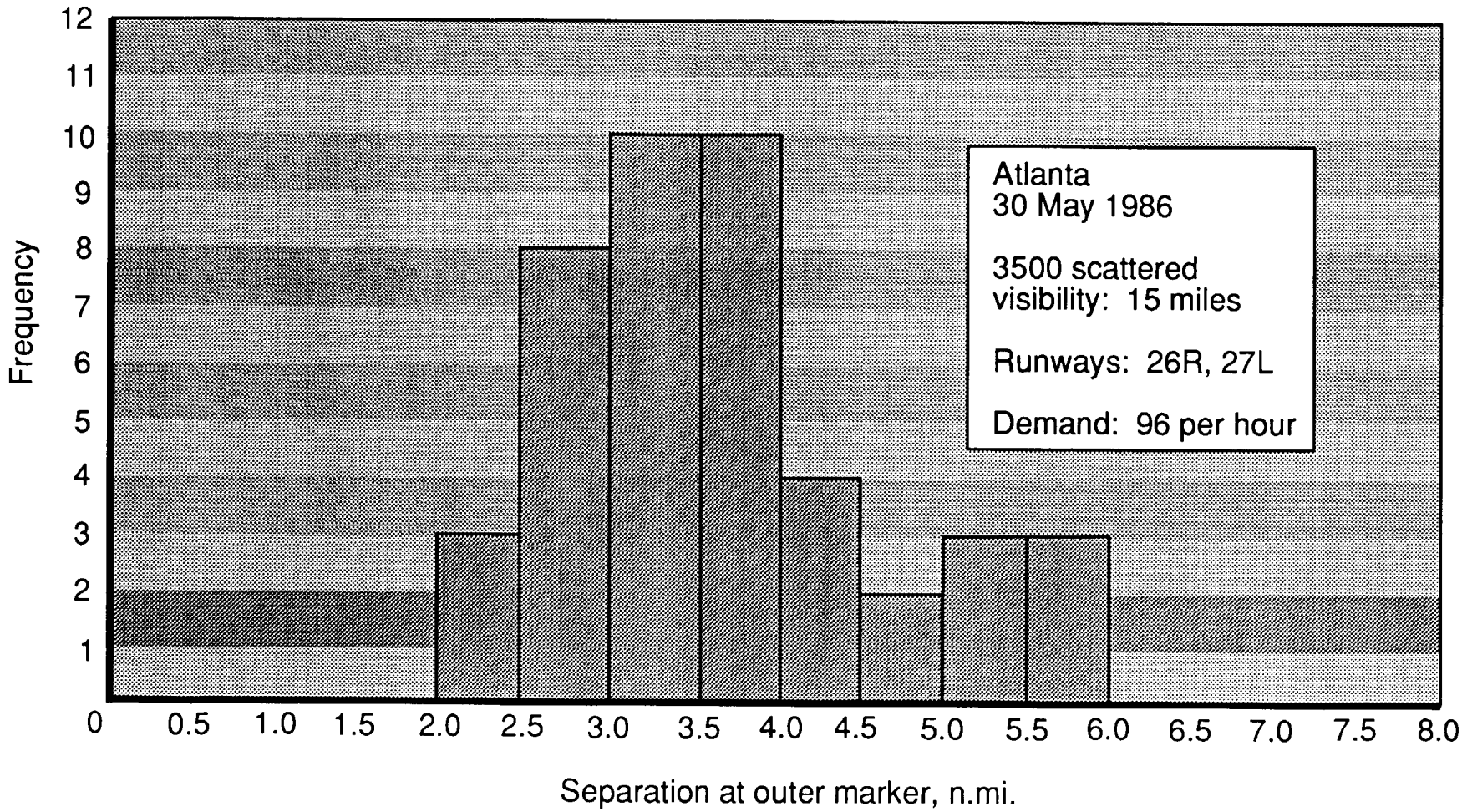

Figure 21. Aircraft-pair separation distribution at William B. Hartsfield Atlanta International Airport (ATL) measured when first aircraft is at outer marker. (Data from MITRE's S.C. Mohleji briefing to FAA Terminal ATC Automation Concept Advisory Group meeting at NASA Ames Research Center, April 30, 1987.)

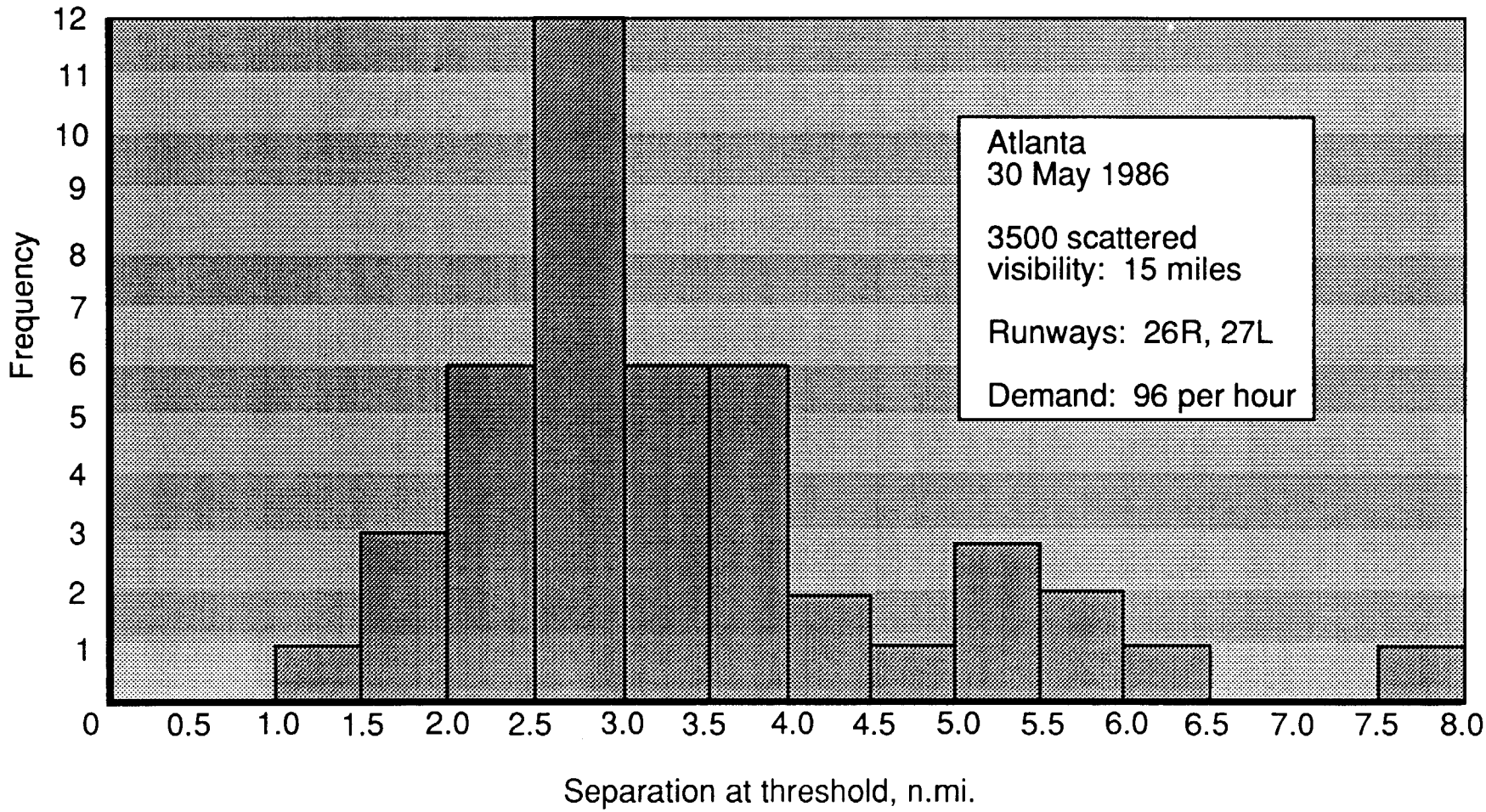

Figure 22. Aircraft-pair separation distribution at William B. Hartsfield Atlanta International Airport (ATL) measured when first aircraft is at runway threshold. (Data from MITRE's S.C. Mohleji briefing to FAA Terminal ATC Automation Concept Advisory Group meeting at NASA Ames Research Center, April 30, 1987.)

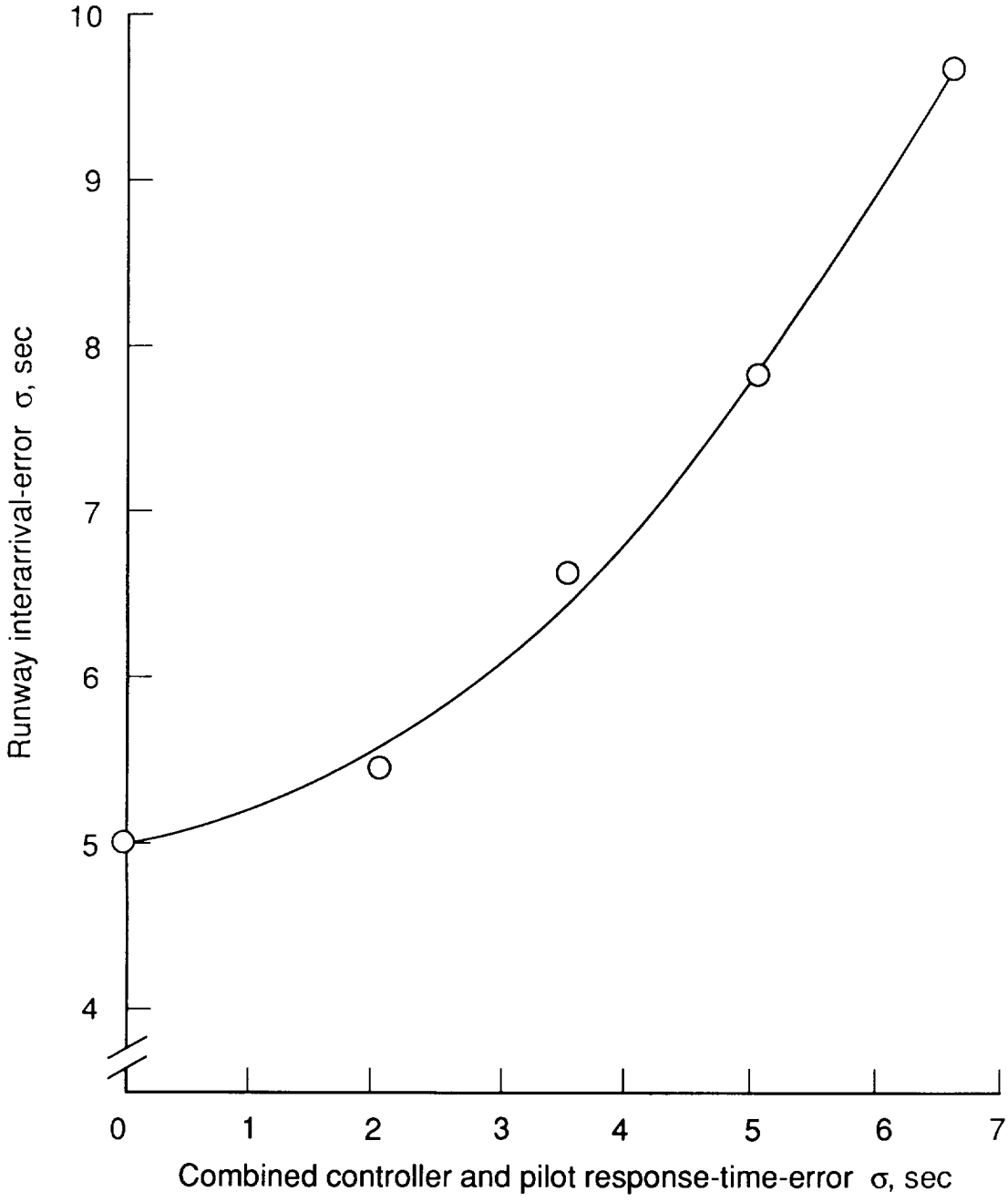

Figure 23. Effect of controller and pilot response times on system runway delivery precision.

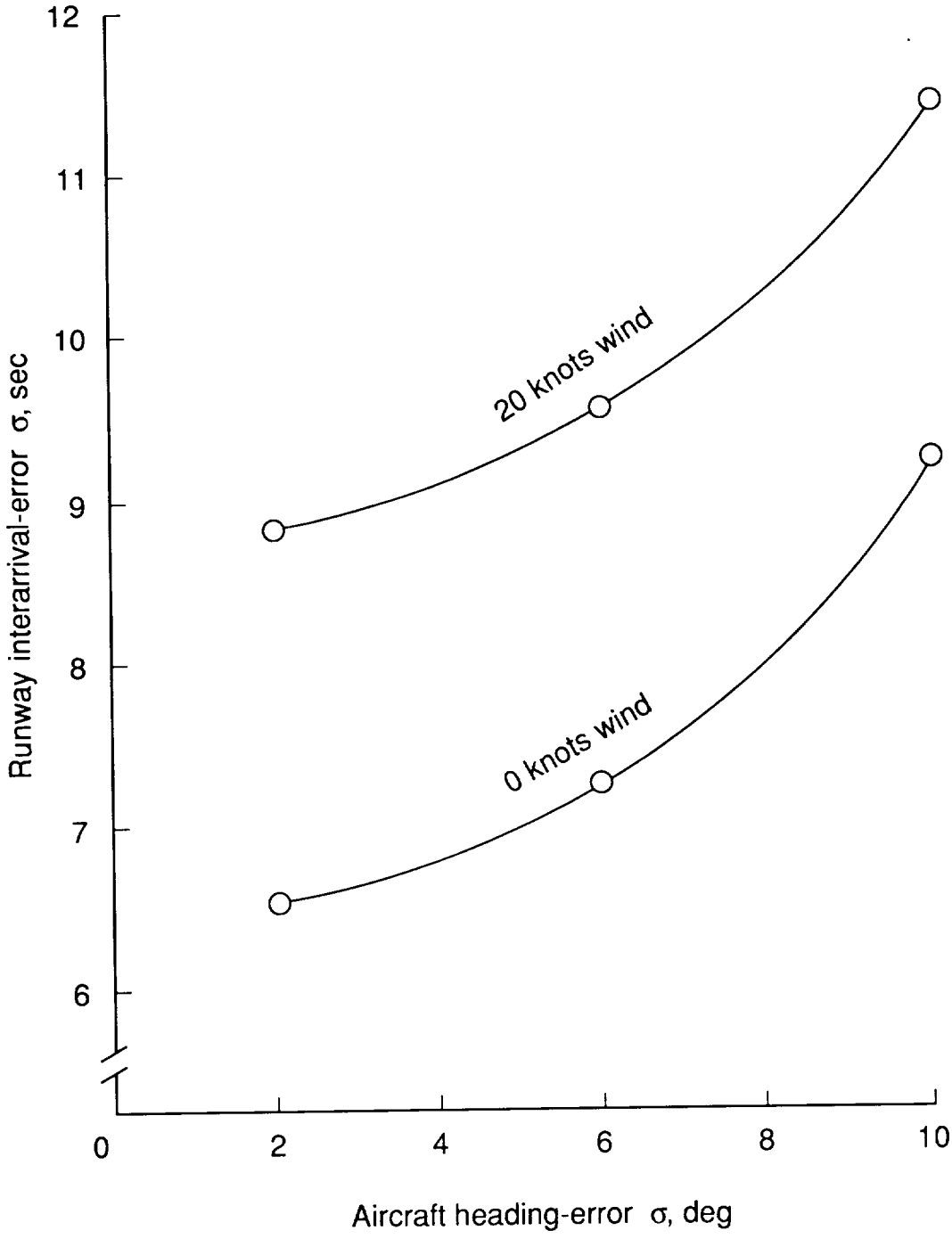

Figure 24. Effect of aircraft heading error on system runway interarrival error. 270° wind direction aligned with runway 3.

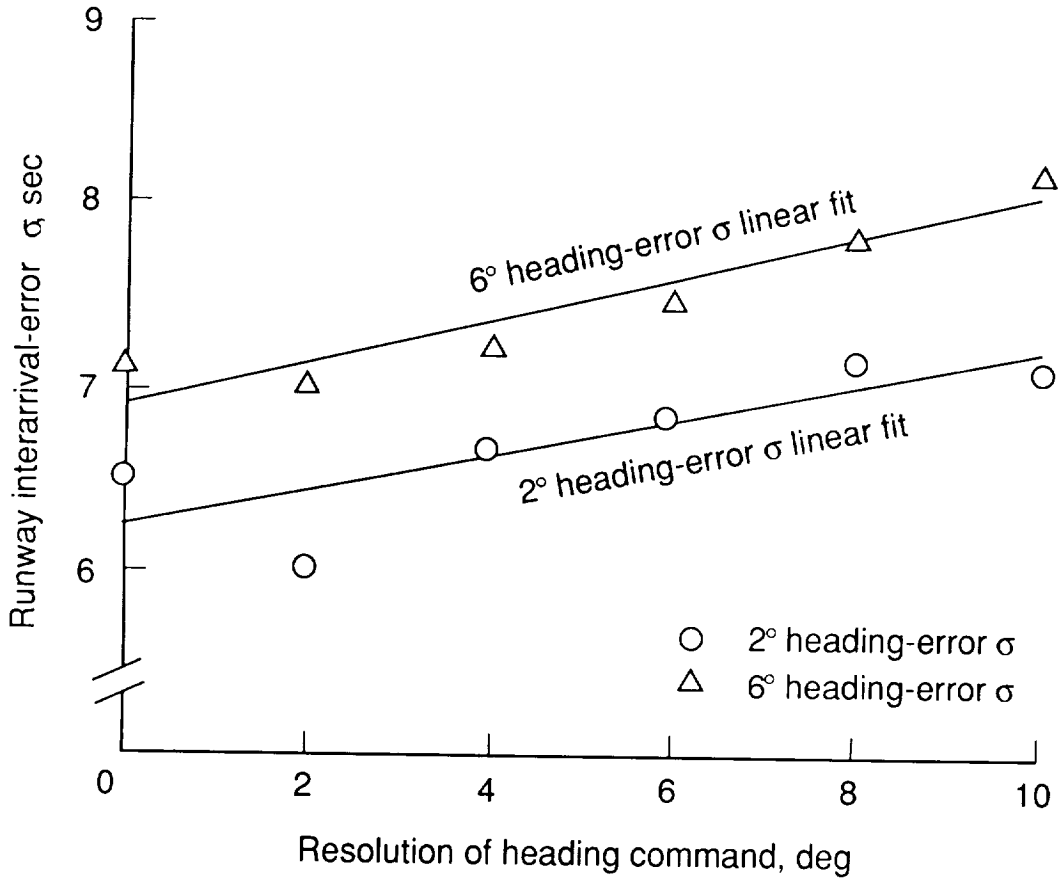

Figure 25. Impact of heading command resolution on system runway interarrival error.

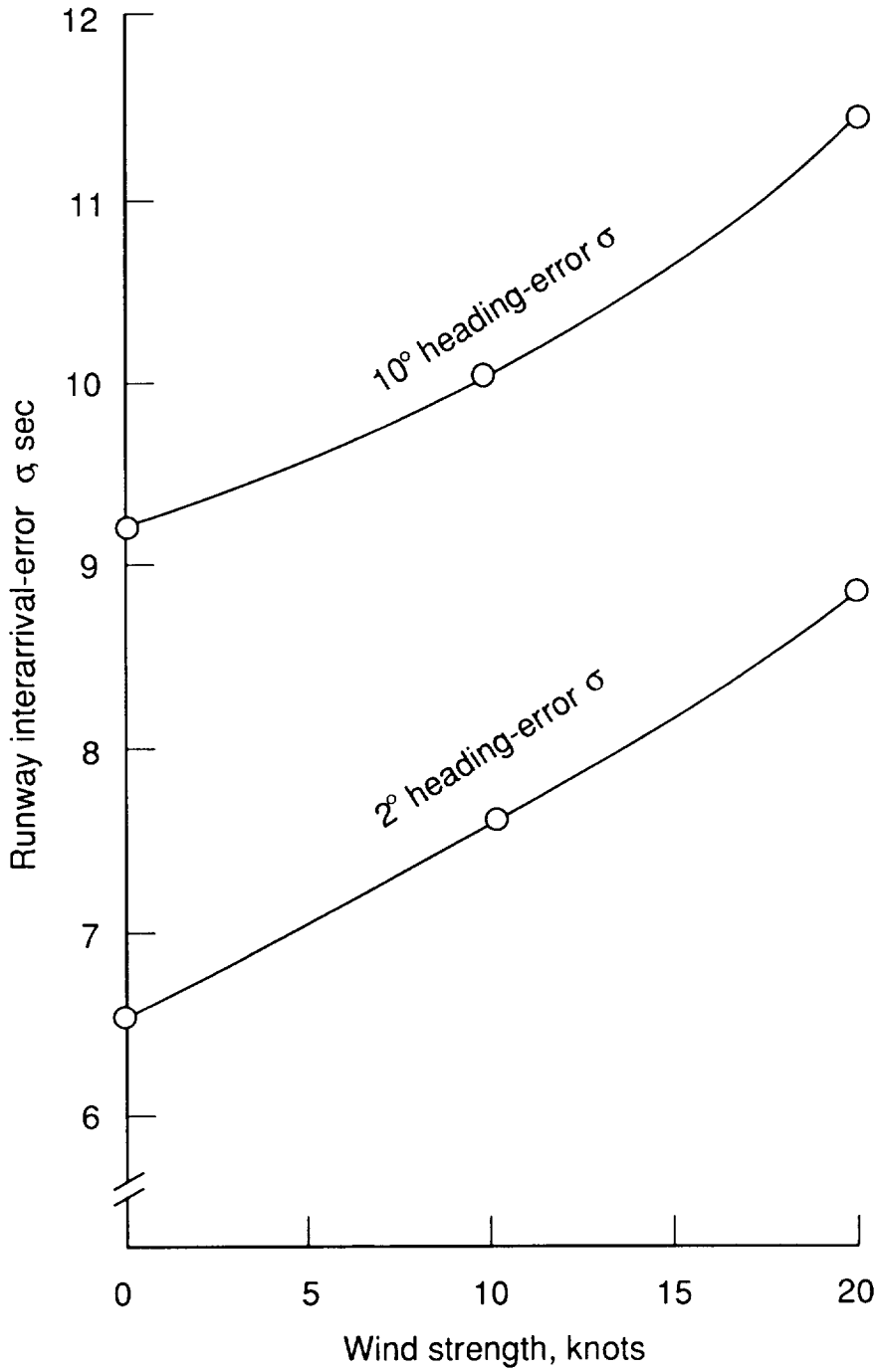

Figure 26. Impact of head-wind strength on system runway interarrival error. 270° wind direction aligned with runway.

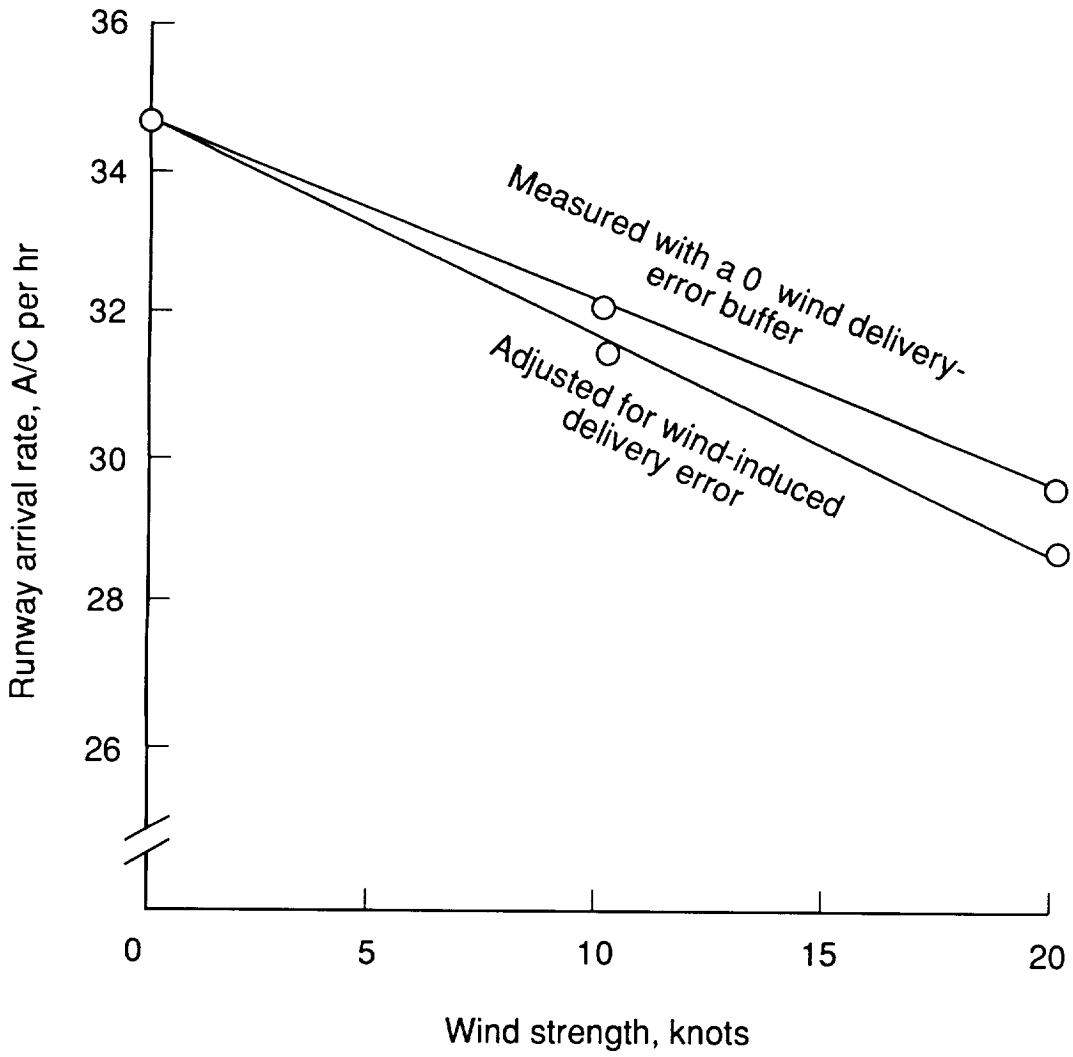

Figure 27. Impact of head-wind strength on runway arrival rate. 270° wind direction aligned with runway.

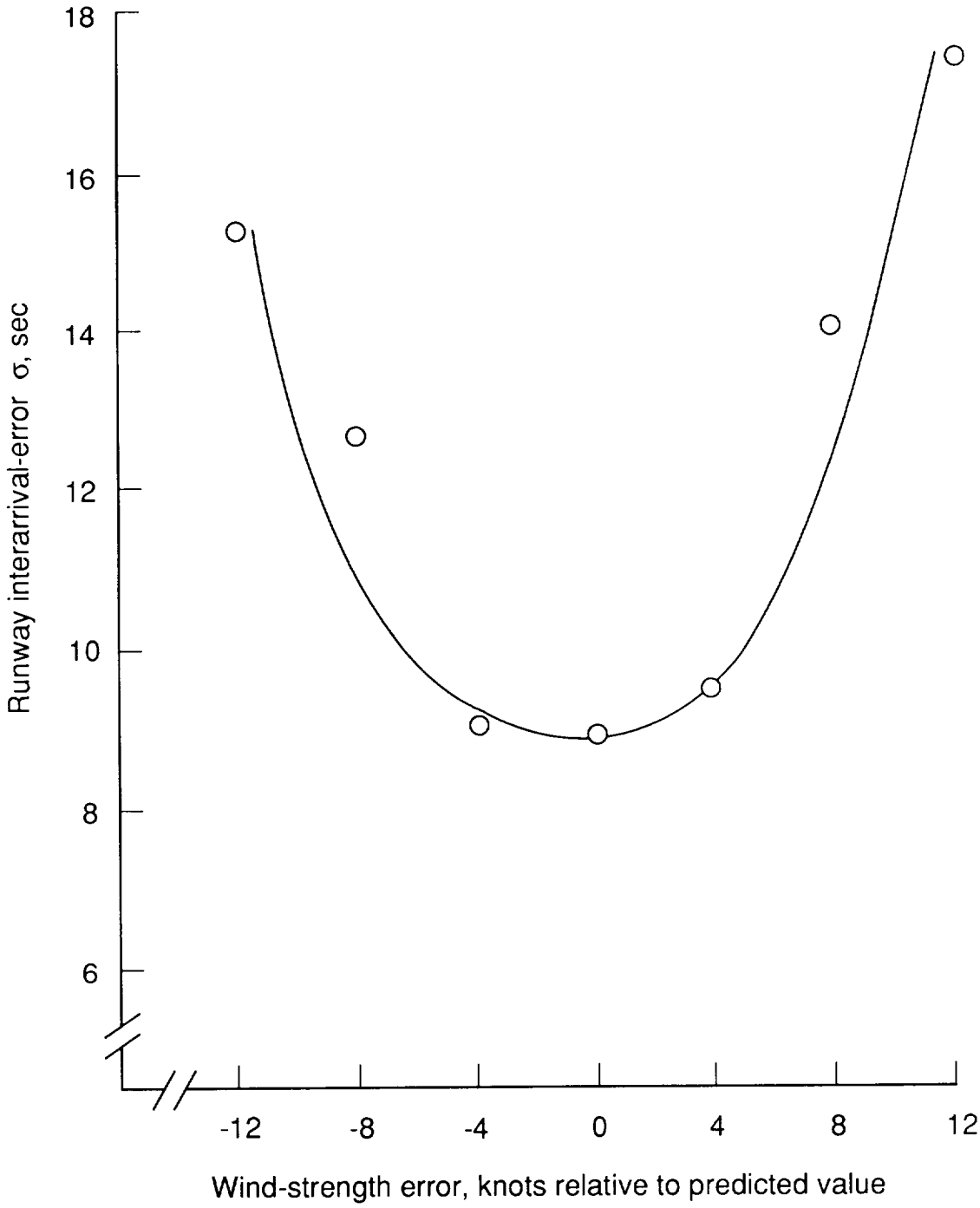

Figure 28. Effect of wind-strength error on system runway interarrival error. 20 knots wind predicted; 270° wind direction aligned with runway.

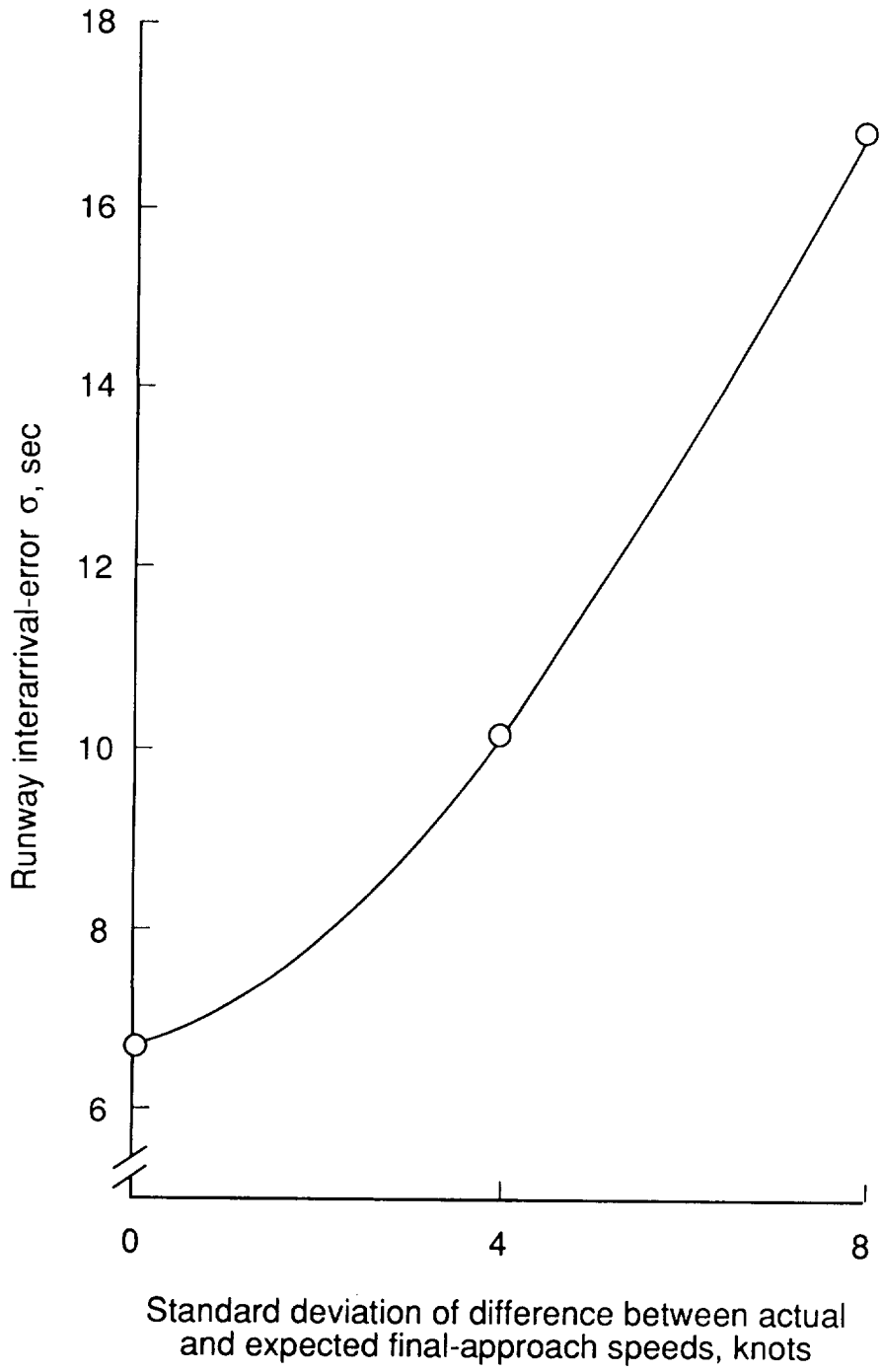

Figure 29. Impact of pilot-induced variability in final-approach speed on system interarrival error. Known landing weight; no wind.

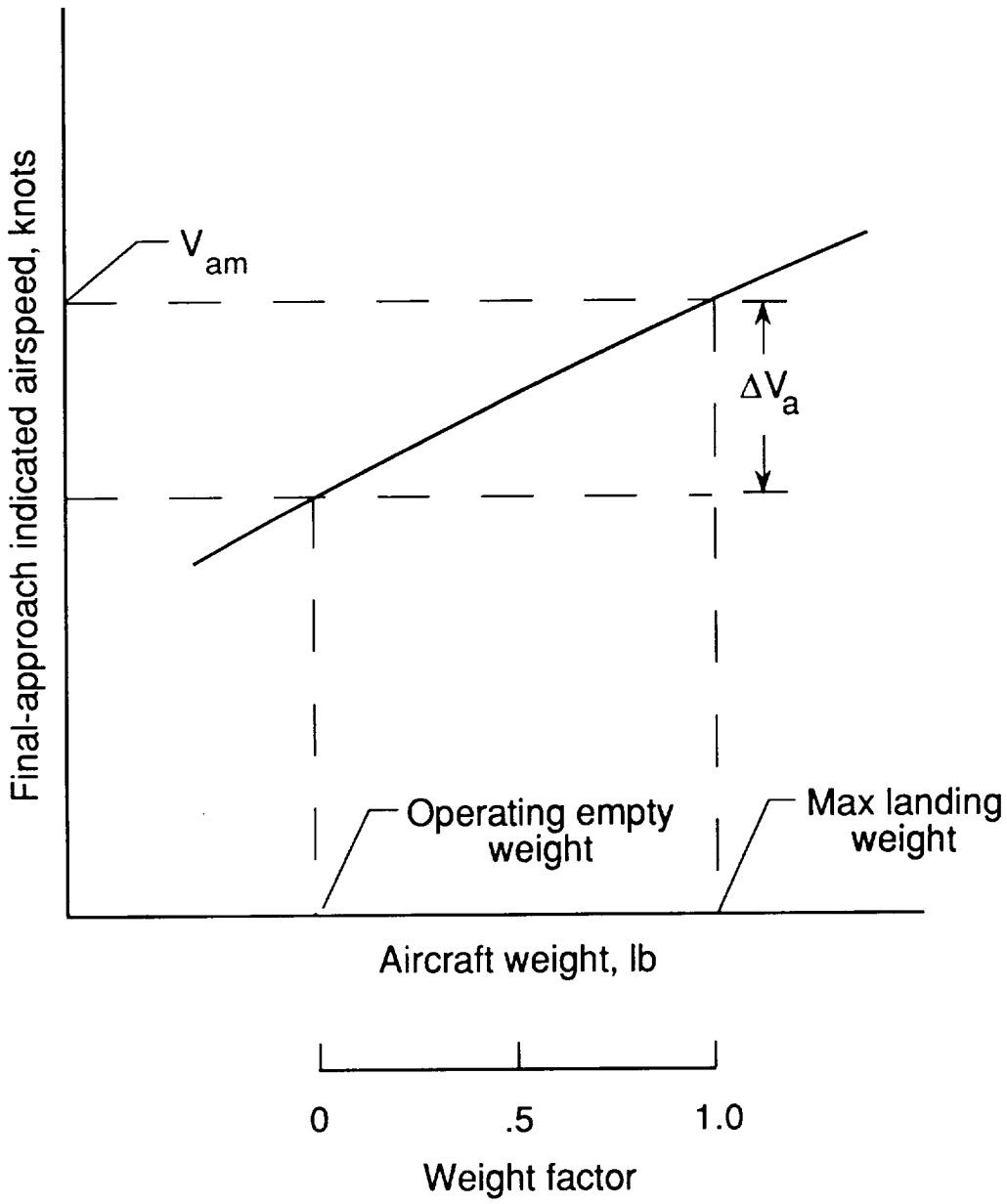

Figure 30. Relationships of aircraft weight, weight factor, and final-approach landing speed.

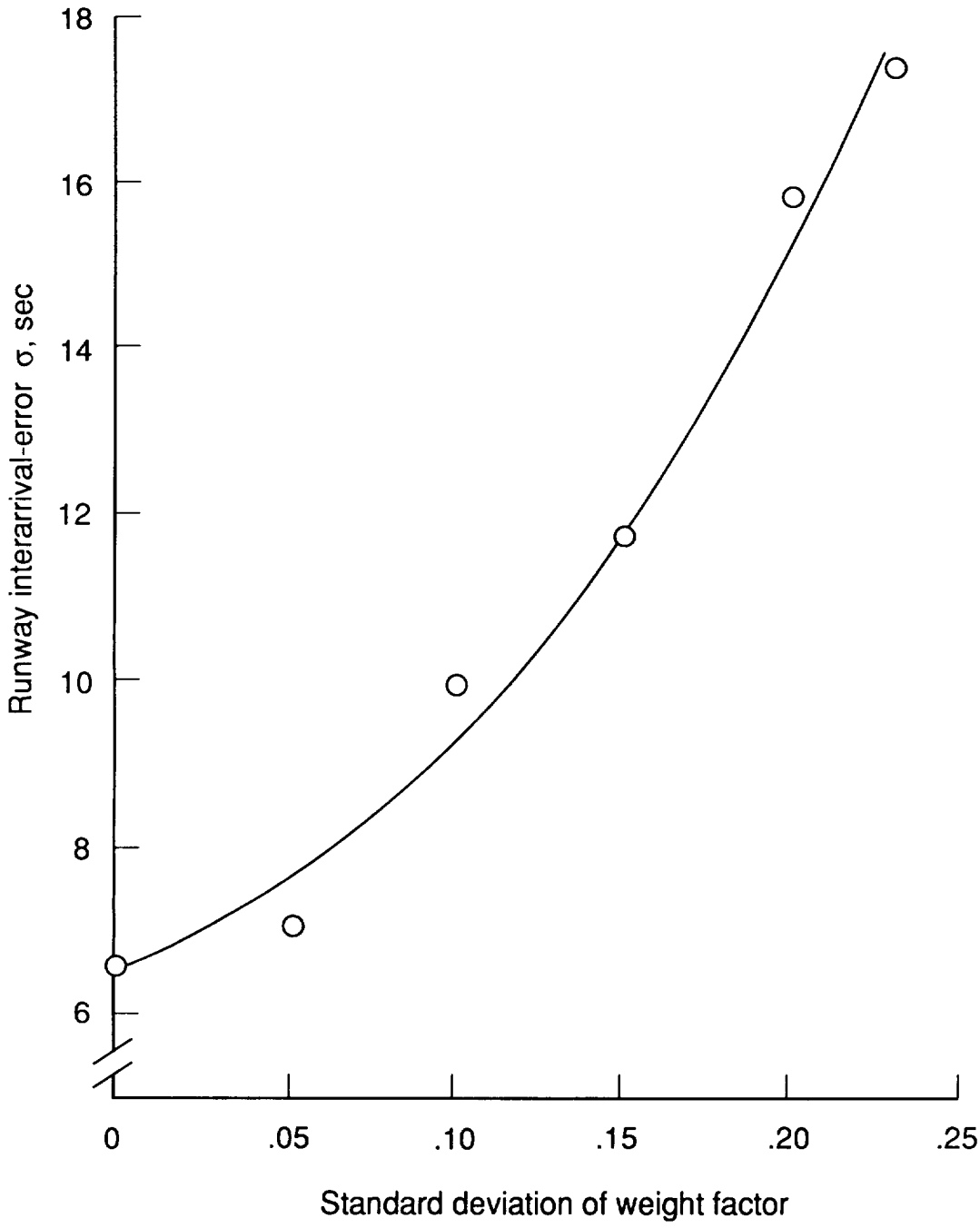

Figure 31. Impact of weight-factor density function on system runway interarrival error. Weight factor mean = 0.5; unknown final-approach speed.

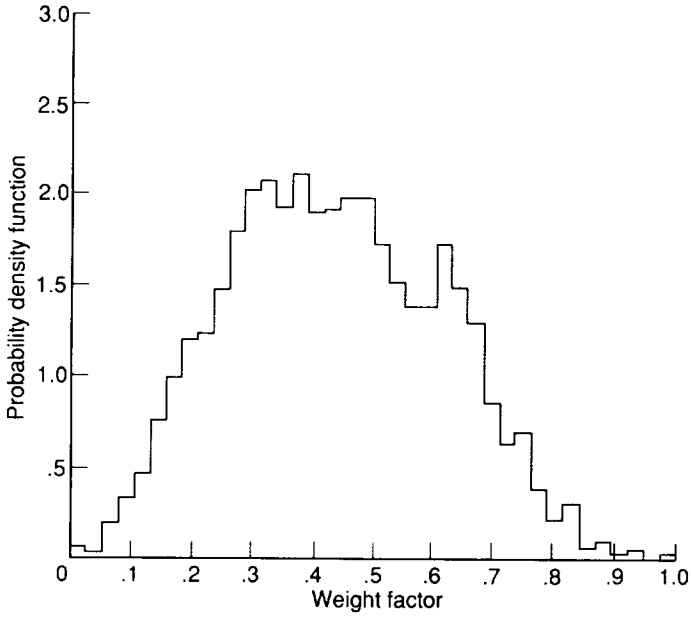

Figure 32. Probability density function of landing weight factor for a major airline's Boeing 737-200A arriving at Chicago's O'Hare International Airport (ORD) between January 1, 1986, and April 30, 1987. The mean was 0.435 and the standard deviation was 0.176.

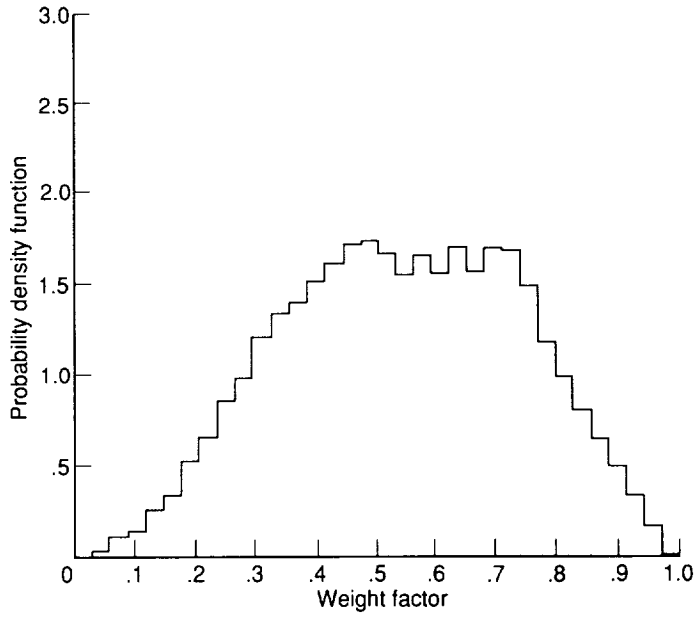

Figure 33. Probability density function of landing weight factor for a major airline's Boeing 737-200 arriving at Chicago's O'Hare International Airport (ORD) between January 1, 1986, and April 30, 1987. The mean was 0.541 and the standard deviation was 0.196.

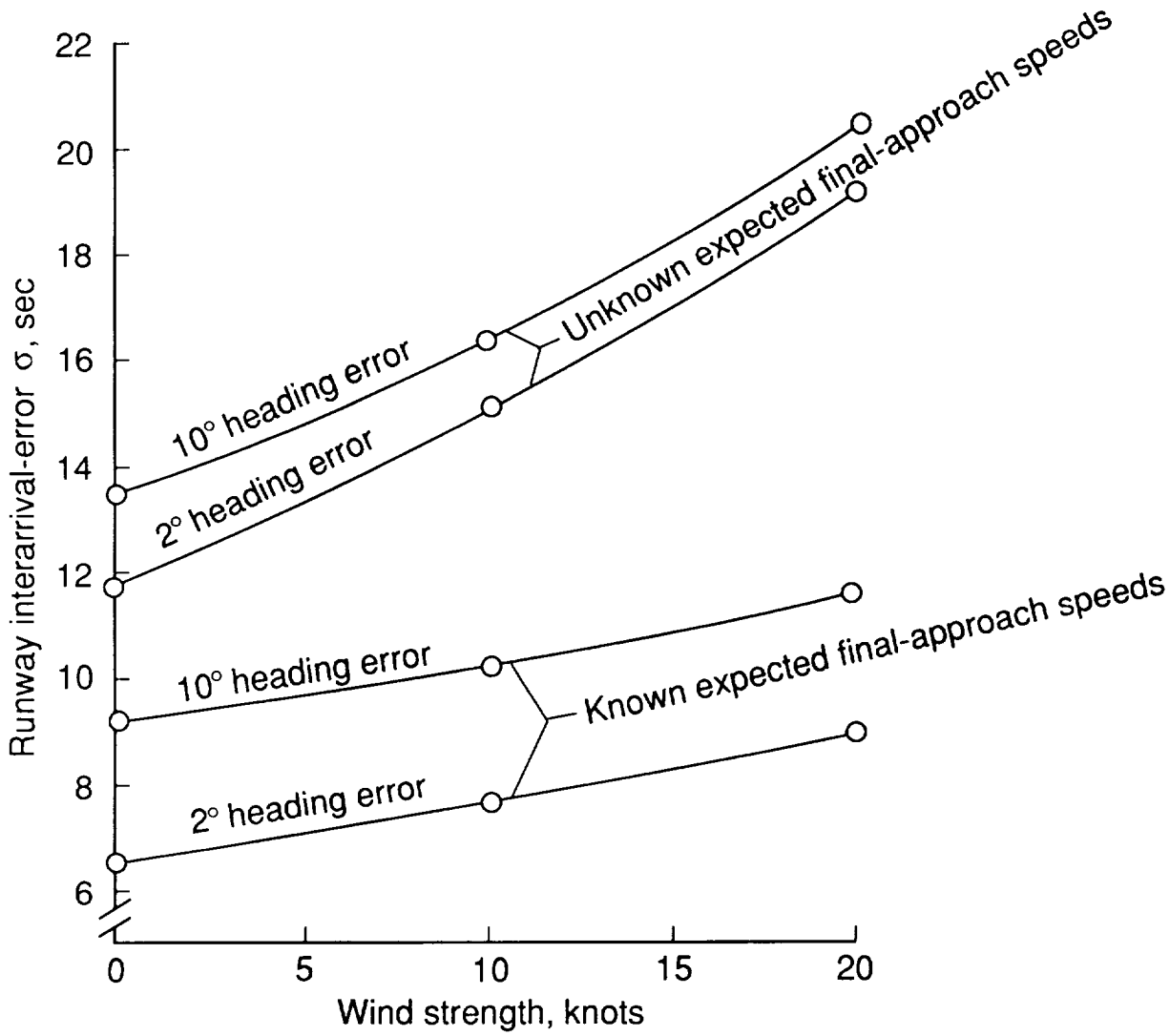

Figure 34. Impact of unknown final-approach speed and head-wind effect on system runway interarrival error. Weight factor mean = 0.5; weight factor standard deviation = 0.15; wind direction aligned with runway.

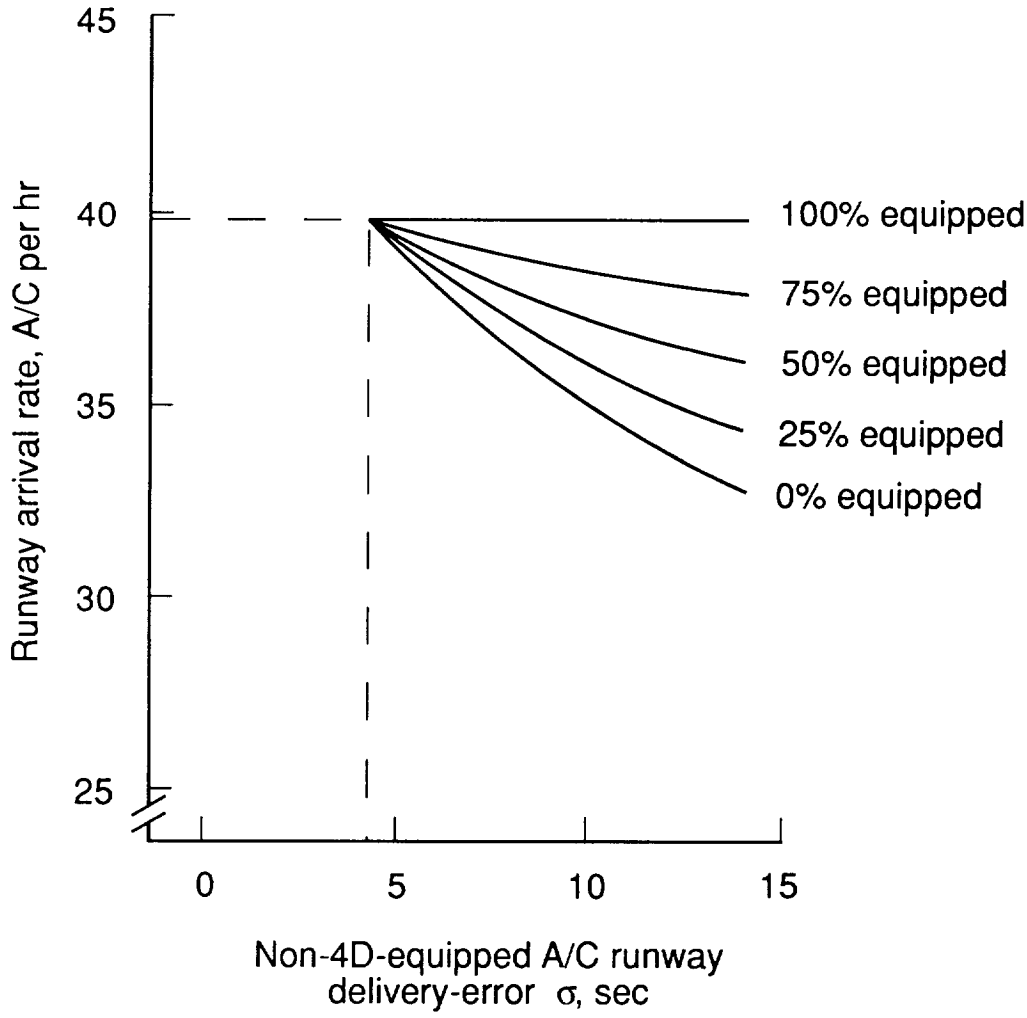

Figure 35. Effect of 4D equipage on capacity. Delivery-error standard deviation of 4D A/C = 4.3 sec; separation criterion is 2.5/3.5/4.5 n.mi.

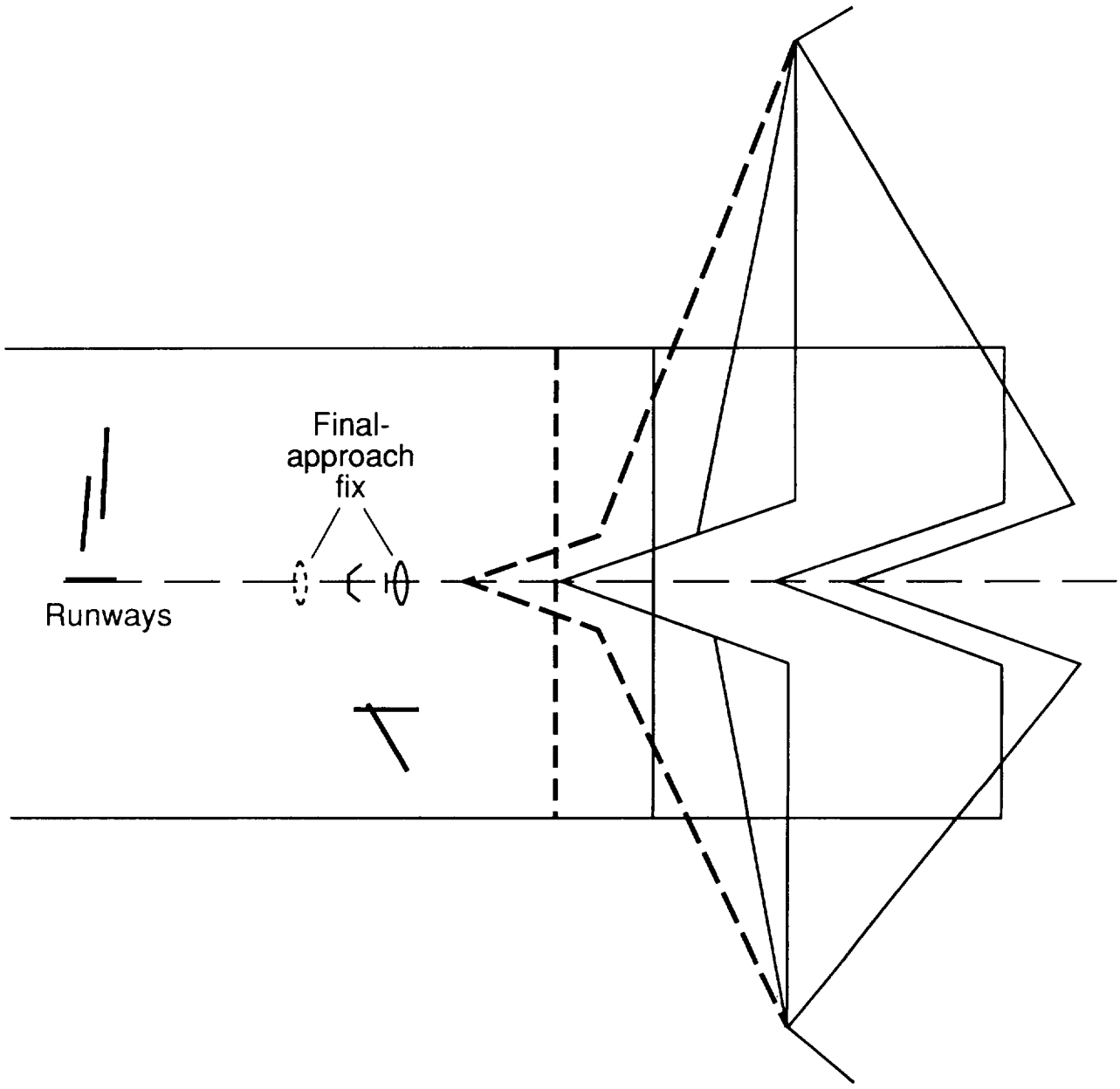

Figure 36. Normal and altered fine-tuning regions.

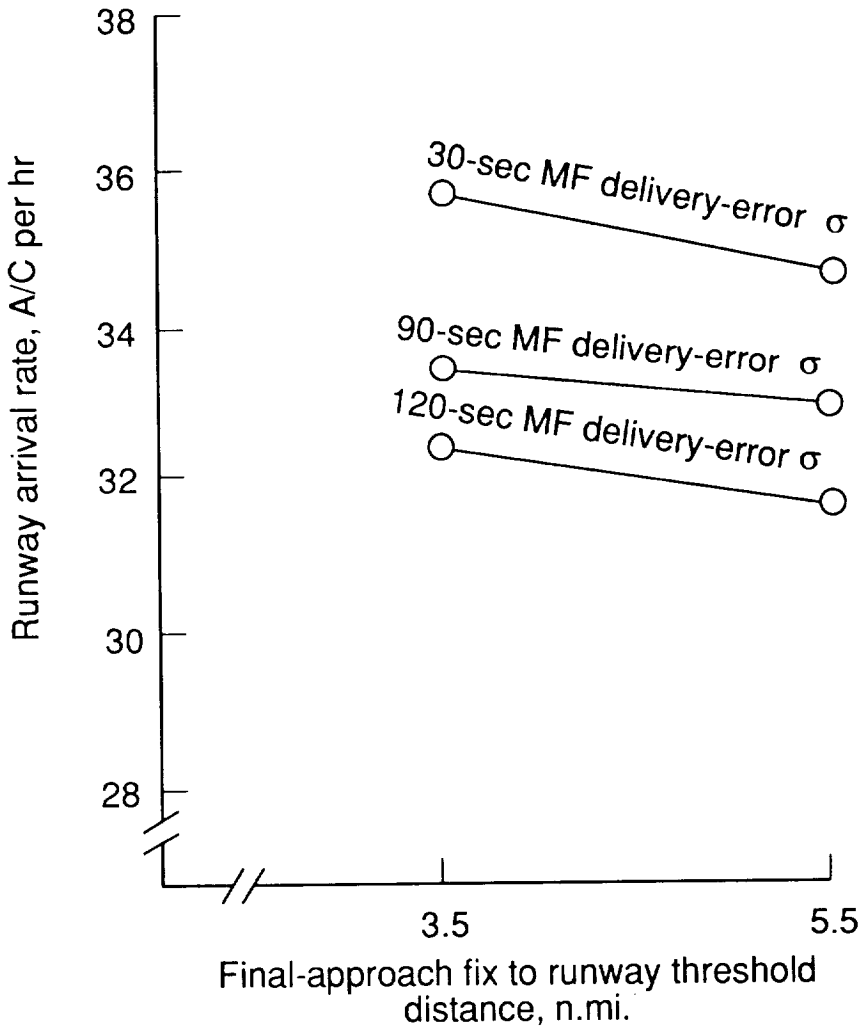

Figure 37. Effect of larger time control as a result of expanding final-approach, fine-tuning area. Separation criterion is 3/4/5 n.mi.

NASA
National Aeronautics and Space Administration

Report Documentation Page

1. Report No.	2. Government Accession No.	3. Recipient's Catalog No.
NASA TP-2870		

4. Title and Subtitle	5. Report Date
Simulation Evaluation of TIMER, a Time-Based, Terminal Air Traffic, Flow-Management Concept	February 1989
	6. Performing Organization Code
7. Author(s)	8. Performing Organization Report No.
Leonard Credeur and William R. Capron	L-16386
9. Performing Organization Name and Address	10. Work Unit No.
NASA Langley Research Center Hampton, VA 23665-5225	505-66-41-01
	11. Contract or Grant No.
12. Sponsoring Agency Name and Address	13. Type of Report and Period Covered
National Aeronautics and Space Administration Washington, DC 20546-0001	Technical Paper
	14. Sponsoring Agency Code

15. Supplementary Notes

Leonard Credeur: Langley Research Center, Hampton, Virginia.
William R. Capron: PRC Kentron, Inc., Aerospace Technologies Division, Hampton, Virginia.

16. Abstract

A description of a time-based, extended-terminal-area air traffic control (ATC) concept called TIMER (traffic intelligence for the management of efficient runway scheduling) and the results of a fast-time computer evaluation are presented. The TIMER concept is intended to bridge the gap between today's ATC system and a future automated time-based ATC system. The TIMER concept integrates en route metering, fuel-efficient cruise and profile descents, terminal time-based sequencing and spacing, and computer-generated controller aids to improve delivery precision for fuller use of runway capacity. Simulation results identify and show the effects and interactions of such key variables as horizon-of-control location, delivery-time error at both the metering fix and runway threshold, aircraft separation requirements, delay discounting, wind, aircraft heading and speed errors, and knowledge of final-approach speed.

17. Key Words (Suggested by Authors(s))	18. Distribution Statement
Terminal flow control Terminal automation Time-based air traffic control Controller aids	Unclassified—Unlimited Subject Category 04

19. Security Classif. (of this report)	20. Security Classif. (of this page)	21. No. of Pages	22. Price
Unclassified	Unclassified	69	A04

NASA FORM 1626 OCT 86 NASA-Langley, 1989

For sale by the National Technical Information Service, Springfield, Virginia 22161-2171